QUANTIFYING THE IMPACT OF ADIPOCYTE-SECRETED FACTORS ON BREAST CANCER METASTASIS

by

Pravalika Irukulla

(Under the Direction of Cheryl T. Gomillion)

ABSTRACT

Breast cancer metastasis is a major cause of mortality in women with cancer, and the role of the breast microenvironment in this process is significant. Adipocytes within breast adipose tissue are the predominant cells in the breast and contribute to metastasis through the secretion of various factors such as leptin, adiponectin and cytokines, which promote cancer cell proliferation and migration. Understanding the collective impact of adipocyte-secreted factors on breast cancer cell behavior is important for developing effective therapies. In this work, a proof-of-concept study was conducted to validate methods for culturing lean and obese adipocytes through assessment of metabolic activity, glucose and triglyceride levels. Co-cultures with breast cancer cells allowed observation of the impact of obese adipocytes on tumor cell behavior, including cell proliferation and migration over time. This work explores the interactions between adipocytes and breast cancer cells, towards identifying the impacts of the microenvironment on cancer progression.

INDEX WORDS: Breast Cancer Metastasis, Adipocytes, Adipocyte-Secreted Factors, Obesity, Co-Culture, Impedance

QUANTIFYING THE IMPACT OF ADIPOCYTE-SECRETED FACTORSON BREAST CANCER METASTASIS

by

PRAVALIKA IRUKULLA

B.S. The University of Georgia, 2022

A Thesis Submitted to the Graduate Faculty of the University of Georgia in Partial Fulfillment of the Requirements for the Degree

MASTER OF SCIENCE

ATHENS, GEORGIA

2023

© 2023

Pravalika Irukulla

All Rights Reserved

QUANTIFYING THE IMPACT OF ADIPOCYTE-SECRETED FACTORSON BREAST CANCER METASTASIS

by

PRAVALIKA IRUKULLA

Major Professor:	Cheryl T. Gomillion
Advisory Committee:	Ross Marklein
	Ramana Pidaparti

Electronic Version Approved:

Ron Walcott
Vice Provost for Graduate Education and Dean of the Graduate School
The University of Georgia
August 2023

DEDICATION

I would like to dedicate this to

my parents, Prasad Irukulla and Prashantha Kanniahgari and my brother Saiesh for always supporting me and guiding me in the right direction.

ACKNOWLEDGEMENTS

I would like to acknowledge

Dr. Cheryl Gomillion ~ who encouraged me and supported me in every step of the way through my Double Dawgs program and my thesis research.

Dr. Ross Marklein and Dr. Ramana Pidaparti ~ for their service in my committee

Damion Dixon, Kyndra Higgins ~ lab mates and friends who made this journey much more fun and special.

Isha Naidu, Asma Hashim, Divya Bhakta, and Amanda Issac ~ for all the love, support and encouragement they gave me through this journey.

TABLE OF CONTENTS

LIST OF TABLES

Chapter 3

Chapter 4

LIST OF FIGURES

Chapter 2

Chapter 3

Chapter 4

CHAPTER 1

INTRODUCTION

Globally, cancer continues to be a major public health concern, with over 17 million new cases diagnosed annually and accounting for approximately 90% of cancer-related deaths, making it the 2nd leading cause of death [1]. Cancer incidence is particularly high, with women having a 1 in 3 chance and men having a 1 in 2 chance of being diagnosed with any type of cancer [2]. Breast cancer, in particular, affects 1 in 8 women and is the 2nd most common cancer among women aged 40-50 or in their postmenopausal phase [3]. Early detection and treatment of breast cancer are critical for improving the chances of survival. If diagnosed at an early stage, there is a 99% chance of survival. However, if diagnosis and treatment are delayed, chances of survival become very low [4]. Metastatic breast cancer accounts for approximately 90% of cancer-related deaths. Metastasis usually occurs in stage 4 breast cancer, when the cancer cells spread from the breast tumor other organs [5]. Therefore, understanding the underlying factors and conditions that influence breast cancer metastasis is essential for developing more effective and personalized treatments.

Breast cancer is a complex disease influenced by various factors, such as genetic predisposition, environmental exposure, hormonal imbalances, and microenvironmental changes. Among these, obesity is a well-known risk factor for breast cancer in postmenopausal women [6]. Adipocytes in the breast adipose tissue play a critical role in breast cancer pathogenesis, as they secrete several factors that support cancer cell proliferation and migration, further facilitating tumor development. As the tumor grows, adipocytes undergo transformation into

cancer-associated adipocytes, which display tumorigenic properties and disturb normal adipose tissue function [7]. Therefore, investigating the molecular mechanisms underlying the interaction between adipocytes and breast cancer cells is crucial to elucidate the impact of obese conditions on metastasis.

Breast cancer has been a significant disease for over 5000 years, but metastatic breast cancer remains an incurable condition [8]. Despite the availability of conventional treatments such as chemotherapy, radiation and hormonal therapies, metastatic breast cancer remains a major cause of mortality worldwide. The effectiveness of these methods varies depending on the cancer subtype, ethnicity, and medical backgrounds of patients [9]. It is crucial to decipher the molecular mechanisms underlying the impact of adipocyte-secreted factors on breast cancer development to pave the way for personalized treatments tailored for obese patients. Thus, understanding the role of adipocytes could result in improving the survival outcomes of obese patients with breast cancer.

Previous research has focused on various aspects of the tumor microenvironment utilizing two-dimensional (2D), three-dimensional (3D), and animal models to study tumor progression, responses to treatment, and correlation with other medical conditions [10]. Specifically, cell culture models have been widely used for assessing the effects of changes in the tumor microenvironment. Prior research has primarily focused on individual adipocyte-secreted factors and their effects on breast cancer cell proliferation [11]. However, the secretion levels of certain factors can influence other secreted factors, thus, altering the adipose tissue microenvironment. Consequently, understanding the cumulative impact of adipocyte-secreted factors on breast cancer development is crucial.

The overarching aim of this thesis is to investigate the effect of adipocyte-secreted factors on breast cancer metastasis and to establish the prevalence of obesity on the low survival rates of

breast cancer patients. The literature review in Chapter 2 provides an overview of breast cancer metastasis and its association with obesity. Chapter 3 outlines a proof-of-concept study that involves the development of adipogenic media formulations to culture lean and obese adipocytes as well as a comparative analysis of their characteristics. Chapter 4 describes a co-culture experiment involving adipocytes and breast cancer cells to observe the effects of adipocytes and adipocyte-secreted factors on breast cancer cell proliferation and migration using impedance measurements. Lastly, Chapter 5 summarizes the findings of this study, presents final thoughts and outlines recommendations for future work.

CHAPTER 2

LITERATURE REVIEW

2.1 Breast Anatomy and Physiology

The breasts are located on the chest, superiorly across from the second rib to the sixth rib [12]. In females, they are specialized organs for milk production through a process called lactogenesis. They synthesize, secrete and eject the milk produced during lactation [13]. The size and shape of the breasts vary depending on genetics, menopausal status, diet and other factors [13]. They are composed of three types of tissue—glandular, fatty, and connective tissues. The glandular tissue holds the mammary glands and produces milk via lobules during lactation. The fatty tissue gives the breast its size and the connective tissue keeps the glandular and fatty tissue in place [14].

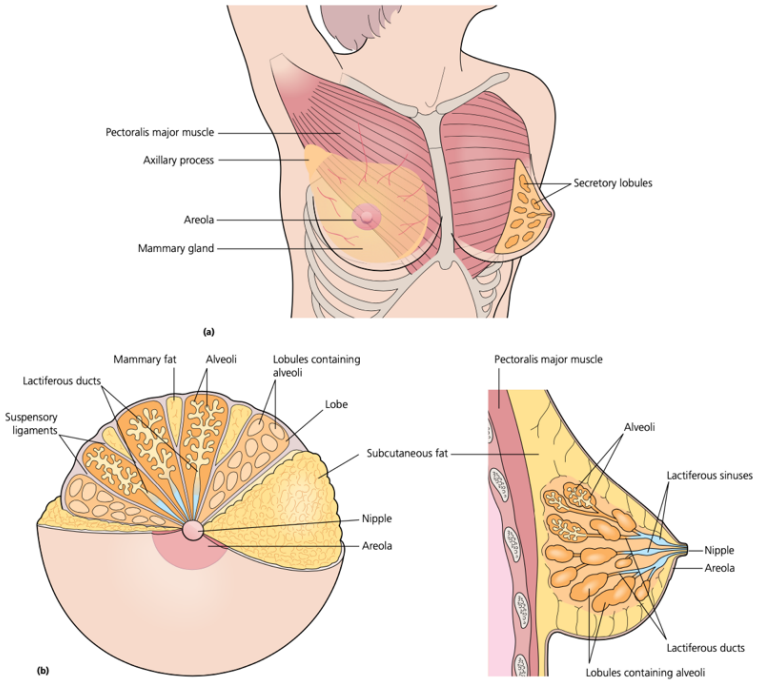

Figure 2.1. Anatomy of the female breast [13]

Structurally, the female breast is comprised of lobes, lobules, mammary ducts, blood vessels, lymph vessels and connecting nerves [14]. The majority of these components make up the nipple-areola complex which is about 3-4 centimeters in diameter and rests in the center of the breast area at the fourth to fifth rib [13]. The areola is the circular dark-colored skin that surrounds the nipple as shown in Figure 1. It holds the Montgomery glands that secrete lubricating oil during lactation [13]. The nipple is in the center of the areola and contains 9 milk ducts and is surrounded by 15-20 lactiferous ducts composed of 20-40 lobules [12, 13]. Each of these ducts contain small bulb-like glands that produce milk. The milk is carried by the mammary or milk ducts from the glandular tissue to the nipple [14].

Prior to puberty, the breast only consists of lactiferous ducts with no alveoli. At the beginning of puberty, estrogen circulates through the breast resulting in ductal and lobular proliferation, thus stimulating vascularity and increasing the volume of connective tissue or adipose tissue [13]. The majority of the breast connective tissue is composed of adipose tissue, which stretches from the collarbone to the underarm and around middle of the ribcage. The adipose tissue secretes several factors and enzymes and supports endocrine functions of the breast [15]. Breast maturity is signified by the shape of the breast and the nipple-areola area. However, it is not until pregnancy that the breast matures to its full volume. During pregnancy, the fluctuation of hormones severely impacts the size and functionality of the breasts [13]. When lactation ceases, the glandular tissue of the breast reaches a resting state. Once a woman is between the ages 40-50, menstruation ceases signifying the start of menopause [16]. This is when there is a drastic reduction of hormones like estrogen and progesterone resulting in the weakening of glandular tissue and connective tissue [13]. Women in menopause are more likely to develop the risk of breast cancer, due to the drastic changes in hormonal factors or the length in exposure to estrogen [17].

Milk production occurs through lactogenesis, which is a process that is primarily controlled by hormone changes and growth factors [13]. The process is divided into three stages, with lactogenesis I occurring in the second half of pregnancy [18]. This stage is characterized as hormone-driven due to high levels of progesterone, which increase the presence of connective tissue and fat in the breast and initiate milk production. By week 16 of pregnancy, milk components can be synthesized and colostrum production begins [19]. Lactogenesis II occurs 30-40 hours after birth, which is initiated by the removal of the placenta in addition to the child's birth. This stage can be delayed or affected by medical conditions like obesity or diabetes. Additionally, if a woman goes through a Caesarean section or gives birth to a premature baby, it would cause adverse effects

on lactogenesis II causing more delays [19]. Lactogenesis III is known as galactopesis and occurs with the ongoing production of milk. It is autocrine controlled and driven by the removal of milk from the breast [19]. All three stages of lactogenesis are regulated by the removal of milk via the nipple which triggers the levels of different hormones resulting in the ongoing milk production [18].

2.2 Breast Cancer and Tumor Progression

Breast cancer is one of the leading causes of mortality in women worldwide. The cancer tumor is initially identified using mammography, which is an x-ray of the breast that enhances benign or malignant abnormalities [20]. Other imaging techniques like Magnetic Resonance Imaging (MRI), ultrasound, Positron Emission Tomography (PET), and others are used for more accurate diagnosis of breast abnormalities [21].

Breast cancer occurs when breast cells evolve into cancerous cells when there are damages in the DNA or there are errors during cell division. During cell division, the body removes cells with damaged DNA. However, as an individual ages, the body's ability to monitor and remove potential cancer cells reduces, thus increasing the risk of a cancer tumor in the breast [22]. As the number of cancer cells in the breast tissue increases, the tissue goes into a phase known as hyperplasia, whether cancer cell proliferation increases, initiating cell build up in the tissue. As cell build up continues, the tissue enters dysplasia, where the cells look abnormal. This also causes changes in the tissue organization. As the severity of changes in tissue organization increases along with more abnormalities in cell structure and function, a cancerous tissue begins to form [22]. As the cancer cells grow uncontrollably, they start to migrate throughout the tissue as shown in Figure

2. Soon the tissue stage 0 of cancer also identified as carcinoma *in situ*, where the cancer cells exhibit non-invasive cancer behavior and do not spread to nearby tissues [23].

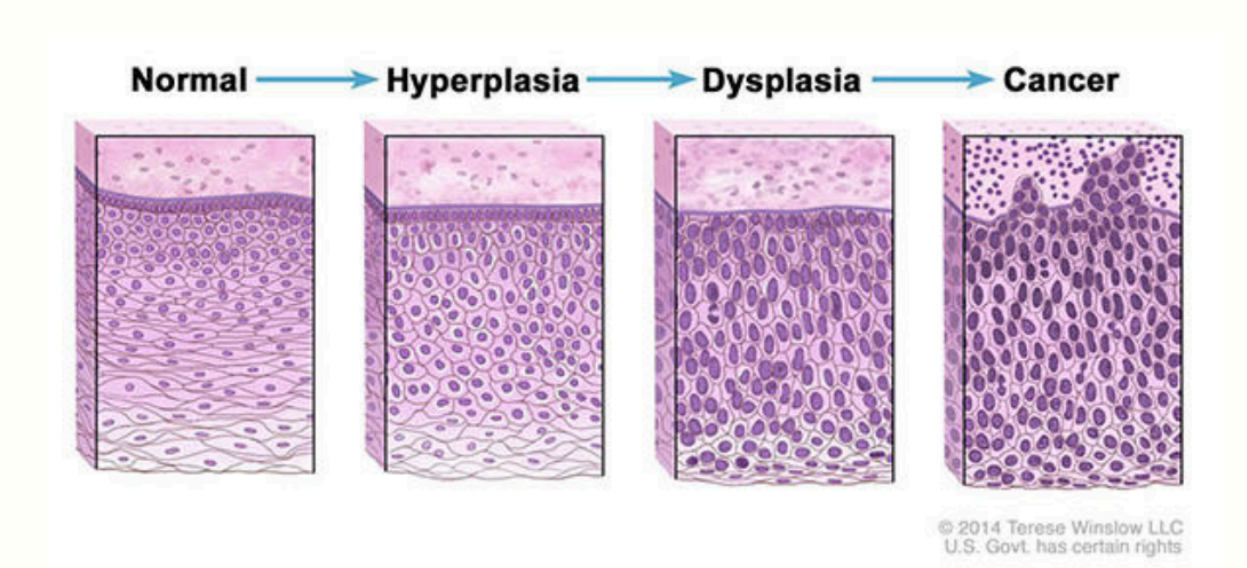

Figure 2.2. Tissue changes from a normal healthy tissue to a cancerous tissue [22].

Once the cancer cells start spreading to other tissues, they develop into carcinoma and exhibit invasive cancer behavior. There are two main areas, where breast cancer can start from: the lobules or the milk-producing ducts. If the cancer cells develop in the milk-producing ducts, it is identified to be an invasive ductal carcinoma (IDC). The cancer cells use the ducts to grow in other parts of the breast tissue [24]. If the cancer cells develop in the lobules, it is identified as invasive lobular carcinoma (ILC). The cancer cells spread to other parts of the breast tissue that are in close proximity to the lobules [24].

Breast cancer is characterized by three main hormone receptors: estrogen (ER), progesterone (PR) and human epidermal growth factor receptor type 2 (HER2). The levels of these hormone receptors categorize the tumor into three specific clinical types: ER/PR-positive breast

cancer, HER2+ and triple negative breast cancer (TNBC) as seen in Figure 3 [25]. Within these main clinical types of breast cancer, there are numerous subtypes that are specified based on the area of origin, molecular stratification, and the impact of the hormone. Triple negative breast cancer is the most aggressive subtype and is also known to have the worst prognosis. However, the tumor composition and progression vary at each stage regardless of the clinical subtype and have their own set of adverse side effects.

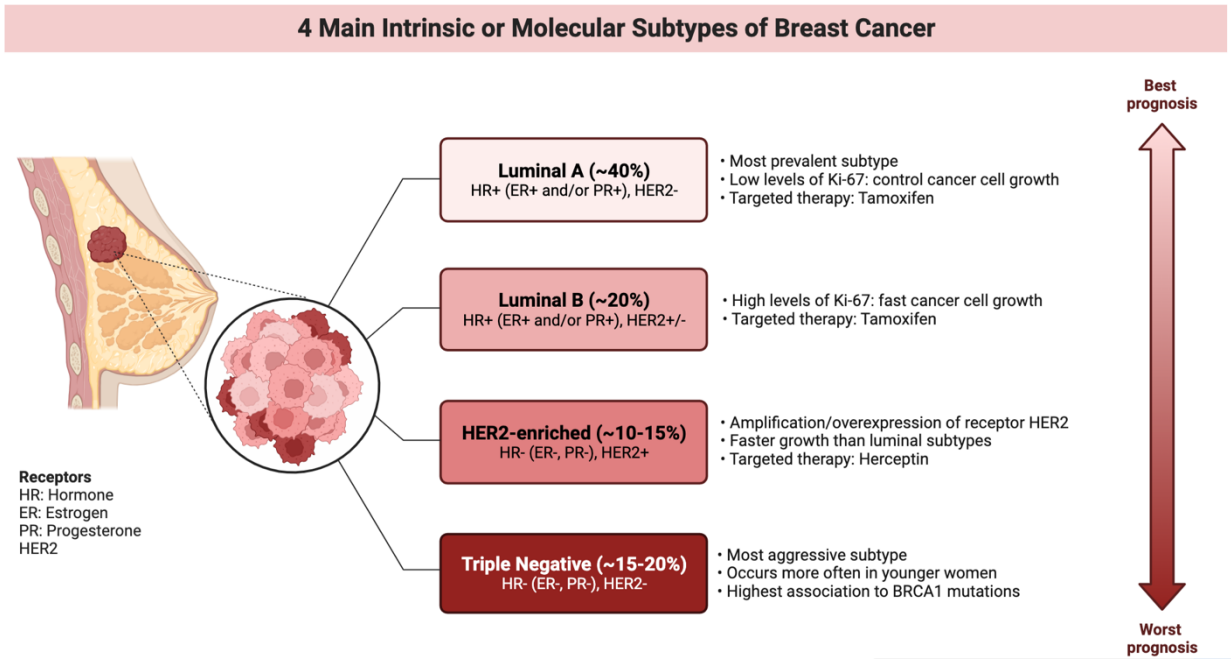

Figure 2.3. Breast cancer can be categorized into subtypes based on the receptors present or absent. The level of aggressiveness and prognosis is also dependent on the receptors. For example, triple negative is receptor negative making it the most aggressive and having the worst prognosis. Adapted from "Intrinsic and Molecular Subtypes of Breast Cancer," by BioRender.com (2023)

2.3 Breast Cancer Metastasis

The invasive behavior of cancer cells describes Stage 1 of breast cancer, where the cells are slowly invading to immediate lymph nodes to spread throughout the breast tissue. In Stage 2, the cancer tumor become larger and invades more lymph nodes [26]. In almost all cases of breast cancer in Stages 1 or 2, the tumor cannot be detected as it is still too small for detection methods [27]. At Stage 3, the tumor is significantly larger and has spread to almost nine lymph nodes and the tissue surrounding the breast [26]. As the tumor transitions into Stage 4 breast cancer, it is adopting a metastatic potential. Metastasis refers to the condition when the tumor spreads to the other organs in the body [28]. At Stage 4, the tumor goes through a metastatic cascade involving five steps: (1) invasion and migration, (2) intravasation, (3) circulation, (4) extravasation, and (5) survival and colonization as shown in Figure 4 [29, 30].

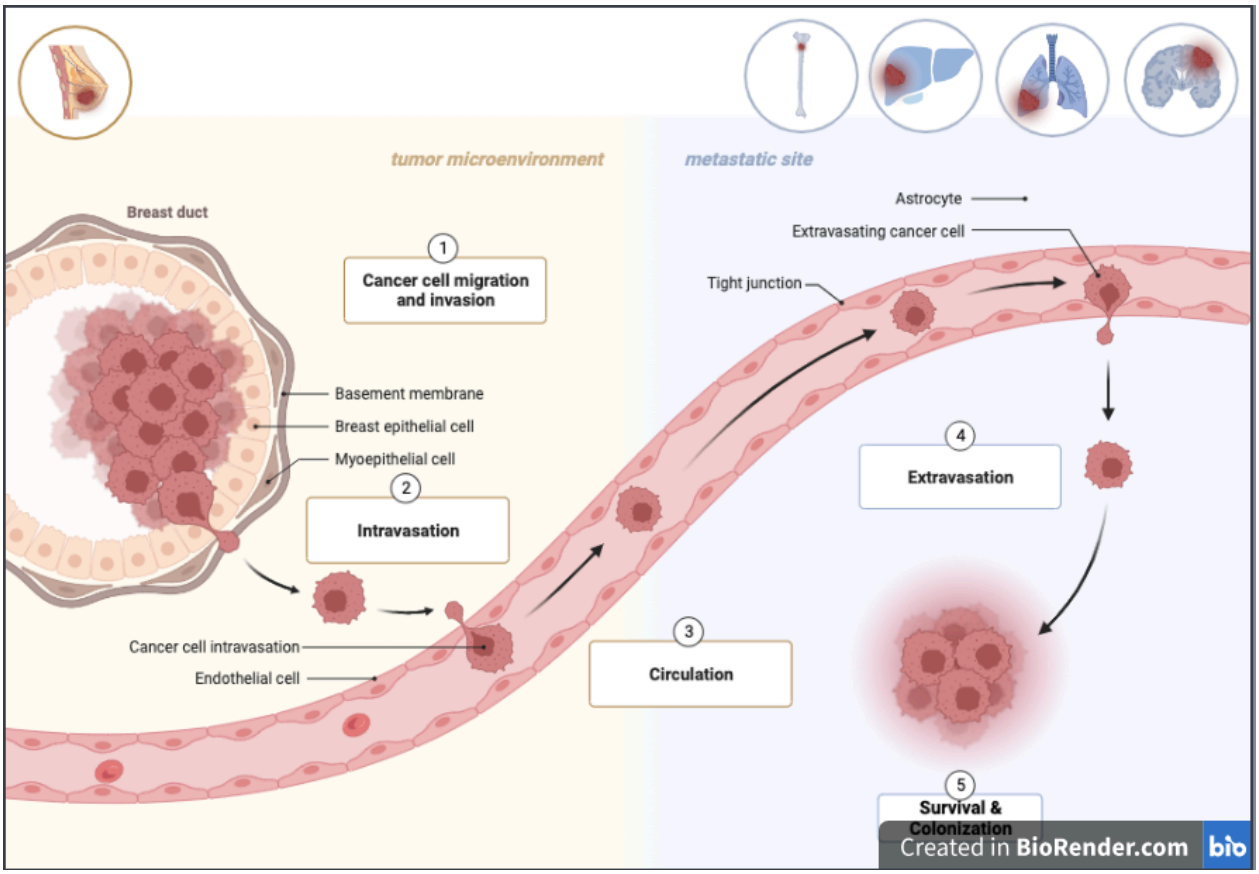

Figure 2.4. Breast cancer metastatic cascade. Breast cancer cells grow uncontrollably and eventually leave the primary tumor to infiltrate other organs in the body. Adapted from "Breast Cancer to Brain Metastasis," by BioRender.com (2023)

During the first step of the cascade, the cancer cells become locally invasive and migratory [31]. They grow uncontrollably and go through a process known as epithelial-to-mesenchymal transition (EMT), where the cells transform from epithelial cell structure to a mesenchymal cell structure as shown in Figure 5.

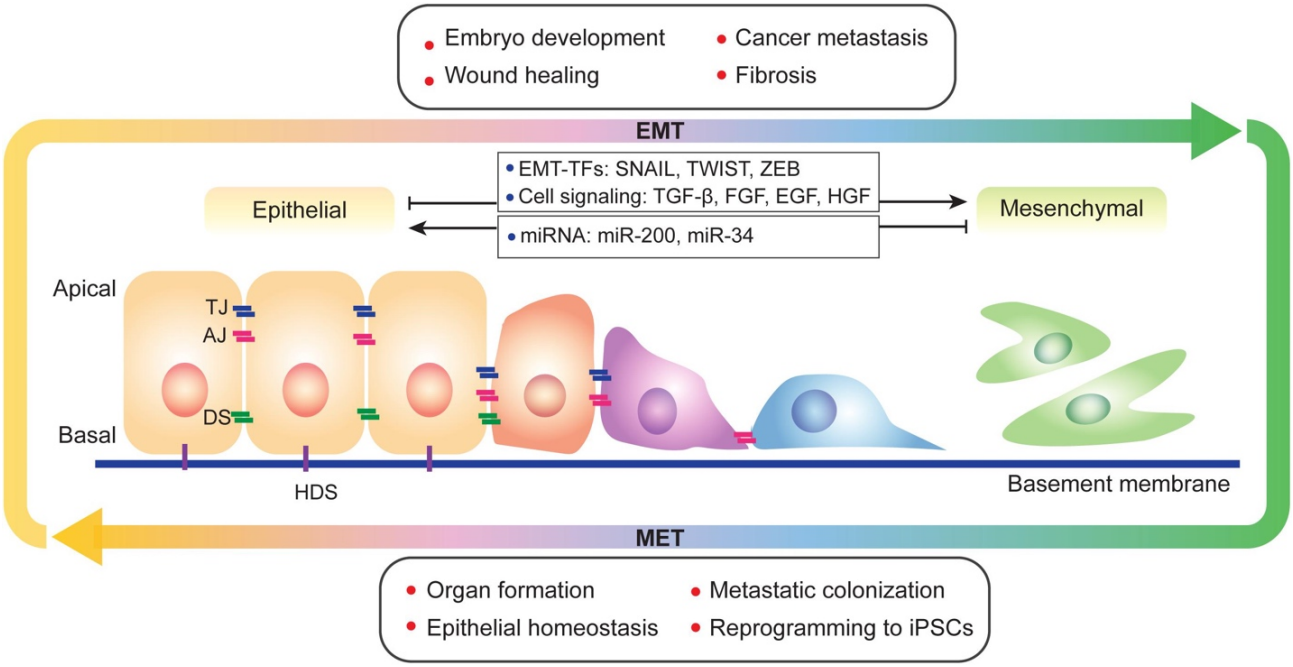

Figure 2.5. Epithelial-to-mesenchymal transition of breast cancer cells [32]

The cells become more migratory and secrete several ECM degrading enzymes like fibronectin, laminin, and other proteins connected to collagen, allowing the cells to invade the local stroma and reach the blood or lymphatic vessels [33, 34]. Then, the primary tumor is vascularized through a process known as angiogenesis. Once the primary tumor is fully vascularized, the cancer cells enter the bloodstream and secrete ECM factors to destroy the enzymes in the local stroma [30]. The tumor cells eventually circulate through the bloodstream to travel to other organs in the body [33]. Once the cancer cells circulate and populate the blood vessels, extravasation starts to occur [30]. The cancer cells leave the blood vessels and enter organs such as the brain, lung, liver or bone [33].

The most important part of the metastatic cascade is survival and colonization. In order for the cancer cells to survive in the new organ, they must be well-equipped to infiltrate through the vascular network. The normal vascular organization of the new organ is different from the origin

of the tumor [30]. The cancer cells adapt extra genes to modify the new stroma to develop a microenvironment where they can grow and populate into a cancer tumor [33]. Then, they go through a process of mesenchymal-to-epithelial transition (MET) to attach to the target site as shown in Figure 5.

The metastatic behavior of the breast cancer cells can be modified by the tissue properties, presence of epithelial or organ cells or internal/external environmental factors. Biochemical stimuli that can cause inflammation, angiogenesis, or promote cell proliferation can further support the tumor growth [5]. Additionally, other medical conditions that directly affect the composition of the breast tissue can also cause modifications of the breast tissue.

If the tumor is diagnosed at an early stage, there are high chances of survival [20]. When the tumor is diagnosed at an initial stage, the patient can undergo treatment with immediate effect to prevent tumor progression and any other side effects the tumor may cause in the body. However, majority of the breast cancer tumors are detected around stage 3 where patients have a survival rate of about 86% [4]. The type of treatment also varies based on when the tumor was diagnosed, the grade of the tumor, where the tumor is, and the subtype of breast cancer the patient is diagnosed with. Some common methods of treatment used after early detection include breast surgery, chemotherapy, radiotherapy, hormonal and targeted therapies [9]. More than one of these methods are used in combination to treat each subtype to provide a more personalized and safe treatment for patients. Even though there are multiple therapies, there is still no cure to breast cancer due to the complexity of the disease. One of the biggest challenges deals with treating patients with TNBC as it is the most aggressive of the subtypes. Survival rates have been very low even with a personalized therapeutic treatments [9]. Another challenge is treating metastatic breast cancer

(MCB). Due to its complexity, therapies for MCB have been developed to combine the common therapies in addition to biological agents to be more personalized for a patient's condition [9, 35].

2.4 Breast Cancer and Adipocytes

About 56% of the breast is composed of adipose tissue [36]. It plays a very significant role in the breast during development, pregnancy, lactation, and breast cancer metastasis. The adipose tissue in the breast is primarily composed of fibroblasts, macrophages, adipocytes (fat cells), an extracellular matrix and immune cells [15]. The adipose tissue secretes proteins, fatty acids and cytokines which influence other cells in the environment and changes in tissue development. Therefore, any changes to the adipose microenvironment can essentially alter the cell morphology and proliferation rates of breast cancer cells and support breast cancer metastasis [37].

The adipocytes in the adipose tissue are primarily responsible for the secretion of factors and the storage of fat and energy [38]. The secreted factors are certain molecules that release into the fat tissue to support the organ via endocrine, autocrine, and paracrine functions. Adipocyte secreted factors like leptin and adiponectin regulate body weight. TNF-α, IL-6, IL-1β, and other cytokines are cause inflammation of the adipose tissue and Ang II and PAI-1 regulate the vascular function [39]. However, leptin, adiponectin and inflammatory cytokines have the most prominent role during breast cancer development.

Leptin is a hormone secreted to regulate the energy balance by inhibiting hunger and reducing the storage of fat in adipocytes. It activates several signaling cascades that play an important role in cell development and invasion [40]. Leptin plays a critical role in inducing the JAK/STAT signal transduction pathway as well as the impact on the mitogen-activated protein kinase (MAPK) and epidermal growth factor receptor (EGFP) pathways [41, 42]. This further

affects the levels of adipokines and other cytokines being secreted by the adipocytes, further affecting the estrogen metabolic pathway and promoting breast cancer cell activity [43]. Leptin tends to enhance cell functionality and proliferation capabilities.

Adiponectin is a hormone that regulates insulin sensitivity and inflammation, controls glucose levels and plays an important role in cell morphology and hypertrophy [44]. In normal adipose tissue, adiponectin acts to reduce or prevent inflammation of the tissue. The molecule also signals several metabolic pathways in breast tissue, skeletal muscles, and the vasculature [44]. Adiponectin levels are usually high in adipose tissue, allowing the proper regulation of inflammation and metabolic activity. In the presence of breast cancer cells, adiponectin inhibits the adhesion and migration of cancer cells. The hormone inhibits tumor growth by elevating LKB1 which is a tumor-suppressing gene [45].

Cytokines also play an important role in cell-to-cell communication and pro-inflammatory factors in adipocytes. More specifically, interleukin-6 (IL-6) and interleukin-8 (IL-8) are cytokines that tend to develop at early stages of cell growth and facilitate cell signaling to ensure faster growth and spread rate [46]. When interacting with breast cancer cells, these factors will also cause cancer cells to grow faster and slightly alter their cell morphology. Eventually, the interaction with breast cancer cells causes the adipocytes to evolve into cancer-associated adipocytes by acquiring behaviors of cancer cells and continuing to provide more nutrients for them [7].

Adipocyte-secreted factors are the key hormones that support the development of the adipose tissue in the breast. During breast cancer, they supply almost all nutrients needed for breast cancer cells to metastasize. Each factor plays its own important role in cell growth, proliferation, and migration of adipocytes and other cells in the environment. Additionally, every factor

influences another adipocyte-secreted factor, which collectively results in greater impact to the adipose microenvironment, especially in the breast.

2.5 Breast Cancer and Obesity

Medical conditions like obesity can stimulate inflammation of breast cancer cells (BCCs) and lead to metastatic behavior of breast cancer by altering the levels of adipocyte-secreted factors [28]. The positive correlation between excess body weight and mortality due to breast cancer has been well established over the past decade [47]. This idea has been the driving factor to understand how obese conditions impact breast cancer development; however, the relationship is not fully validated with evidence. The overall survival rate of breast cancer patients who are considered obese, based on their Body Mass Index (BMI), is low as seen in Figure 6 [48]. Many patients have also shown to have poor prognosis irrespective to the tumor subtype [49].

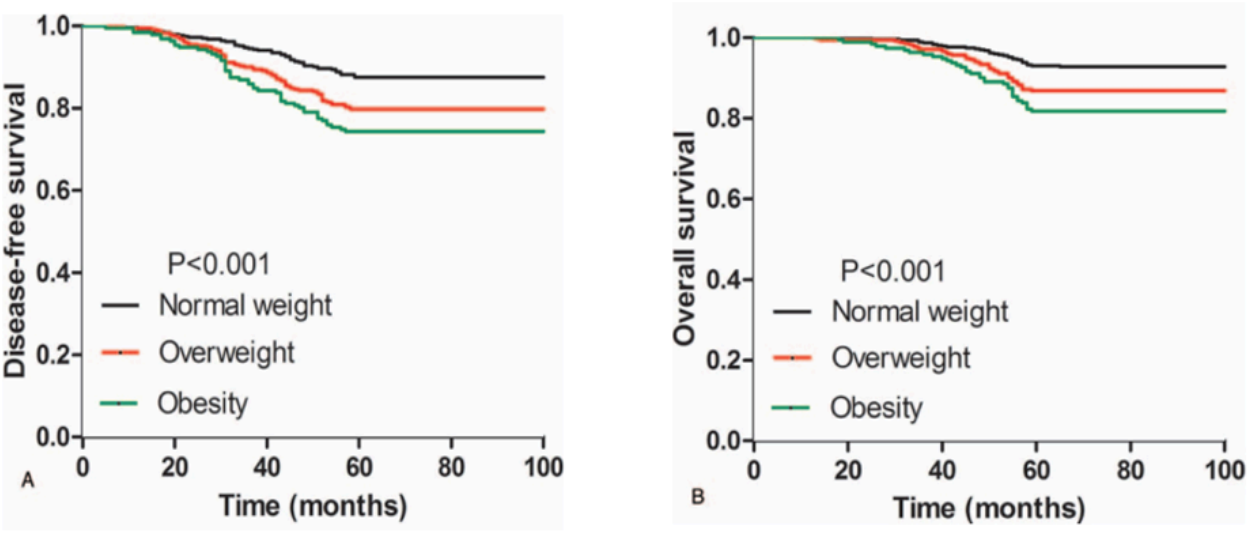

Figure 2.6. 5-year survival outcomes of breast cancer patients based on BMI visualized using a Kaplan-Mier analysis. (A) shows disease-free survival rates and (B) shows the overall survival rates [48].

Obesity is a condition that describes excessive body fat which influences other health conditions and increases mortality risks. Obese patients are at risk of developing cardiovascular diseases, type 2 diabetes, joint and muscular disorders, and other health issues [50]. If an adult's BMI is 30.0 or higher, they are considered obese [51]. The transition from a lean to an obese condition initiates chronic low-grade inflammation of the adipose tissue [50].

About 48.5% of women in the initial stages of breast cancer are diagnosed as obese, whereas 67.3% women in Stage 4 of breast cancer are diagnosed as obese [52]. Women in their postmenopausal phase are more likely to become obese due to the changes in their body rather than the physical gain in weight and change in BMI. The BMI measurement accounts for an individual's weight-to-height ratio, which does not accurately consider the muscle mass loss or the redeposition of adipose tissue, leading to imprecise conclusions about an individual's weight

condition. Even though a woman's BMI is the same peri- and post-menopause, she could be considered obese [53]. During post-menopause, a woman's body goes through significant physical changes such as decrease in height, body weight fluctuations, reorganization of the adipose tissue or the decrease in skeletal muscle mass [54].

The changes in fat storage and mass directly impact the estrogen and insulin levels in the body [52]. Estrogen has several important roles in the mammary gland along with hormonal changes in the adipose and skeletal system [55]. It is primarily responsible for the distribution of fat in the female body. The fluctuations of estrogen levels and synthesis processes before, during and after menopause result in improper depositions of fat, increasing a women's risk of obese post-menopause. During perimenopause, estrogen is synthesized in the ovaries. In post-menopause, estrogen is synthesized in peripheral sites, which initiates the changes in adipose tissue redeposition. Estrogen synthesis in obese postmenopausal women occurs in the adipose tissue increasing the chances of estrogen deposition near breast tumors [56]. Along with the changes in estrogen levels near the breast tumor, the constant change in adipose tissue causes the adipocytes to secrete different levels of adipocyte secreted factors, further supporting the breast tumor growth.

Normally, adipocytes produce lipid droplets to regulate the storage and hydrolysis of lipids in the body. Many studies have investigated the microenvironment of obese conditions, which showed that adipocytes swell up due to the accumulating lipids droplets, making them appear dysfunctional and diseased as shown in Figure 7. Under obese conditions, lipid droplets accumulate at a faster rate and secrete more inflammatory cytokines and factors that support cell proliferation [39].

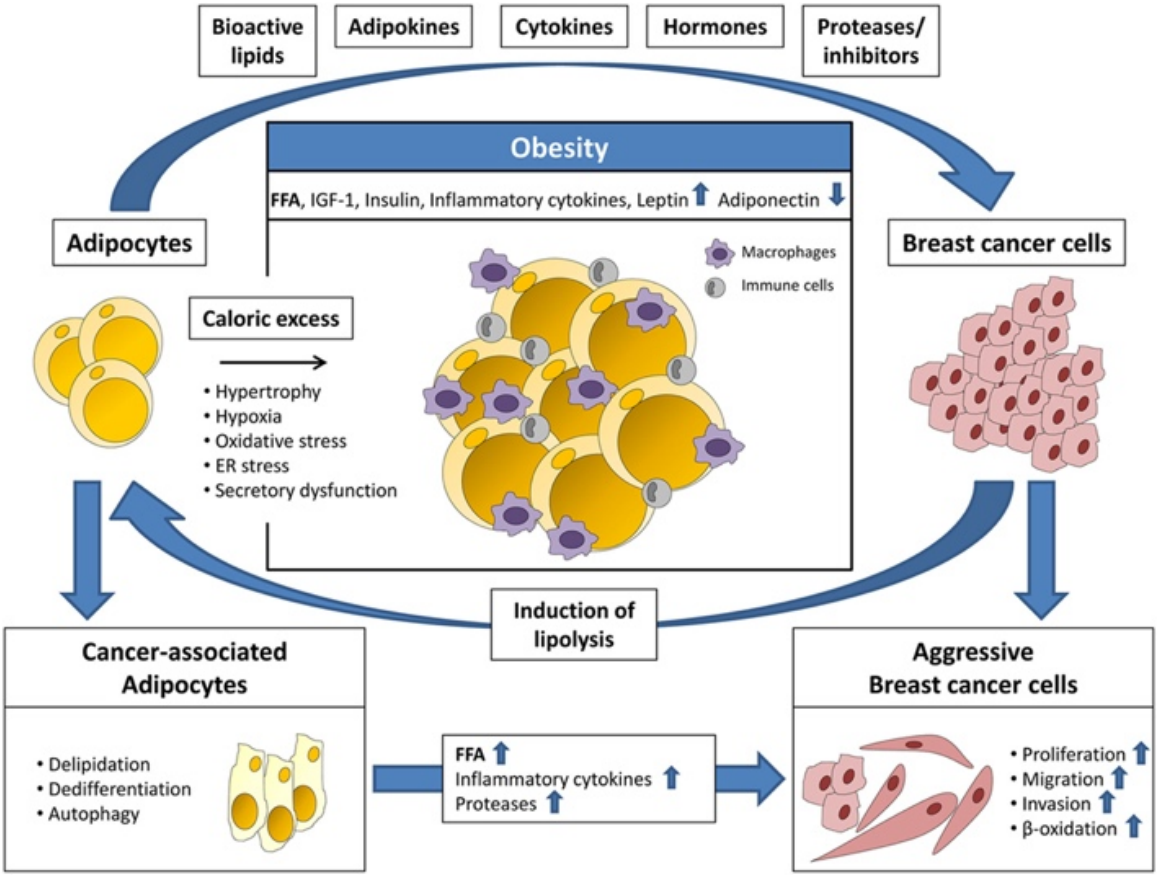

Figure 2.7. Impact of adipocytes in obese conditions on breast cancer cells. Secretion of adipocyte-secreted factors impact breast cancer cell proliferation. The aggressiveness of breast cancer cells also makes the adipocytes evolve into cancer-associated adipocytes [7].

During obese conditions, adipocytes secrete different levels of leptin, adiponectin and inflammatory cytokines that further support cell proliferation making the cancer cells more aggressive as shown in Figure 7 [28, 57]. Adipocytes secrete excess leptin which supports the cross-talk between breast cancer cells and adipocytes [58]. Studies have shown that increased levels of leptin have been associated with obesity-associated cancer development [46]. Likewise, obese conditions are characterized by low levels of adiponectin [59]. The increase in leptin levels also supports the suppression of adiponectin causing adipocytes to grow faster and look "fat." Due

to the low levels of adiponectin in obese conditions, there is no proliferation inhibitor of breast cancer cells in the microenvironment, increasing the chances of tumor progression to metastasis. Obese adipocytes also secrete more inflammatory cytokines, which drive inflammatory and angiogenic processes supporting tumor progression as well.

The majority of the nutrients needed for breast cancer cell survival and colonization in the breast tissue are supplied by adipocyte-secreted factors, making conditions like obesity a detrimental factor to tumor progression. Therefore, it is important to understand how these factors influence each other and provide nutrients to the breast cancer cells. Thus, this work will focus on assessing the impact of obese adipocytes on breast cancer cell proliferation and behaviors.

2.6 2D In Vitro Culture Analysis

Cell culture models are widely used in breast cancer research to assess diagnosis methods, impact of specific conditions or therapeutic effects on cancer growth. Scientific research has been conducted using various *in vitro* or *in vivo* models. Over the past decade, *in vitro* and *in vivo* models have been very useful in understanding the mechanisms and pathways of metastatic breast cancer. However, they have their own set of advantages and limitations.

In vivo models are usually animal models which are used to study disease progression, test new therapies, and assess the efficacy of new drugs. Animal models are used as animals share a similar physiology to a human, making it more feasible to understand the impacts and other reactions a body can have due to the disease or treatment [60]. However, there are a number of ethical concerns revolving around the use of animal models for scientific research, which create many challenges in experimental procedures and scientific analysis. One common ethical concern is related to euthanizing or sacrificing the animals after experimentation. Many ethicists have

argued that animals cannot be sacrified for the benefits of human health [61]. Likewise, the use of animal models in research is expensive, limiting the number of studies that can be completed.

On the other hand, *in vitro* models are more cost-effective and easier to use. These models are developed using cell lines derived from animals and humans, which can be used for a longer time [62]. 2D models can also be developed using simulations or mathematical models. While a 2D cell culture does not accurately represent the physiology and microenvironment of the human body, it provides an easier way to make qualitative and quantitative observations with reduced ethical concerns. 2D cell cultures have been used in scientific research since the 1900s and have been a well-established method to efficiently analyze diseases and treatment delivery methods. Likewise, there is more comparative data to support current 2D culture model studies [63]. Therefore, 2D cell culture models are more feasible to develop to use analysis techniques like terminal and non-terminal assays as well as imaging for precise initial observations.

Majority of breast cancer research is initially conducted using 2D *in vitro* cell culture models. These cultures are usually created by culturing breast cancer cell lines in tissue culture plastics like flasks, plates, or Petri dishes, with culture medium. The medium provides appropriate nutrients and molecules needed for cell growth and can be altered based on the condition of the cells or the microenvironment that need to be observed. These models can be developed using different culture approaches. A common culture approach involves changing the media used to culture the cells. Media can be conditioned by adding supplements or extra serum concentrations to impact cell growth or differentiation. Many studies like the one conducted by Guo et al. culture cells in media for a period of time and collect the media samples for future conditioned media studies [64]. Therapeutic or drug treatments can also be added to the media to observe the impact of new therapies on the breast cancer cells [65]. For example, antibodies, reagents, or drug doses

can be added to the media throughout an experiment timeline to observe different aspects of the cell culture like proliferation, viability, and morphology [64].

Another culturing approach involves culturing multiple cell lines together in a co-culture. In co-cultures, different cell lines are cultured together to observe the impact on cell growth rate and cell-to-cell behaviors. Co-cultures are accurate in representing different cell populations in one culture, similar to the human body. However, due to the use of different cell lines, optimization of the culture condition can become a challenge [65]. These models are usually developed using Transwell inserts or in 3D *in vitro* models [66]. In the Transwell inserts, one cell line is cultured into the tissue culture plastic (i.e. well plates) and the other cell line is cultured on to the insert which is then placed on top of the first cell line in the tissue culture plastic well-plate as shown in Figure 8.

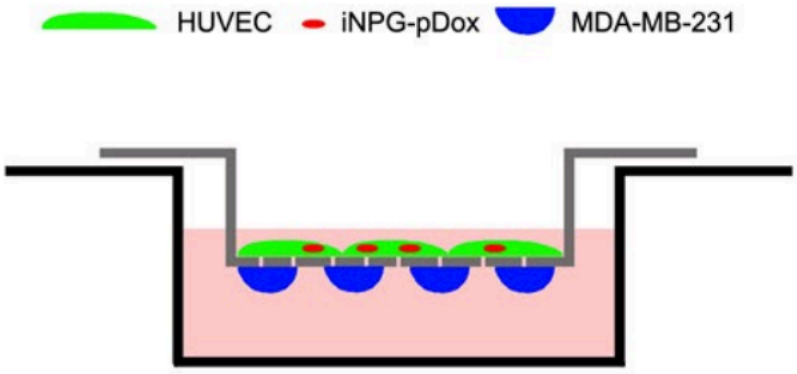

Figure 2.8. Use of a Transwell insert to co-culture human umbilical vein endothelial cells (HUVEC) with triple negative breast cancer cells (MDA-MB-231) [67].

Co-culture 2D models provide a bigger picture about the impact one cell type has on the other cell line. They provide data about the maintenance and build-up of the tissue or disease solely

based on the cell-to-cell interactions [68]. In a co-culture study with breast cancer cells and adipocytes conducted by Crake et al, they showed the impact on several metabolic pathways of the cancer cells, which proved to be a good platform to investigate paracrine function during metastasis [69].

In a number of studies, 3D cell culture models are used after the initial studies with 2D cell culture models have been conducted and have proven to show supportive results. However, it is imperative to have accurate observations and results from a 2D culture system prior to developing a model in 3D to avoid extra expense and false validations.

The primary goal of this work is to develop a 2D cell culture model using Transwell inserts to co-culture conditioned adipocytes with different breast cancer cell lines to observe the impact of adipocyte-secreted factors on breast cancer tumor progression by analyzing cell proliferation and migration rates. The first part of the work will focus on developing an adipogenic media formulation with specific additives to culture lean and obese adipocytes, which will be discussed in Chapter 3. Then in Chapter 4, the lean and obese adipocytes will be cultured with various breast cancer cell lines. Real-time data about cell proliferation and migration will be collected using the Axion BioSystems MaestroZ instrument, an impedance-based assay system to continuously monitor cell growth. Overall, the 2D co-culture model will provide evidence to the low survival rate of obese patients suffering from breast cancer metastasis. However, these studies can be improved for better models. The final chapter provides a summary of the findings and recommendations for future studies.

CHAPTER 3

QUANTIFYING THE DIFFERENCES BETWEEN LEAN AND OBESE AIDPOCYTES

3.1 Introduction

Obesity is a prevalent condition that affects a significant portion of the global population, with a prevalence of 38% [70]. In the United States particularly, the prevalence of obesity was documented to be 41.9% between 2017-2020, impacting about 2 in 5 adults [71, 72]. This condition is characterized by the excessive body fat accumulation, which contributes to the development of various medical conditions and increases mortality risk. Obesity primarily impacts cardiovascular diseases, type 2 diabetes, joint and muscular disorders, and breast cancer [71]. Individuals with a Body Mass Index (BMI) of 30.0 or higher are considered obese [72]. It can be impacted by various factors such as genetic, environmental, or behavioral factors. Poor diet and lack of physical activity are the primary contributions to the development of obesity, while sleep patterns and degree of time with electronic devices also make a significant contribution [72]. Additionally, socioeconomic status, cultural factors and access to healthy food and physical activity opportunities may influence the prevalence of obesity. However, obesity is a preventable condition that can be managed with a healthy lifestyle. A proper diet that includes the necessary fats, carbohydrates, sugars, fruits/vegetables, grains/nuts and regular physical activity can improve one's overall health [73]. In some cases, individuals with other conditions such as breast cancer must take extra care to maintain a healthy diet and engage in regular physical activity to avoid any complications.

Obesity primarily impacts the adipose tissue which comprises about 20-25% of the entire body weight [38]. It is a connective tissue primarily composed of adipocytes or fat cells along with fibroblasts, immune cells, and endothelial cells [74]. The adipose tissue stores excess energy in the form of triglycerides. The functions of the adipose tissues are regulated by various hormones including insulin, glucagon, cortisol, estrogen, etc. The adipocytes in the tissue secrete factors like leptin, adiponectin and other cytokines which perform important metabolic activities in the endocrine pathway to maintain energy balance, food intake and inflammatory responses [38].

The transition from a lean to an obese condition initiates chronic low-grade inflammation of the adipose tissue [50]. The inflammation causes imbalances in adipocyte secreted factors impacting the metabolic activities of the endocrine system that induce food intake and maintain energy balance. Thus, making the adipose tissue dysfunctional and diseased. In a diseased adipose tissue, leptin levels are high which constantly induces the feeling of hunger, resulting in more food intake [40]. The high leptin levels also influence the decrease in adiponectin levels which regulates the inflammatory response of the tissue. The low level of adiponectin hinders the proper regulation of inflammatory pathways supporting the low-grade inflammation of the tissue. Likewise, there are fluctuating levels of various cytokines such as IL-6, IL-8, etc. that support the inflammation of tissue and secrete more factors [46]. The diseased adipose tissue makes a significant contribution on the disease outlook of type 2 diabetes, muscular and joint disorders, and breast cancer. The fluctuations of adipocyte-secreted factors impact the disease progression by influencing the primary hormones of the diseases.

Many studies have created two-dimensional (2D) models to observe the differences between lean and obese adipocytes by using a variety of cell lines or a variety of reagents in the media formulations. This study will focus on using bone-marrow derived mesenchymal stromal

cells (D1 MSCs) to derive lean and obese adipocytes with different media formulations. To derive obese cultures, different concentrations of stearic acid with bovine serum albumin (BSA) will be used to induce an increase in the inflammatory response of the MSCs during differentiation [75]. This proof-of-concept study is intended to determine the best media formulation to grow obese adipocytes by using stearic acid and bovine serum albumin as additional inflammatory reagents.

3.2 Materials and Methods

3.2.1 Materials

Murine bone marrow-derived mesenchymal stromal cells (D1) were obtained from the American Type Culture Collection (ATCC, Manassas, VA, USA). 24-well tissue culture treated, and 96-well black walled/clear bottom tissue culture treated plates were purchased from Fisher (Hampton, NH, USA). 96-well CytoViewZ plates were purchased from Axion Biosystems (Atlanta, GA, USA). Penicillin-Streptomycin (P/S), Dulbecco's Phosphate Buffered Saline (PBS, -Ca, -Mg), Low-glucose (1 g/L) and High-glucose (4.5 g/L) Dulbecco's Modified Eagle's Medium (DMEM) were purchased from Gibco (Waltham, MA, USA). Fetal Bovine Serum (FBS) was purchased from Atlanta Biologics (Atlanta, GA, USA). Dexamethasone, Indomethacin, Rosiglitazone, Insulin, Isobutyl-1-methlxanthile (IBMX), Stearic acid, and Bovine Serum Albumin (BSA) were purchased from Sigma-Aldrich (St. Louis, MO, USA). The MaestroZ impedance-based assay system was purchased from Axion Biosystems (Atlanta, GA).

3.2.2 Cell Culture

The D1 MSCs at passage 8 were originally cultured in DMEM-Complete (Low Glucose DMEM, FBS, P/S) in 24-well plates, 96-well black walled/clear bottom plates and a 96-well

CytoView plate. Different adipogenic medias were made as shown in Table 3.1. After 48 hours, once the plates were confluent, the different adipogenic medias were added to the culture samples in replicates of 4. The cultures were observed in their specific medias for 14 days. They were harvested at 3 different timepoints: Day 3, Day 7, and Day 14 of differentiation.

Table 3.1 Media formulations used to differentiate the D1 MSCs into lean and obese adipocytes

Media Type	Formulation
ndMSC Media	LG DMEM + 10% FBS + 1% P/S
Lean Media	HG DMEM + 10% FBS + 1% P/S + 1% IBMX + 0.1% Insulin + 0.02% Dexamethasone + 10 μM Rosiglitazone + 100 μM Indomethacin
Obese Media 1 (200 μM Stearic Acid)	HG DMEM + 10% FBS + 1% P/S + 1% IBMX + 0.1% Insulin + 0.02% Dexamethasone + 10 μM Rosiglitazone + 100 μM Indomethacin + 200 μM Stearic Acid + 1% BSA
Obese Media 2 (500 μM Stearic Acid)	HG DMEM + 10% FBS + 1% P/S + 1% IBMX + 0.1% Insulin + 0.02% Dexamethasone + 10 μM Rosiglitazone + 100 μM Indomethacin + 500 μM Stearic Acid + 1% BSA
Obese Media 3 (700 μM Stearic Acid)	HG DMEM + 10% FBS + 1% P/S + 1% IBMX + 0.1% Insulin + 0.02% Dexamethasone + 10 μM Rosiglitazone + 100 μM Indomethacin + 700 μM Stearic Acid + 1% BSA
Obese Media 4 (900 μM Stearic Acid)	HG DMEM + 10% FBS + 1% P/S + 1% IBMX + 0.1% Insulin + 0.02% Dexamethasone + 10 μM Rosiglitazone + 100 μM Indomethacin + 900 μM Stearic Acid + 1% BSA

3.2.3 Lipid Droplet Quantification

Oil Red O (ORO) staining was performed to quantify the lipid droplets in the cell cultures. Cells were washed with PBS and fixed with 10% formalin. Then, cells were washed with 60% isopropanol and allowed to dry at room temperature. A stock solution of ORO was created by combining ORO powder (Sigma-Aldrich, St. Louis, MO, USA) with 100% isopropanol and

stirring overnight. Then, the stock solution was filtered and diluted to a working solution containing 6 parts ORO stock solution and 4 parts DI water. The working solution was added to the cell cultures and incubated for 10 minutes at room temperature with gentle shaking on a rocker. The cells were washed 4 times with DI water and imaged using a microscope.

The ORO staining was quantified by obtaining the absorbance readings of the ORO destained solution. 500 μL of 100% isopropanol was added to each well and incubated for 15 minutes at room temperature to destain the cultures. The absorbance values of the destained solution were measured using a BioTek Cytation|1 imaging reader (Fisher, Hampton, NH, USA) at 500 nm. A solution of 100% isopropanol was used as a reference.

3.2.4 Lipid Droplet Hypertrophy

To assess the hypertrophy or size of the lipid droplets, the ORO-stained culture images were used with ImageJ (National Institutes of Health, Bethesda, MD, USA). The software was initially calibrated to the assess 40x images taken by the EVOS Imaging System (Life Technologies, Hampton, NH, USA). Then the image was split into 5 areas indicated by the yellow boxes in Figure 3.1. Two measurements from each of the yellow boxes, for a total of 10 measurements were taken, without any duplicates. To do so, the free hand tool was used to select the lipid droplet and the area of the lipid was measured using the analysis option in the software (Appendix A). The average of areas was used and compared among all cell cultures.

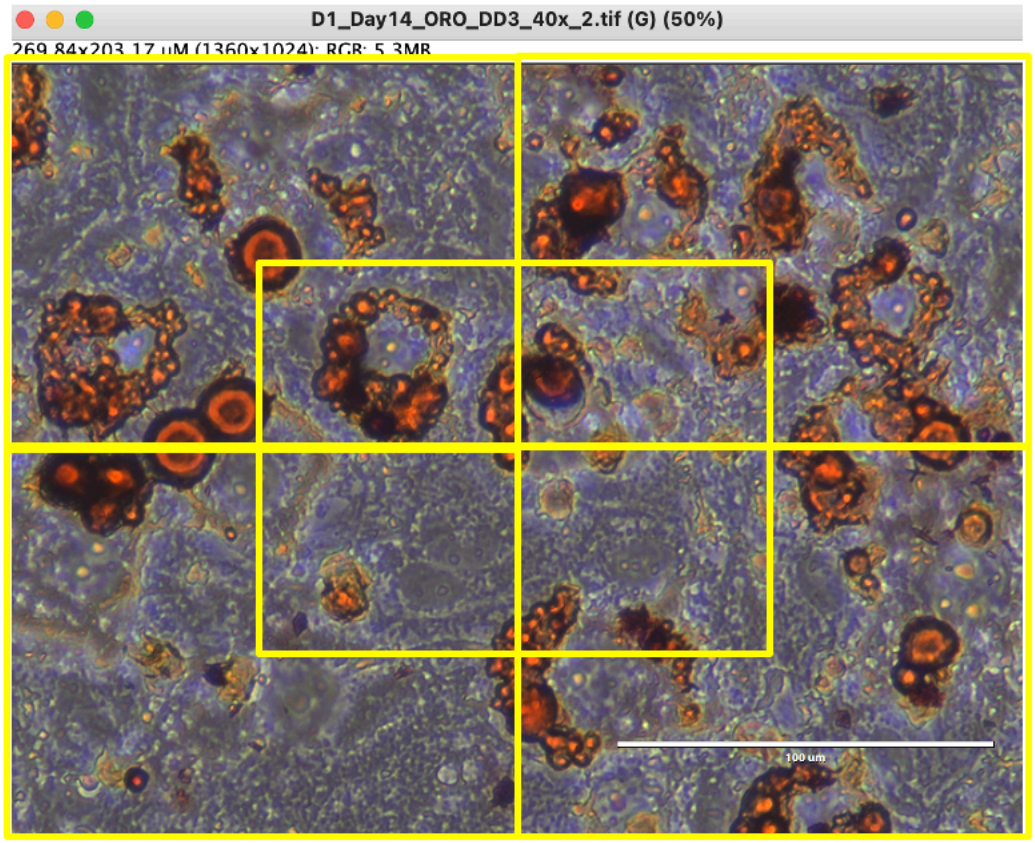

Figure 3.1 ImageJ analysis of ORO stained image. The ORO stained image was split into 5 areas for randomization in lipid droplet area measurement collection.

3.2.5 Metabolic Activity

The metabolic activity of the cell cultures was assessed using AlamarBlue® (Pierce Biotechnology, Rockford, IL, USA). At each timepoint, 10% v/v of AlamarBlue® reagent was added to the wells. The culture plate was incubated for 1.5 hours at 37˚C and 5% CO_2. Then, absorbance readings of the samples were measured at 570 nm and 600 nm.

3.2.6 Glucose Uptake

A glucose uptake cell-based assay (Cayman Chemical, Ann Arbor, MI, USA) was used to determine the glucose uptake levels. At each timepoint, the cell cultures were incubated for 30 minutes with 100 μL of glucose-free Dulbecco's Modified Eagle's Medium (DMEM) (Gibco, Waltham, MA, USA). Then 200 μg/mL of fluorescence tagged glucose derivative (2-NBDG) was added to the cultures and incubated for 1.5 hours. The cells were then placed on a rocker for 5 minutes. Then the media was aspirated and replaced with 200 μL of glucose buffer. The plate was placed on a rocker for 5 minutes and the buffer was aspirated again. 100 μL of glucose buffer was added to the cells and fluorescence readings were collected at 485 nm and 535 nm.

3.2.7 Triglycerides

The triglyceride content of the cultures was determined by using a triglyceride liquid stable reagent, Infinity™ (Fisher, Hampton, NH, USA). First, Glycerol standard solutions were prepared according to the sample solutions shown in Table 3.2 and incubated with the Infinity™ reagent in a 1:200 ratio of sample:reagent for 15 minutes in a 96-well plate. The absorbance readings of the samples were recorded at 490 nm using the BioTexCytation|1 Imaging reader (Fisher, Hampton, NH, USA).

Table 3.2 Glycerol standard solutions made by using Glycerol and deionized water.

No.	Glycerol Concentration (μM)	Glycerol Amount (μL)	dd Water (μL)
1	0	0	1050
2	3.125	1.14	1048.59
3	6.25	2.28	1047.72
4	12.5	4.5	1045.5
5	25	9.09	1040.91
6	50	18.3	1031.7
7	100	36.3	1013.7
8	200	72.6	997.4

The cell samples were first washed with PBS and placed in the -80˚C for 10 minutes. Then, the cultures were thawed at 37˚C for 10 minutes. The cycle was repeated twice. Then 1 mL of 1% Triton X-100 (Sigma-Aldrich, St. Louis, MO, USA) was added to each culture and incubated for 30 minutes at room temperature. The wells were scraped and swirled. The solutions with cell debris were transferred to microtubes and centrifuged at 3000 rpm for 10 minutes. 100 μL of each sample was added to a 96-well plate in triplicates along with 100 μL of the Infinity™ triglyceride reagent in a 1:1 sample:reagernt ratio and incubated for 15 minutes at room temperature. The absorbance readings of all samples were also recorded at 490 nM using the BioTexCytation|1 Imaging reader (Fisher, Hampton, NH, USA).

3.2.8 Impedance & Barrier Index

Cell impedance and barrier index data were obtained from the Axion Biosystems Maestro Z impedance-based instrument (Atlanta, GA, USA). The CytoView-Z plate was coated with 50 μL poly-D-lysine and incubated at room temperature for 1 hour. Then, the wells were washed with

50 μL PBS twice. The plate was allowed to dry before adding 100 μL of desired media to the wells and 8 mL sterilized room temperature DI water to the reservoirs of the plate. The plate was docked to the instrument for a Media Only Baseline test. Then the 100 μL cell suspension containing D1 MSCs were seeded to the CytoView-Z plate. The plate was placed in room temperature for 1 hour and then docked to the MaestroZ instrument. After 48 hours, once the cell cultures were confluent, the different media conditions were added to the appropriate group to observe adipogenic differentiation for 12 days.

3.2.9 Statistical Analysis

All statistical analyses were performed using GraphPad Prism (GraphPad Software, Inc., San Diego, CA, USA). Two-way ANOVA was performed followed by Tukey post-tests for multiple comparisons to determine significance between individual sample groups at each timepoint. The significance was set at $p < 0.05$. All the data is expressed as the mean with standard deviation indicated by the error bars.

3.3 Results

3.3.1 Adipogenic Cell Culture

The obese culture was identified to have larger lipid droplets which was seen on Day 14. More specifically, the cultures with 500 μM and 700 μM stearic acid had more droplets compared to the other obese cultures as seen in Figure 3.2. The obese media culture with 500 μM stearic acid shows a large quantity of lipid droplets covering a larger area of the culture, with a few large, unilocular droplets. The culture with 700 μM stearic acid shows a higher quantity of large, unilocular droplets.

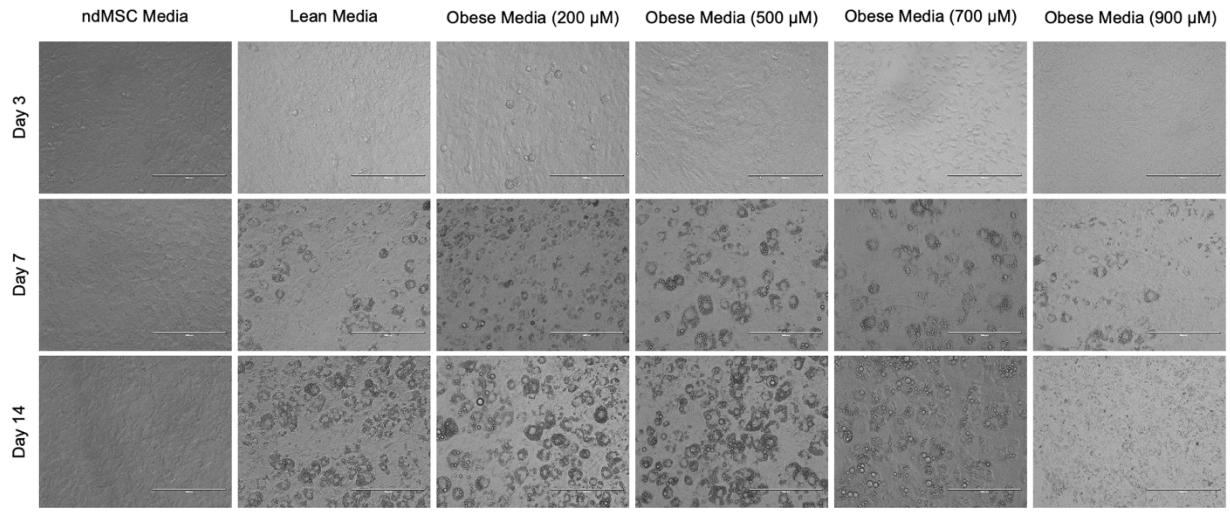

Figure 3.2. Differentiated cultures had clusters of adipocytes over time with the obese cultures having larger, unilocular lipid droplets.

3.3.2 Lipid Droplet Quantification

ORO staining was used to confirm the presence of lipid droplets in the cell culture. As seen in Figure 3.3A, the quantity of lipid droplets in the cultures increased during the 14-day differentiation period. The ORO staining proved the presence of large unilocular droplets in the obese cultures. Over time, the obese media with 700 µM stearic acid had large unilocular lipid droplets by Day 14 compared to the other obese cultures. On the other hand, obese media with 900 µM stearic acid culture looked very similar to the ndMSC media culture.

The destained solutions quantified a higher stain coverage in the lean cultures as seen in Figure 3.3B. Among the obese cultures, the culture with 700 µM stearic acid had a higher coverage proving the presence of larger lipid droplets. On Day 7, the obese culture with 700 µM stearic acid was significantly different ($p < 0.001$) from the lean culture as well. On Day 14, the obese cultures were significantly different ($p < 0.0001$) from the ndMSC media cultures. However, the lean

culture was not as significantly different from the obese media with 700 µM stearic acid, showing a similar coverage of lipid droplets in the culture. Though the 900 µM stearic acid obese media visibly had less droplets, the absorbance was still significantly higher ($p < 0.0001$) than the ndMSC media culture. The ORO solution is known to also stain the exosomes of non-adipogenic cells or pre-adipogenic cells, which could have occurred in the 900 µM stearic acid media [76].

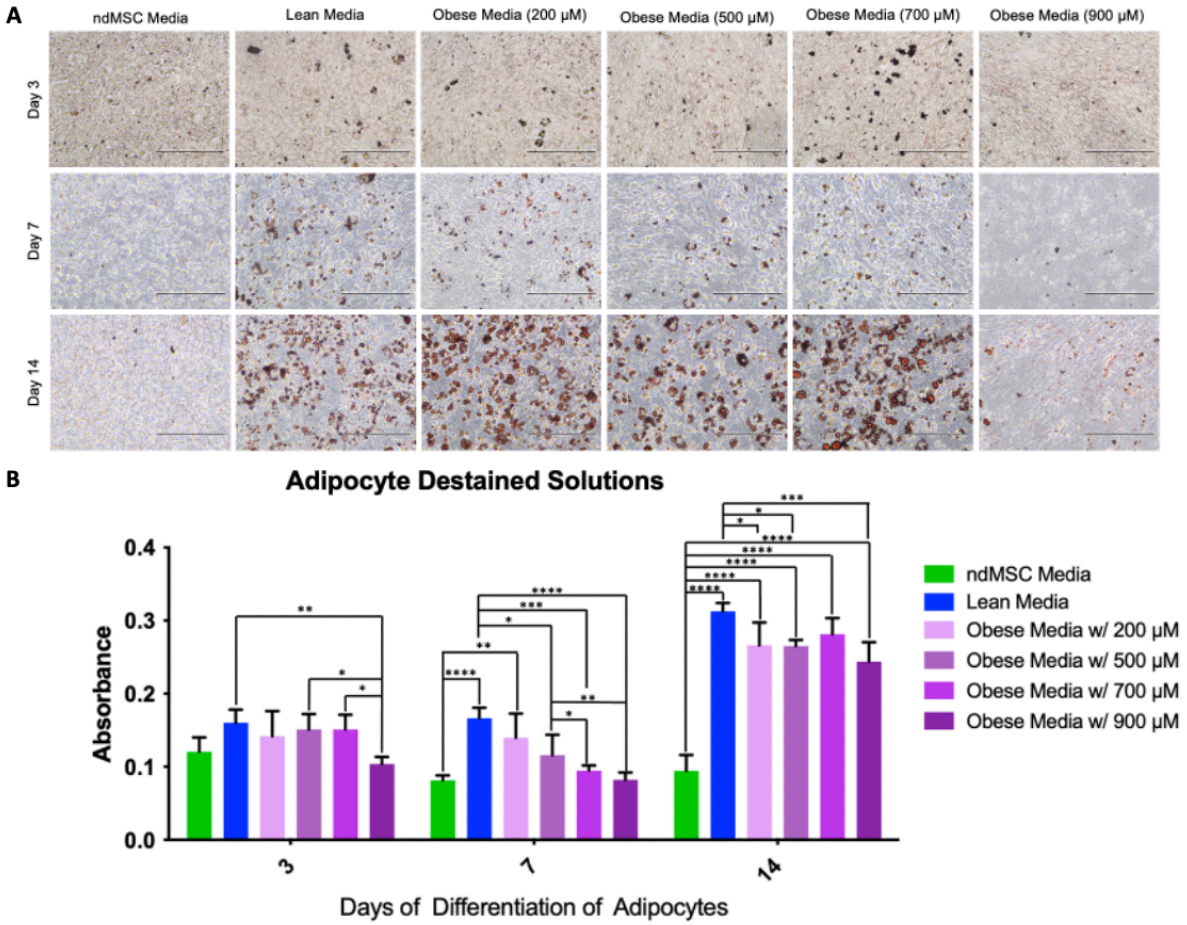

Figure 3.3. Oil Red O staining of lipid droplets to (A) visualize the differences between different culture groups and (B) quantify the red stain coverage of the culture.

3.3.3 Lipid Droplet Hypertrophy

Hypertrophy measurements of the different cultures showed visible lipid droplets in the obese and lean cultures on Day 14 of differentiation. The lean culture had lipid droplets with an average area of 65 μM^2, whereas the obese cultures had lipid droplets over 80 μM^2. Overall, the obese cultures had higher average areas of lipid droplets, with the obese culture with 700µM stearic acid having the highest area as seen in Figure 3.4G. The obese culture with 700µM had lipid droplets with an average area of 145 μM^2 which were signficantly larger ($p < 0.01$) than the lipids in the lean culture. The size of the lipid droplets are visuzally larger and unilocular in the obese cultures as shown in Figure 3.4A-F. Additionally, the culture with 900 µM stearic acid had little to no lipid droplets, visually simular to the ndMSC media cultures as seen in Figure 3.4A and F.

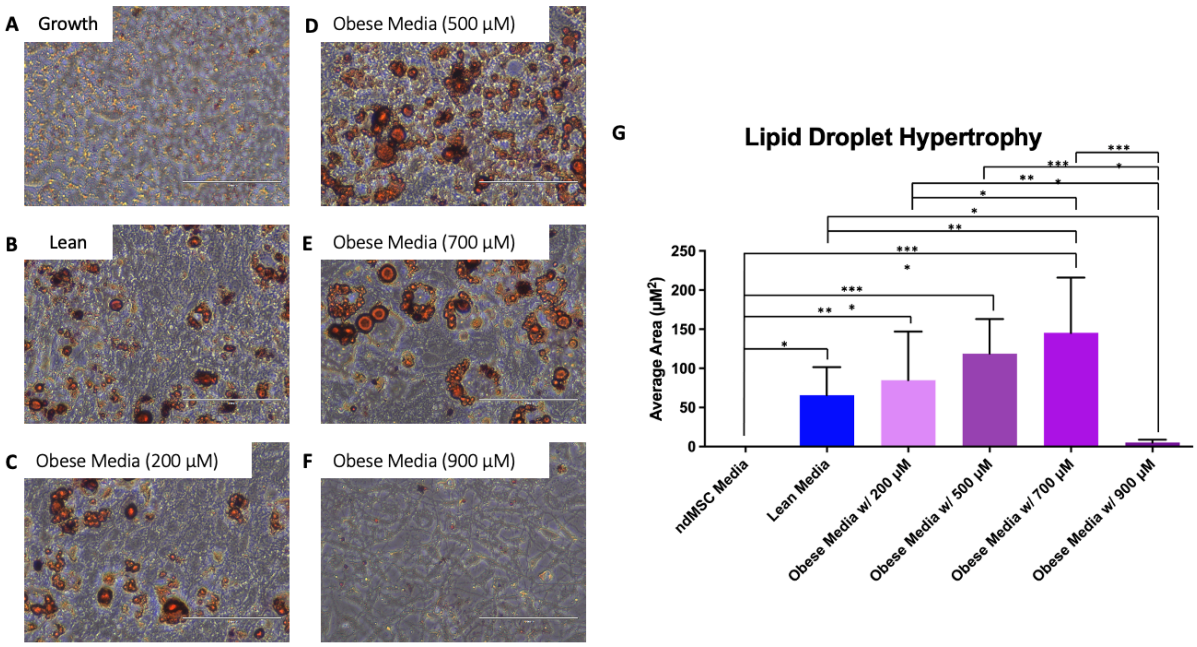

Figure 3.4. ORO stained images of (A) ndMSC media culture, (B) lean media culture, (C) obese media with 200 µM stearic acid, (D) obese media with 500 µM stearic acid, (E) obese media with 700 µM stearic acid and (F) obese media with 900 µM stearic acid used for hypertrophy measurments. The average area of 10 random lipid droplets from each culture is shown in G. Scale bar = 100 µM.

3.3.4 Metabolic Activity

AlamarBlue™ analysis of the obese cultures showed significant differences ($p < 0.001$) over time as shown in Figure 3.5. There was stable metabolic activity for the non-differentiated cells that were no longer proliferating due to reaching confluence. The addition of adipogenic media resulted in decreased metabolic activity in the lean media culture. There was higher metabolic activity observed in the obese cultures, especially on Day 7 and Day 14. More

specifically, on Day 7 and Day 14, the obese culture with 200 µM stearic acid was the most viable ($p < 0.0001$) from the other cultures (Appendix B).

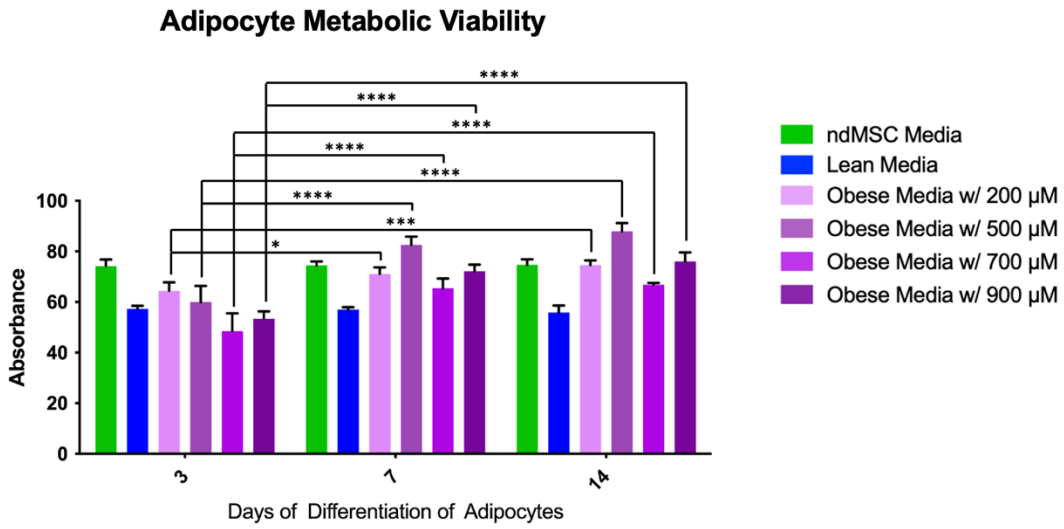

Figure 3.5. Metabolic assessment of lean and obese cultures throughout the 14-day differentiation period.

3.3.5 Glucose Uptake

The relative fluorescence (RFU) measurements are directly proportional to the glucose uptake levels of the cultures. The glucose uptake cell-based assay analysis shows no significant differences amongst the different cultures on day 3, day 7 and day 14 of differentiation. However, the lean and obese culture with 200 µM stearic acid were significantly different ($p < 0.05$) between Day 7 and Day 14. On day 3, the glucose uptake of the ndMSC culture and lean culture were slightly higher than all of the obese cultures. However, on day 7, the obese culture with 200 µM stearic acid was slightly higher than all of the other cultures. The obese cultures with 500 µM, 700 µM and 900 µM stearic acid were still relatively lower than the ndMSC and lean cultures. The analysis on day 14, followed the same trend as day 7, with overall low levels of glucose uptake in

all of the cultures (Figure 3.6). The obese culture with 500 µM, 700 µM and 900 µM had lower fluorescence readings compared to the other cultures, signifying a lower glucose uptake.

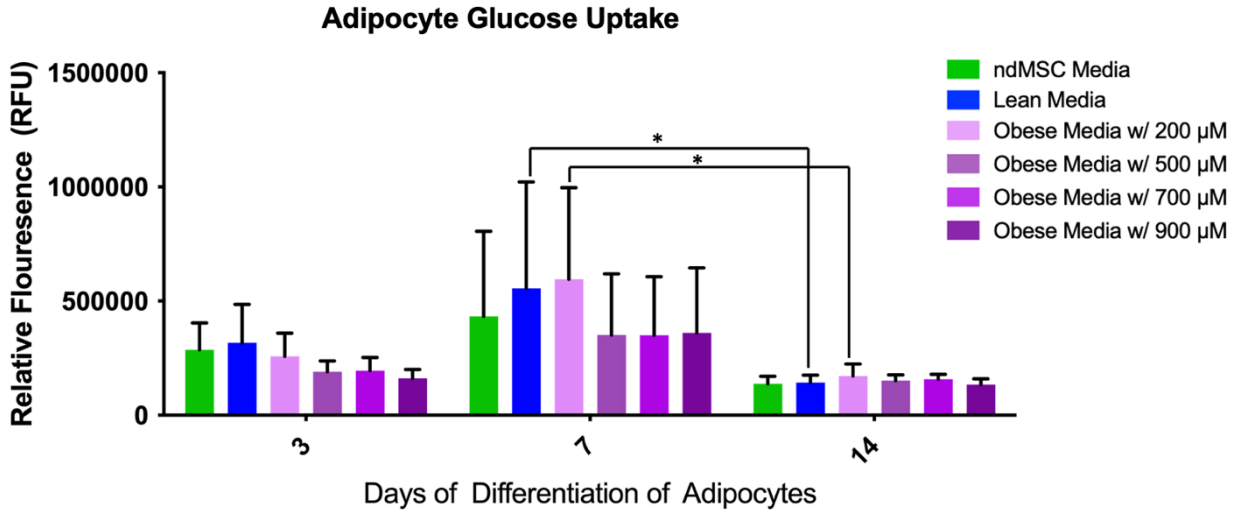

Figure 3.6. Glucose uptake analysis of the different culture groups compared over the 14-day differentiation period.

3.3.6 Triglycerides

The absorbance of the triglyceride analysis is directly correlated to the triglyceride concentrations in the cell culture samples. There were no significant differences among the cultures at each individual timepoint, as shown in Figure 3.7. On Day 3, the ndMSC and lean media cultures had slightly higher triglyceride concentrations compared to the obese cultures but was not significant. By Day 7, there was a slight increase in triglyceride content in the obese cultures compared to the ndMSC and lean media cultures. As the cells became more mature over time, the triglyceride concentrations increased ($p < 0.001$), with the highest triglyceride content observed on Day 14. The obese cultures having slightly higher concentrations compared to the lean and ndMSC groups. Of the obese cultures, the culture with 200 µM stearic acid had the higher concentrations but was not significant when compared to the other obese cultures containing stearic acid.

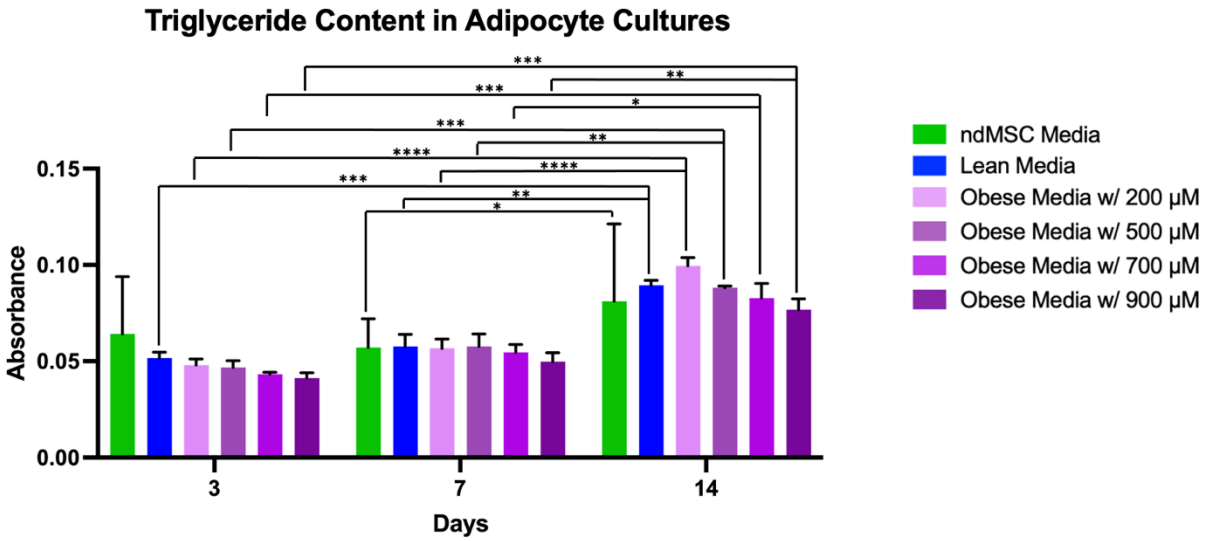

Figure 3.7. Triglyceride measurements of the cultures were directly correlated to the absorbance readings of the cultures. determined from a standard solution curve.

3.3.7 Impedance & Barrier Index

The D1 MSCs were differentiated in the CytoView-Z plates for 7 days which showed higher impedance in the lean cultures than the obese cultures. The obese cultures had relatively same impedance values regardless of the concentration of stearic acid in the media (Figure 3.8A). The ndMSC media culture had negative impedance values after Day 6 of seeding, which could have been due to over confluence in the well plate leading to cell death.

The barrier index readings were derived from the transepithelial electrical resistance (TEER) measurements to assess the small, transient disruptions in barrier permeability. There were low barrier index readings recorded for the obese cultures supporting larger area and signifying the presence of large lipid droplets in the culture (Figure 3.8B). More specifically, the obese culture with 700 μM stearic acid had the lower barrier index readings amongst the obese cultures. The obese cultures have reduced barrier integrity leading to weak barrier permeability compared to the lean and growth media cultures. Thus, resulting in more nutrient flow allowing the fusion of multiple droplets into unilocular lipids in the adipocytes.

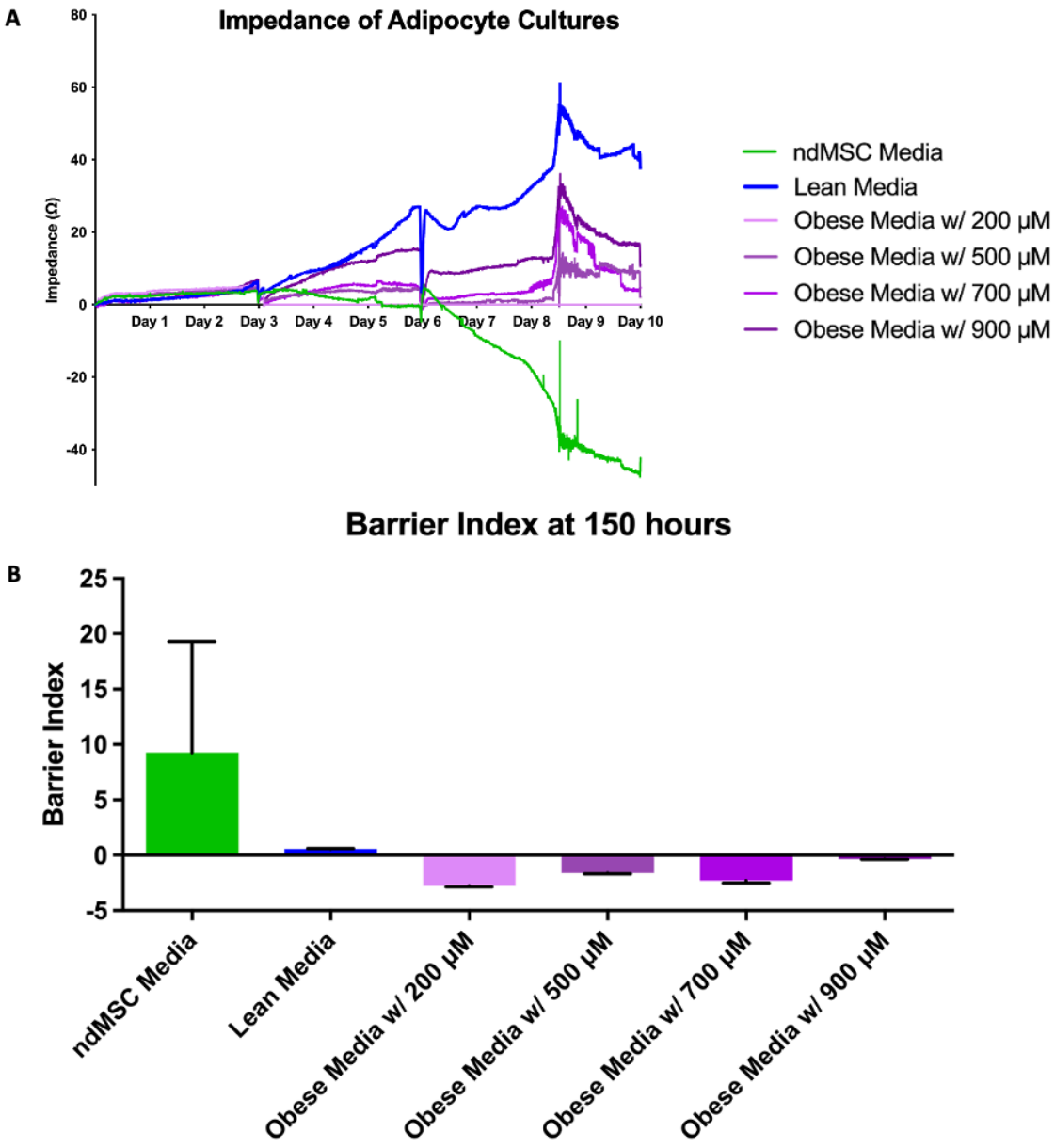

Figure 3.8. MaestroZ instrument analysis of the differentiation process of the D1 MSCs shown as (A) impedance and (B) barrier index.

3.4 Discussion

The adipose tissue plays an important role for various organs in the body, such as the heart, breast tissue, and other muscles [77]. It is an important regulator of homeostasis and other

metabolic functions of the body. Any small changes to the adipose tissue can impact medical conditions like cardiovascular diseases, diabetes, or various types of cancers. In the past, obesity has been closely linked to adipose tissue dysfunction. Obesity is described as an energy surplus in the body causing excess body weight. It primarily occurs due to the imbalance between calorie intake versus expenditure [78]. The imbalance causes excess adiposity and fluctuations in metabolic processes resulting in worse prognosis for heart diseases and breast cancer [78, 79]. Consequently, understanding the changes that occur in the adipose tissue during obesity is vital for evaluating the impact of obesity on other medical conditions.

The purpose of this work was to identify the optimal media formulation to develop an obese culture of adipocytes. It was important to quantify the differences between a lean and obese condition to confirm the right media formulation for obese adipocytes. MSCs are adipocyte precursors and can be used to assess various aspects of adipogenicity [80]. The MSCs were differentiated into lean adipocytes using reagents like Dexamethasone, Rosiglitazone, IBMX, Indomethacin and Insulin, that have been recognized to induce inflammation in cell cultures [81]. These reagents induce adipogenesis and allow the MSCs to adapt adipocyte characteristics primarily seen through the presence of small lipid droplets in the cultures.

Obesity is characterized with a higher fat content, evident through the fast accumulation of lipid droplets, eventually fusing into large unilocular lipid droplets in a cell culture [82]. The obese adipose tissue has elevated levels of fatty acids like stearic acid, oleic acid, and palmitic acid [83, 84]. Therefore, to differentiate MSCs into obese adipocytes, different concentrations of stearic acid, ranging from 200 μM to 900 μM were added to the lean media formulation to observe the differentiation of an obese adipocyte culture.

Throughout the differentiation period, the viability of the cell culture must be maintained as the adipocytes differentiate into a lean and obese condition. AlamarBlue™ is often used as an indicator of cell proliferation and metabolic activity. During proliferation, the actively proliferating cells would exhibit greater metabolic activity due to a high rate of cell division which was seen in the ndMSC cultures. During differentiation, the adipocytes go into a dormant state, where proliferation ceases to undergo adipogenesis. Adipogenic cultures usually show low levels of absorption indicating slow proliferation rates as the cells differentiate [85]. The analysis showed the obese cultures had higher metabolic activity on Day 7 and Day 14 indicating alterations in cell metabolic state of the obese cultures compared to the lean cultures. Additionally, the analysis of the different obese cultures showed significantly low absorbance levels compared to the growth culture, indicating the low proliferation rates. More importantly, the obese culture with 700 µM showed low values amongst the other obese culture, signifying its differentiating capability while maintianing cell viability. Additionally, the lower impedance levels observed in the obese cultures compared to the lean cultures also support the subdued proliferation rates of the obese adipocytes, affirming the differentiation potential of the adipocytes while maintaining cell viabilitiy.

During the differentiation process, previous studies have observed the formation of small lipid droplets over a period of 10-14 days [86]. The adipogenicity of cell cultures was visualized through the presence of lipid droplets in the culture. Many studies have also used ORO staining for better visualization of the lipid droplets [87]. The ORO staining also shows how much of the cell culture is stained, indicating the presence of lipid droplets. Thus, showing the adipogenic potential of the culture. The majority of the obese culture was stained in red compared to the control group, which showed a successful differentiation of adipocytes. Additionally, the

absorbance readings of the destained solutions quantify the amount of lipid in the culture, which showed a higher stain coverage in the 700 μM stearic acid media culture.

One of the biggest visual differences between a lean and an obese adipocyte culture is the size of the lipid droplets. An obese culture has large, unilocular lipid droplets due to the increase in inflammation and formation of lipid droplets [88]. The over accumulation of lipid droplets causes the small lipid droplets to fuse into large droplets, resulting in larger unilocular lipids in the obese cultures compared to the lean cultures. Adipogenic studies have observed the size of lipid droplets ranging from 50 μM to 150 μM [89]. By the end of the differentiation period, the obese cultures had lipid droplets with an average area ranging from 100 μM^2 to 150 μM^2, whereas the lean culture had droplets with an average area near 50 μM^2. Additionally, the low barrier index values support the fusing ability of the lipid droplets in the adipocytes. The barrier index values signify the barrier integrity and permeability of the cells [90]. Therefore, the low barrier index values prove a low integrity of the cells and a weak permeable membrane that allows more nutrients to flow into the adipocytes which essentially turned into fat droplets indicating the fusion of multiple small lipid droplets. The obese cultures had very low barrier index values compared to the ndMSC culture and the lean culture signifying the presence of unilocular lipid droplets in the cultures.

Triglycerides and glucose are two very important molecules that play important roles in the adipose tissue. The adipose tissue regulates systematic glucose metabolism and lipid homeostasis [91]. Some studies have suggested the influence of the adipose tissue led to a better control over glucose metabloism in the body [92]. However, some suggest that the adipose tissue may impair the glucose and lipid metabolism in the body [93]. Thus, making it an important aspect when addressing the differences between lean and obese conditions. The chronic inflammation of

the adipose tissue causes an increase in body fat, interfering the insulin signaling pathway. This inhibits the glucose uptake ability of the adipocytes, characterizing the obese condition with high blood glucose concentrations. Therefore, in obese conditions the adipocytes have impaired glucose uptake, resulting in low glucose uptake levels [94]. Though not significantly different from the lean condition, this phenomena was also observed through the glucose uptake test conducted in this study. The obese culture with 700 μM stearic acid had slightly lower glucose uptake levels than the lean media and ndMSC cultures throughout the differentiation period. Thus resulting in slightly higher glucose levels in the body, impacting the functions of adipocytes in the adipose tissue. This also stimulates the synthesis of fatty acids in the adipose tissue to form triglycerides [95]. Triglycerides serve as a major energy source in the adipose tissue and play a huge role in the metabolic processes of the adipocytes [96]. The bodily functions infleunce the energy levels available in the body. The energy availability and regulation is primarily monitored through triglyceride synthesis and hydrolysis [97]. During obese conditions, the inflammation of the adipose tissue causes a signfiicant increase in triglyceride content on the adipose tissue. The elevated triglyceride levels also influence the levels of adipocyte-secreted factors released into the microenvironment [98]. Thus, making it an imparitive measure to differentiate an obese condition from a lean condition. Over the course of the 14-day differentiation period, the triglyceride concentration increased, which was expected as the cells became more mature. All of the obese cultures had higher triglyceride concentrations comapred to the ndMSC and lean cultures. Of the obese cultures, the culture with 200 μM stearic acid had higher concentrations of triglcyerides, but was not significant when compared to the other cultures grown with stearic acid.

3.5 Conclusion

With this proof-of-concept work, the differentiation of obese adipocytes was successfully demonstrated with the use of stearic acid in the lean media formulation. The different aspects of the obese cultures were targeted proving the presence of large unilocular lipids in culture and the ability of the differentiated culture in maintaining stable viability while exhibiting slow proliferation rates. Additionally, the obese cultures also had low glucose uptake and high triglyceride content compared to the lean and ndMSC cultures. The obese media created with lean media and 700 μM stearic acid clearly showed the different aspects of an obese culture resulting in better differentiation while maintaining the cell viability for an obese adipocyte condition. Thus, making it an ideal formula to evaluate the impact of obese adipocytes on other diseases like breast cancer. The results of the study can be further used for different research aspects of obesity. Future work of this proof-of-concept will entail using the obese adipocytes grown with lean media and 700 μM of stearic acid in a co-culture or conditioned media studies with other diseased cells, like breast cancer cells. Eventually, a full picture about the impact of obesity on medical conditions will help improve the personalization of treatments to help improve disease prognosis and the overall health of patients.

CHAPTER 4

QUANTIFYING THE IMPACT OF LEAN AND OBESE ADIPOCYTES ON BREAST CANCER CELL PROLIFERATION

4.1 Introduction

Breast cancer is the second leading cause of death in woman [99]. It is characterized by three main hormone receptors: estrogen (ER), progesterone (PR) and the human epidermal growth factor receptor type 2 (HER2). The levels of these hormone receptors in the body distinguish breast cancer into specific clinical types, where triple negative breast cancer is known to be the most aggressive type and having the worst prognosis [25]. Regardless of the breast cancer subtype, the composition and progression of the tumor varies at every stage leading to adverse side effects and deterioration in patient health.

About 90% of the breast cancer deaths are due to the metastatic behavior of the tumor [5]. When the tumor enters stage 4 of breast cancer, it becomes metastatic. This is when the tumor spreads to other organs in the body by adapting to the tissue microenvironment [28]. Once the tumor in the breast is large, the tumor cells break away from tumor and enter the body vasculature. The tumor cells circulate to go to target organs like the lung, liver, brain, or bone. Once they identify a target site, they exit the vasculature and adapt to the conditions in the target site to survive and colonize into a new tumor [30]. The spread of the tumor can be mediated by various factors such as tissue properties, the presence of other cells or environmental factors.

Medical conditions like obesity impact the metastatic behavior of breast cancer cells by providing nutrients to support cell proliferation and migration. About 56% of the breast is

composed of adipose tissue that is composed of mature adipocytes [36]. These adipocytes provide energy for homeostasis, secrete cytokines to develop and support the tissue in normal, lean conditions [40]. During obese conditions, the adipocytes tend to swell up due to the accumulation of lipid droplets and look dysfunctional and diseased. This also causes the adipocytes to secrete more inflammatory cytokines and nutrients that allow breast cancer cells grow and metastasize faster [39].

Mature adipocytes secrete several different factors that provide the necessary nutrients to the cancer cells. Factors such as leptin, adiponectin, IL-6, IL-8, and other inflammatory cytokines have known to support the metastatic behavior [40]. Many studies have also shown that the fluctuations in adipocyte secreted factors like leptin have been associated with obesity-associated cancer development as well [46].

Studies have also shown the differences between a lean and obese conditions via adipocyte-secreted factors. However, a majority of these studies focus on one specific adipocyte-secreted factor at a time, rather than the entire adipocyte prolife. For example, researchers have investigated the differences of leptin levels between lean and obese conditions and their impact on other disease progressions like breast cancer [46]. However, it is important to observe the differences of all adipocyte-secreted factors together as they influence each other in normal and obese conditions. The goal of this study is to develop co-culture and conditioned media culture models of adipocytes with various breast cancer subtypes to identify and observe the impact of obesity on breast cancer cell proliferation and migration.

4.2 Materials and Methods

4.2.1 Materials

Murine bone marrow-derived mesenchymal stromal cells (D1) were obtained from the American Type Culture Collection (ATCC, Manassas, VA, USA). MCF-10A cells (fibrocystic disease, ER-, Caucasian donor), MCF-7 cells (adenocarcinoma, ER+/PR+, Caucasian donor), MDA-MB-231 cells (triple-negative breast cancer, ER-/PR-/HER2-, Caucasian donor), HCC-1806 cells (triple-negative breast cancer, ER-/PR-/HER2-, African-American donor) were obtained from the American Type Culture Collection (ATCC, Manassas, VA, USA). Low-glucose (1 g/L) and high-glucose (4.5 g/L) Dulbecco's Modified Eagle's Medium (DMEM), Penicillin-Streptomycin (P/S) and Dulbecco's Phosphate Buffered Saline (PBS, -Ca, -Mg) were purchased from Gibco (Waltham, MA, USA). Fetal Bovine Serum (FBS) was purchased from Atlanta Biologics (Atlanta, GA, USA). Dexamethasone, Indomethacin, Rosiglitazone, Insulin, Isobutyl-1-methlxanthile (IBMX), Stearic Acid, and Bovine Serum Albumin (BSA) were purchased from Sigma-Aldrich (St. Louis, MO, USA). Mammary Epithelial Cell Growth Medium (MEGM) Bullet-kit was purchased from Lonza/Clonetics Corporation (Basal, Switzerland). Cholera toxin from *Vibrio cholerae* was purchased from Sigma-Aldrich (St. Louis, MO, USA). The Axion Biosystems Tray Z impedance-based system (Axion Biosystems, Atlanta, GA, USA) was used.

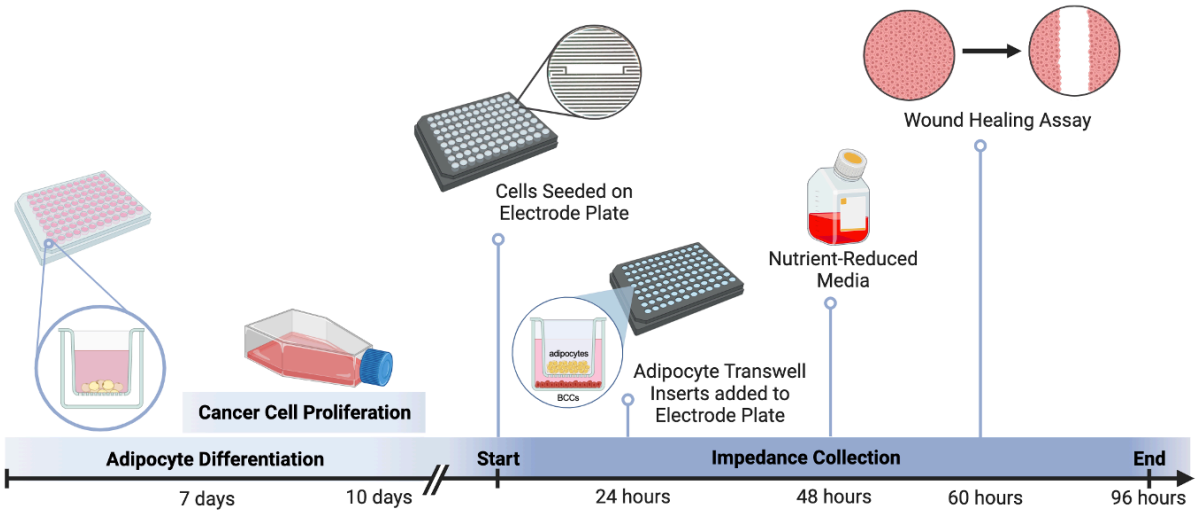

Figure 4.1. Timeline of experiment

4.2.2 Seeding Transwell Inserts

96-well Transwell inserts were purchased from Corning (Corning, NY, USA). D1 MSCs at passage 10 were seeded into the inserts and cultured with DMEM-Complete (Table 4.1). Once the cultures were confluent, the two different adipogenic medias, as shown in Table 4.1, were added to the cultures in replicates of 8. The MSCs were cultured in differentiation media for 10 days as shown in Figure 4.1.

Table 4.1 Media formulations used to differentiate D1 MSCs into lean and obese adipocytes

Media Type	Formulation
Growth Media (DMEM-Complete)	LG DMEM + 10% FBS + 1% P/S
Lean Media	HG DMEM + 10% FBS + 1% P/S + 1% IBMX + 0.1% Insulin + 0.02% Dexamethasone + 10 µM Rosiglitazone + 100 µM Indomethacin
Obese Media	HG DMEM + 10% FBS + 1% P/S + 1% IBMX + 0.1% Insulin + 0.02% Dexamethasone + 10 µM Rosiglitazone + 100 µM Indomethacin + 700 µM Stearic Acid + 1% BSA

4.2.3 Seeding CytoView-Z Plates

The CytoView-Z plates from Axion Biosystems (Atlanta, GA, USA) were used to culture the cancer cells in their respective medias shown in Table 4.2. The plates were coated with 50 μL poly-D-lysine and incubated at room temperature for 1 hour. Then, the wells were washed with 50 μL PBS twice. The plates were allowed to dry before adding 100 μL of desired media to the wells and 8 mL sterilized room temperature DI water to the reservoirs of the plates. The plates were docked to the Tray Z impedance-based instrument (Axion Biosystems, Atlanta, GA, USA), to measure the Media Only Baseline. Then 100 μL cell suspension of each type of cancer cell line was seeded to the CytoView-Z plates. The plates were placed in room temperature for 1 hour before docking it to the Maestro Z instrument.

Table 4.2 Media formulations for cancer cell cultures

Cancer Cell	Culture Media Formulation
HCC-1806	LG DMEM + 10% FBS + 1% P/S
MDA-MB-231	LG DMEM + 10% FBS + 1% P/S
MCF-7	LG DMEM + 10% FBS + 1% P/S + 0.01 mg/mL Insulin
MCF-10A	MEGM + Additives (excluding gentamycin-amphotericin B mix (GA-1000)) + 100 ng/mL Cholera Toxin

4.2.4 Impedance Analysis

The Cyto-View plates were docked onto the Tray Z to observe the cancer cell growth without any conditions for 24 hours. At the 24-hour mark, the Transwell inserts were added to the Cyto-View plates. The adipocytes would be directly on top of the cancer cells in the Cyto-View plate as shown in Figure 4.2.

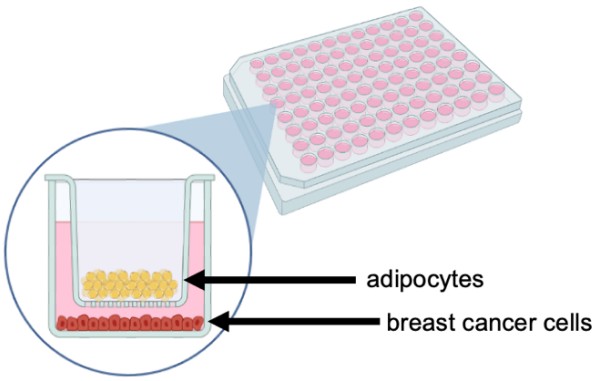

Figure 4.2. Co-culture set-up of breast cancer cells and adipocytes

Additionally, cancer cell cultures were also cultured with conditioned media. At day 10 of adipocyte differentiation, media was collected from adipogenic cultures. The media was centrifuged to avoid cell debris. In the inserts without adipocytes, the conditioned media was added to culture the cancer cells in conditioned media.

4.2.5 Wound Healing Assay

After 48 hours of the co-culture, the cancer cell medias were replaced with nutrient-reduced medias described in Table 4.3.

Table 4.3 Nutrient-reduced media formulations for cancer cell cultures

Cancer Cell	Nutrient-Reduced Media Formulation
HCC-1806	LG DMEM + 2% FBS + 1% P/S
MDA-MB-231	LG DMEM + 2% FBS + 1% P/S
MCF-7	LG DMEM + 2% FBS + 1% P/S
MCF-10A	MEGM

After 12 hours in the nutrient-reduced medias, a wound healing assay was conducted by scratching the cancer cell surface in the CytoView-Z plates by using a multi-channel pipet and applying pressure as the pipet tip interacts with the cancer cell surface. 2 replicates from each treatment group were left unscratched for comparison. The cultures were then observed for 36 hours to assess migration rates of the cancer cells by observing wound closure rates. The wound healing assays are feasible in observing the migration rates of the cancer cells [100, 101].

4.2.6 Secretome Analysis

The adipocyte secreted factors in the lean and culture media were assessed using a Human Cytokine Antibody Array (RayBiotech, Norcross, GA, USA). D1 MSCs were cultured in 6-well plates and differentiated to adipocytes using the lean media and obese media formulations mentioned in Table 4.1. The media samples were collected at three different timepoints mentioned in Table 4.4 and frozen at -80˚C. After all samples were collected, they were sent to RayBiotech for inhouse servicing.

Table 4.4 Sample collection points for each media culture

Lean Media	**Obese Media**
Media Only: No contact with cells	Media Only: No contact with cells
Day 1: 24 hours of contact with cells	Day 1: 24 hours of contact with cells
Day 10: 10 days of differentiation	Day 10: 10 days of differentiation

At RayBiotech, the samples were incubated with an antibody array chip containing different proteins. Then, the array chip was incubated with biotinylated AB and labeled streptavidin, before being read by a chemiluminescence detection device (Figure 4.3).

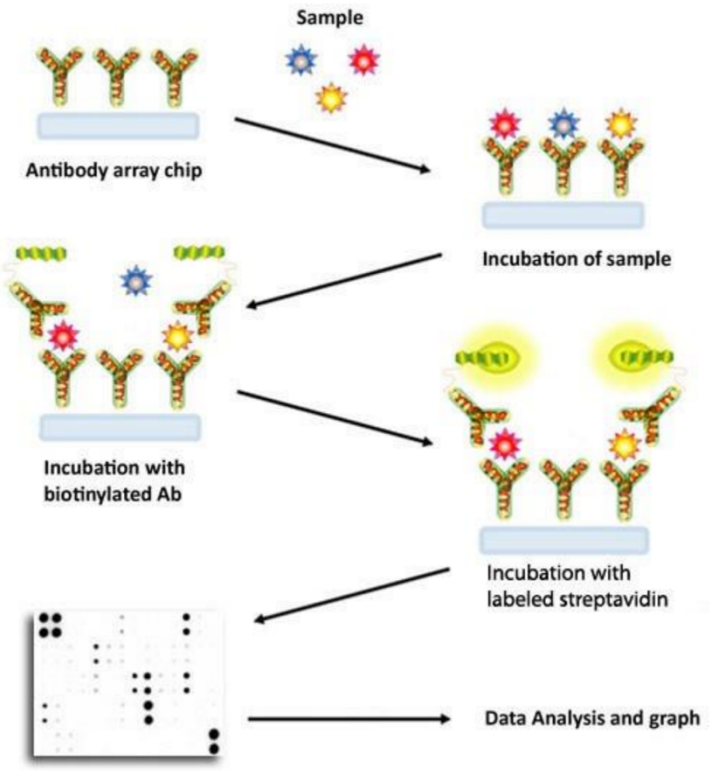

Figure 4.3. Human Cytokine Antibody Array procedure conducted by RayBiotech. *Adapted from RayBiotech AAH-CYT-1000 protocol*.

4.2.7 Statistical Significance

All statistical analyses were performed using GraphPad Prism (GraphPad Software, Inc., San Diego, CA, USA). Two-way ANOVA was performed followed by Tukey post-tests for multiple comparisons to determine significance between individual sample groups at each timepoint. The significance was set at $p < 0.05$. All the data is expressed as the mean with standard deviation indicated by the error bars.

4.3 Results

4.3.1 Secretome Analysis

The secretome analysis was done using the cytokine array which analyzed multiple cytokines using chemiluminescence. The signal intensities from the assay are directly proportional to the concentrations of the cytokine proteins in the media samples. Overall, the analysis of leptin from the human cytokine array showed significantly higher levels ($p < 0.01$) in the obese culture compared to the lean culture as seen in Figure 4.4. From the media only to Day 10, the leptin signals in the lean media and obese media decreased over time. When there was no contact with cells, the obese media had a higher signal closer to 14,000 compared to the lean media, which had a signal close to 10,000 ($p < 0.05$). On Day 10 of differentiation, the leptin signals of the obese media samples were significantly higher ($p < 0.01$) than the signals of the lean media, suggesting higher concentrations in the obese media culture.

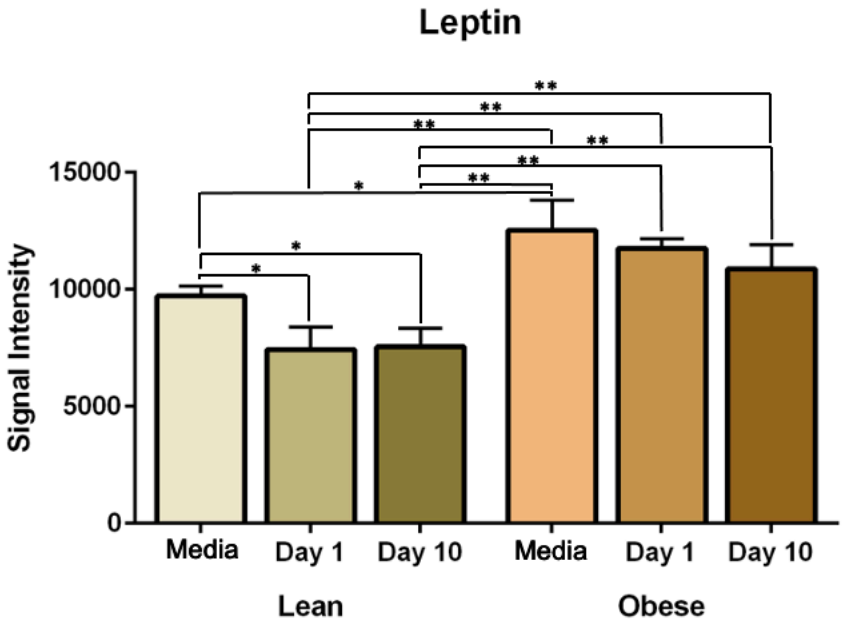

Figure 4.4. Leptin protein signal intensity measured in the lean culture medium and obese culture medium during the adipogenic differentiation period.

Adiponectin is an anti-inflammatory cytokine and should follow the opposite trajectory of the pro-inflammatory cytokines in the obese cultures. The analysis of the adiponectin protein does show a steady decrease in signal intensity in the obese media from the media only to Day 10 of differentiation as seen in Figure 4.5. For the lean media, the adiponectin signals increased from after 24 hours of contact with cells and dropped drastically by Day 10 of differentiation, however, it was not significant. The adiponectin signals of the obese media steadily decreased from the media only to Day 10 of differentiation. When comparing the two medias, the signal intensity of adiponectin is lower in the obese media on Day 1, but slightly higher in the media only and Day 10 of differentiation samples.

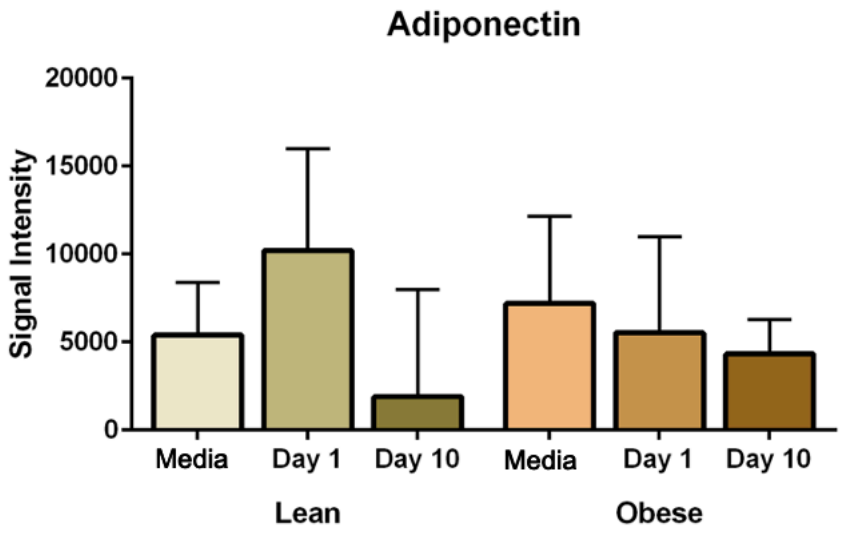

Figure 4.5. Adiponectin signal intensity measured in the lean culture medium and obese culture medium during the adipogenic differentiation period.

The analysis of the pro-inflammatory cytokine IL-6 shows higher signals in the obese media compared to the lean media as seen in Figure 4.6. However, when the media was added to the cells, the IL-6 signals were lower than the media control samples. On Day 1, after 24 hours of contact with the cells, the IL-6 signals were still slightly lower in the lean media compared to the obese media. Most importantly, on Day 10 of differentiation, the IL-6 signals were slightly higher in the lean cultures compared to the obese cultures but were not significant. Overall, the IL-6 signals decreased ($p < 0.001$) throughout the 10-day differentiation period in both media cultures.

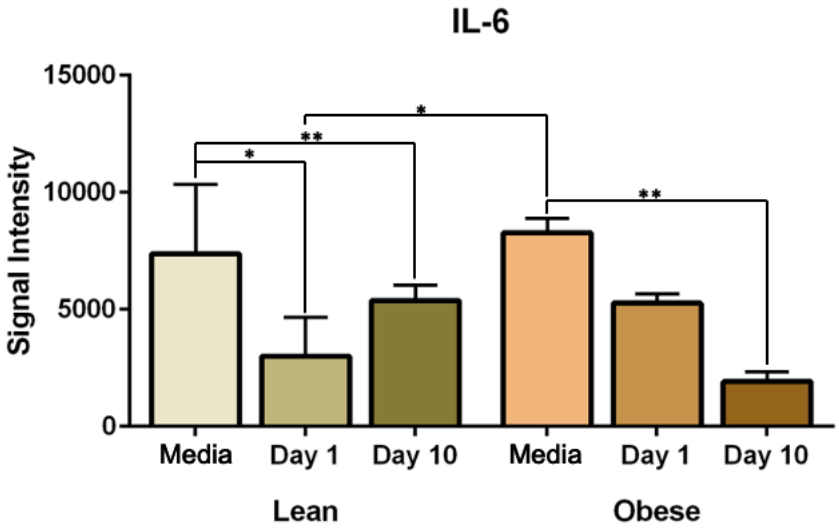

Figure 4.6. IL-6 protein signal intensity measured in the lean culture medium and obese culture medium during the adipogenic differentiation period.

Analysis of the pro-inflammatory cytokine IL-8 were about the same in the lean and obese media samples as seen in Figure 4.7. The IL-8 signals follow the same trajectory in both media samples. The IL-8 signal intensities were around 30,000 in both media only samples. Once the medias were added to the cultures, there was an immediate increase in signal intensity. However, after 10-days of differentiation, the IL-8 levels decreased in both media cultures and were not significantly different. Though the signal intensity of the obese culture on Day 10 was slightly higher than the lean culture, it was not significant.

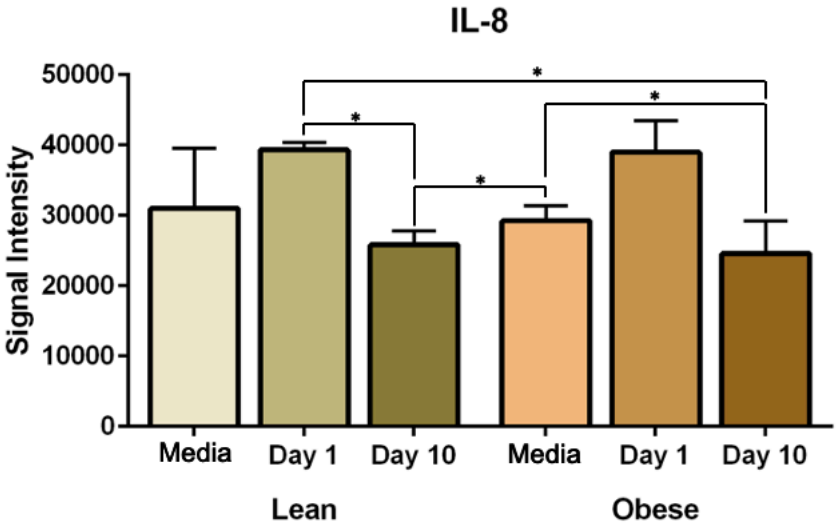

Figure 4.7. IL-8 protein signal intensity measured in the lean culture medium and obese culture medium during the adipogenic differentiation period.

The analysis of the TNF-α protein had higher signals in the obese media samples compared to the lean media samples as seen in Figure 4.8. In the media only samples, the lean media had higher signals compared to the obese media. After 24 hours of contact with the cells, the obese media had a higher signal intensity than the lean media, but it was not significantly different. After 10 days of differentiation, the obese culture had a higher signal intensity at about 7,500 compared to the lean culture, which had a signal intensity at 5,200. Throughout the differentiation period, there was a significant decrease in TNF-α signal intensities in the lean media ($p < 0.01$) and slightly in the obese media ($p < 0.05$). Overall, the TNF-α signal intensities were slightly higher in the obese media than the lean media, though a decrease was observed throughout the 10-day differentiation period.

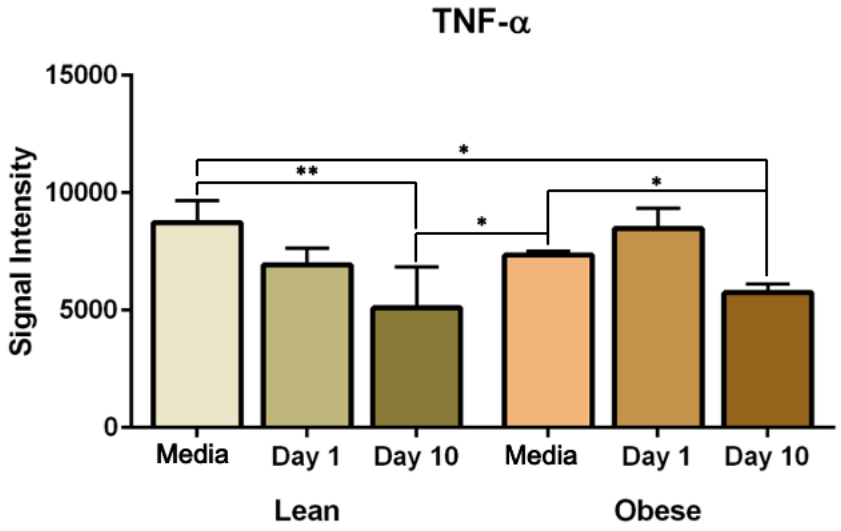

Figure 4.8. TNF-α protein signal intensity measured in the lean culture medium and obese culture medium during the adipogenic differentiation period.

The signal intensities of the TGF-β1 protein were slightly higher in the obese media samples compared to the lean media samples as seen in Figure 4.9. There were higher signal intensities in the media samples compared to the other timepoints. More specifically, the lean media sample had slightly higher levels compared to the obese media samples. After 24 hours of contact with the cells, the same trend followed but with lower signal intensities in both cultures. After 10 days of differentiation, the signal intensity of TGF-β1 in the obese culture was slightly lower compared to the lean media. Overall, the TGF-β1 signal intensities fluctuated through the 10-day differentiation period but were higher in the lean media after the 10 days of differentiation.

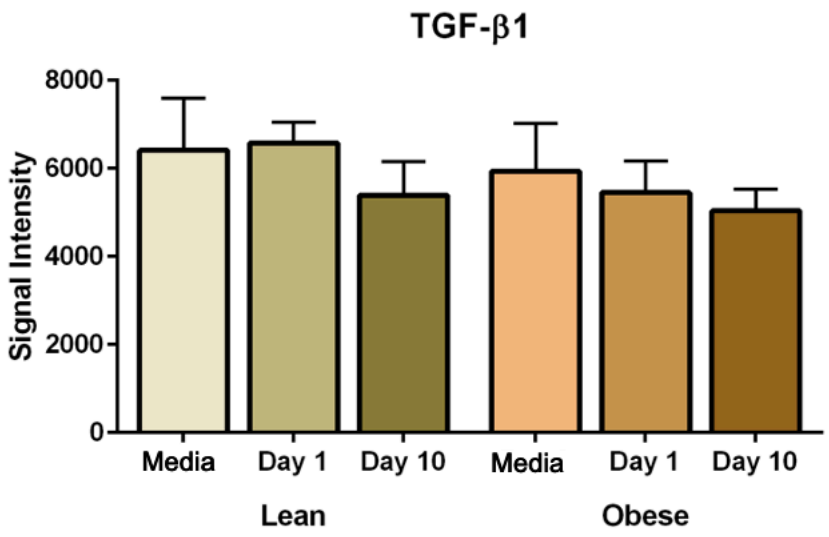

Figure 4.9. TNF-β1 protein signal intensity measured in the lean culture medium and obese culture medium during the adipogenic differentiation period.

The angiopoietin-2 protein signal intensities significantly decreased ($p < 0.05$) throughout the 10-day differentiation period as seen in Figure 4.10. Overall, the signal intensity of angiopoietin-2 were higher in the obese cultures compared to the lean cultures. Prior to any contact with the cells, a signal intensity of about 33,000 was observed in the obese media sample, whereas a signal intensity of about 27,000 was observed in the lean media sample. After 24 hours in contact with the cells, the signal intensity in the lean culture was slightly higher than the obese culture. However, after 10 days of differentiation, the obese culture had slightly higher signal intensities compared to the lean culture. Though there was a significant decrease ($p < 0.05$) in signal intensity of the lean culture from Day 0 to Day 10 of differentiation, the signal intensity initially increased on once the media was added to the cells and drastically decreased ($p < 0.05$) by Day 10 of differentiation. On the other hand, a gradual decrease ($p < 0.05$) in angiopoietin-2 signal intensities were observed in the obese culture throughout the 10-day adipogenic differentiation period.

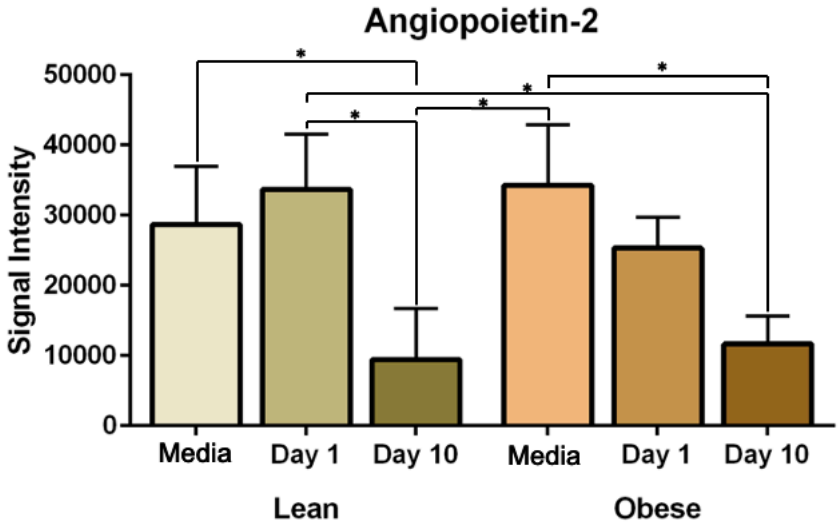

Figure 4.10. Angiopoetin-2 protein signal intensity measured in the lean culture medium and obese culture medium during the adipogenic differentiation period.

4.3.2 Impedance Analysis

The MCF-10A breast immortalized cell line is known to have fast proliferation rate. Prior to any conditions, they exhibited a steady increase reaching an impedance value of 50. Once the different conditions were added to the breast cells, all of the conditioned groups proliferated faster than the MCF-10A control group, between 24-60 hours (Figure 4.12D). As seen in Figure 4.11A, all of the cultures were very confluent. More specifically, the conditioned media and co-culture groups had higher impedance values than the MCF-10A control group as seen in Figure 4.12B. The D1 growth culture and the lean culture were significantly higher ($p < 0.01$) than the MCF-10A control group (Figure 4.12B).

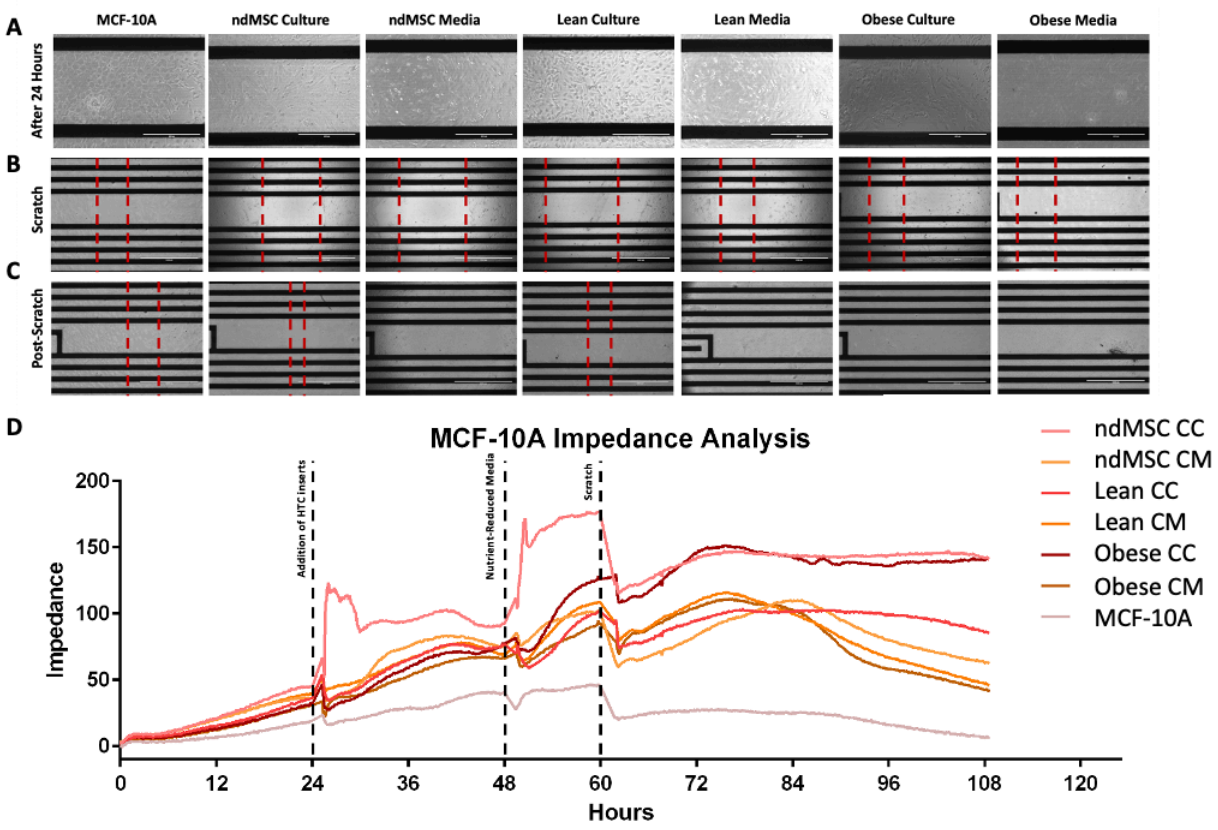

Figure 4.11. MCF-10 benign breast cell line co-culture and conditioned media analysis visualized (A) after 24 hours of seeding, (B) at the induced wound via a scratch and (C) 36 hours after the scratch where (D) the impedance values recorded at real-time for the duration of the study.

At 60 hours, a scratch was induced as seen in Figure 4.11B. After the scratch, there was an immediate increase in impedance values. However, after 12 hours, the impedance values started to decrease and stabilize. The D1 growth culture and obese culture had the highest impedance values from the scratch to the end of the study. After 12 hours from the scratch, the obese culture was the only condition that was significantly higher than the MCF-10A control group (Figure 4.12C). Almost all of the cultures had almost complete wound closures, signified by a wound coverage higher than 1, which was not expected. By the end of the study, all of the culture group

expect the MCF-10A control group had complete wound coverage which is also reflected in the visuals seen in Figure 4.11C. However, towards the end, the growth culture and conditioned growth media were significantly higher ($p < 0.05$) than the MCF-10A control group.

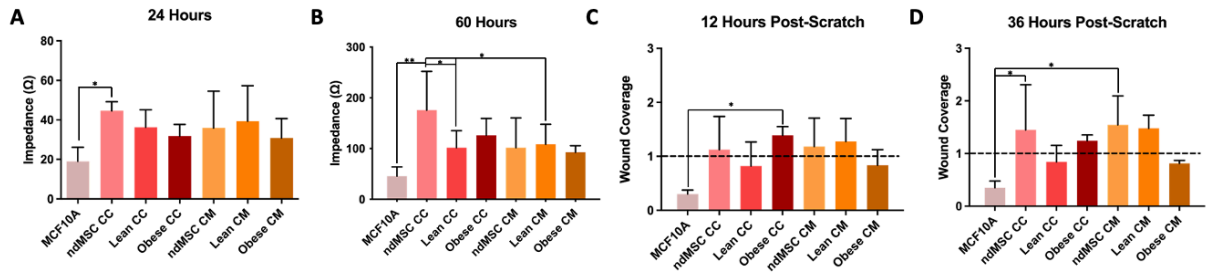

Figure 4.12. Impedance of MCF-10A assessed (A) after 24 hours of seeding, (B) at 60 hours (prior to scratch), (C) at 12 hours post-scratch and (D) at 36 hours post-scratch (end of study).

The MCF-7 breast cancer cell line is known to have slow proliferation and migration rate as it is a luminal-A breast cancer. The impedance values of the cancer cells were between 0-50 prior to any co-culture or conditioned media as seen in Figure 4.13D. Once the different conditions were added to the cancer cells, the impedance gradually increased, which is also reflected by the visual growth of the cells as seen in Figure 4.13A. More specifically, the conditioned media groups had higher impedance values compared to the co-culture of adipocytes. The lean conditioned media group had impedance values similar to the MCF-7 control group (Figure 4.14B). Additionally, a majority of the groups had impedance values significantly lower ($p < 0.0001$) than the MCF-7 control group.

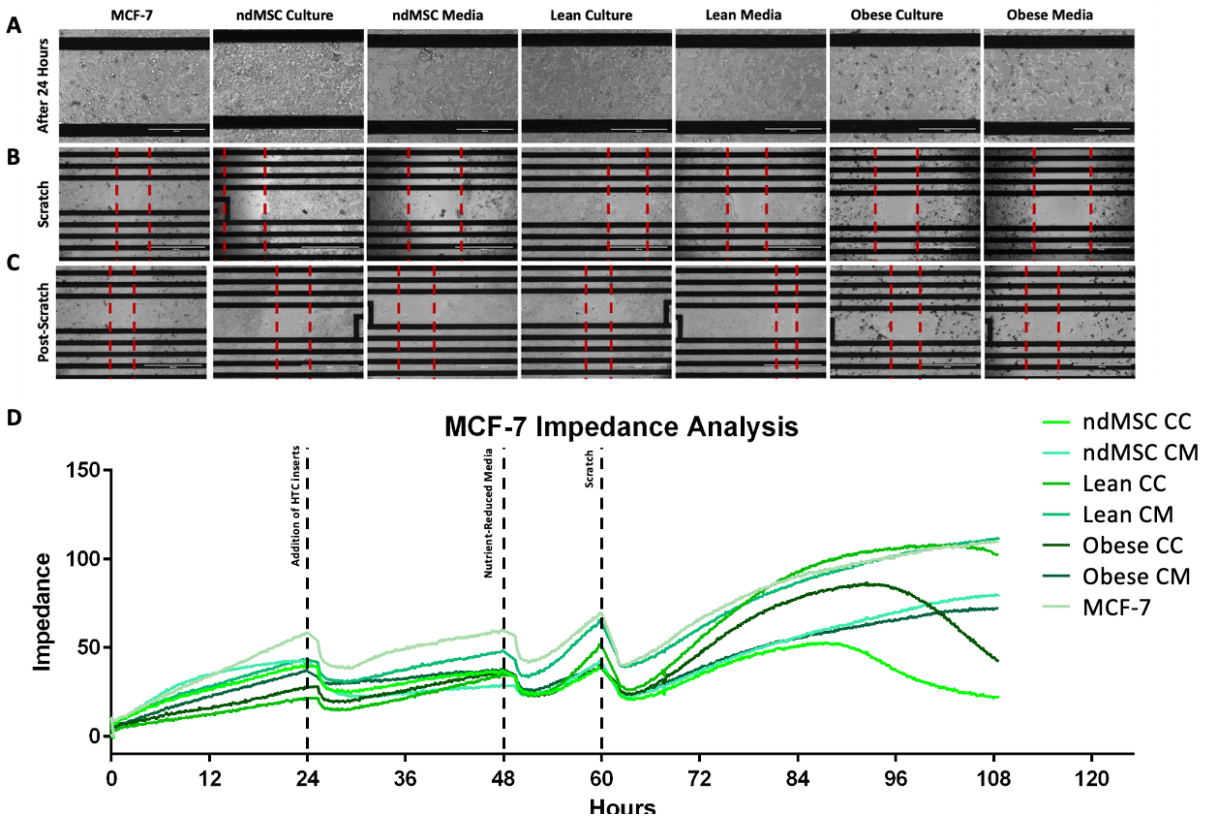

Figure 4.13. MCF-7 breast cancer cell line co-culture and conditioned media analysis visualized (A) after 24 hours of seeding, (B) at the induced wound via a scratch and (C) 36 hours after the scratch where (D) the impedance values recorded at real-time for the duration of the study.

At 60 hours, a scratch was induced to observe the migratory capabilities of the cancer cells in the presence of adipocytes (Figure 4.13B). Immediately after the scratch an exponential increase in impedance values was observed. After 12 hours from the scratch, about 50% of the wound was covered in the majority of the treatment groups, which was significantly different ($p < 0.0001$) compared to the unscratched groups. At the end of the study (96 hours), there was about than 50% wound coverage in all of the conditioned media groups, which is reflected by the smaller wounds as seen in Figure 4.13C as well as the wound coverage being below 1 in Figure 4.14D. The adipocyte co-cultures groups were significantly below unscratched bar ($p < 0.01$)., signified by the

dotted line at 1 (Figure 4.14D). The majority of the wounds were still open as seen in Figure 4.13C. The conditioned media groups exhibited better wound closure than the co-culture groups as seen in Figure 4.14D.

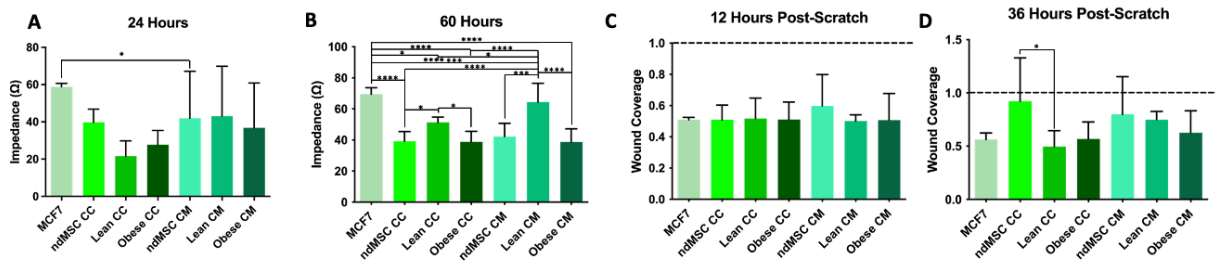

Figure 4.14. Impedance of MCF-7 assessed (A) after 24 hours of seeding, (B) at 60 hours (prior to scratch), (C) at 12 hours post-scratch and (D) at 36 hours post-scratch (end of study).

HCC-1806 breast cancer cells are a triple negative breast cancer, which are known to have fast proliferation and migration rates due to their aggressive behavior. They are more sensitive to the changes in the environment and proliferate faster. As the cancer cells proliferated before any conditions were added, the impedance values were between 0-65 as seen in Figure 4.15D. After the different conditions were added to the cancer cells, there was an immediate decrease in impedance, followed by a gradual increase, which became stable by the 60th hour. The lean and obese cultures had significantly higher ($p < 0.0001$, $p < 0.01$) impedance than the HCC-1806 control group (Figure 4.18B). Additionally, both the lean and obese culture groups had significantly higher ($p < 0.0001$, $p < 0.01$) impedance values than any of the other groups.

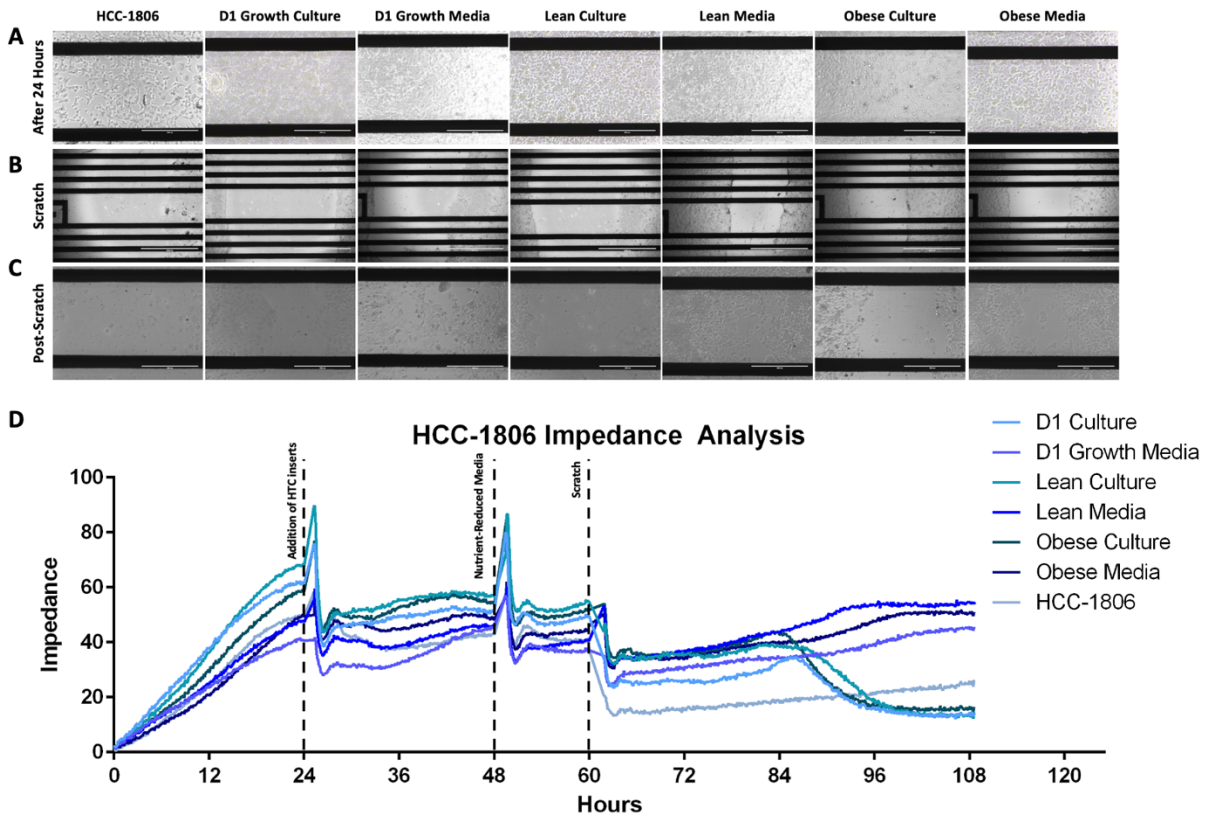

Figure 4.15. HCC-1806 breast cancer cell line co-culture and conditioned media analysis visualized (A) 24 hours after seeding, (B) when a scratch was induced in the culture, and (C) 36 hours after the scratch, where (B) the impedance values were recorded in real-time for the duration of the study.

At 60 hours, a scratch was induced to assess the migratory capabilities of the HCC-1806 cancer cells, which is seen in Figure 4.15B. After the scratch, there was a sharp decrease in impedance, after which the impedance stabilized until the end of the study. In Figure 4.16C, the dotted line signifies the unscratched groups signifying no wound, by which it was deduced that after 12 hours from the scratch, the majority of the groups exhibited about 50% wound closure. However, the HCC-1806 control group was below the 0.5 mark ($p < 0.01$) whereas the lean conditioned media group was slightly above the 1.0 mark, suggesting faster wound closure rates.

By the end of the study, the lean culture and lean conditioned media were the closest to complete wound coverage (Figure 4.18D). The obese culture and obese conditioned media also were close to complete wound overage which was visible as seen in Figure 4.15C. The HCC-1806 control group was still significantly below the unscratched mark at 1.0 and the other treatment groups.

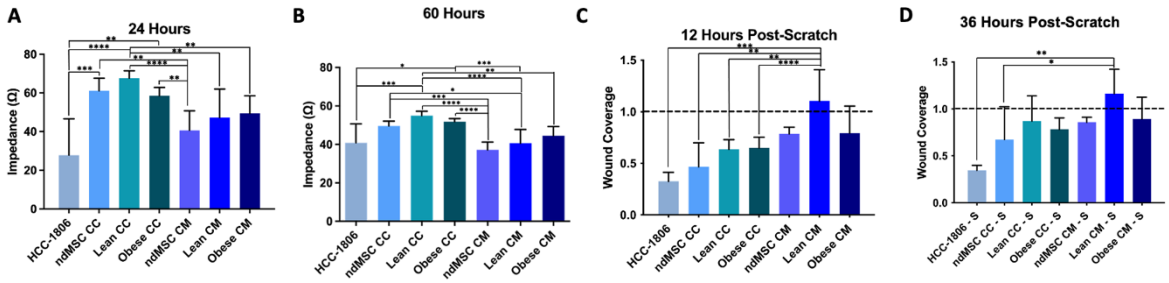

Figure 4.16. Impedance of HCC-1806 assessed (A) after 24 hours of seeding, (B) at 60 hours (prior to scratch), (C) at 12 hours post-scratch and (D) at 36 hours post-scratch (end of study).

The MDA-MB-231 are the other triple negative breast cancer cell line, which also have high proliferation and migration rates due to their aggressive behaviors. Prior to any conditions, the impedance values of the cancer cells steadily increased between 0-8 (Figure 4.17D). After the adipogenic cells and media were added, there was a slight increase in impedance values, which is also visualized in Figure 4.17A. The MDA-MB-231 control group had significantly higher ($p < 0.0001$) impedance values compared to the other groups (Figure 4.18A). Prior to the scratch, at 60 hours, the D1 growth culture had the highest impedance values and was significantly higher ($p < 0.001$) than the other culture groups (Figure 4.18B).

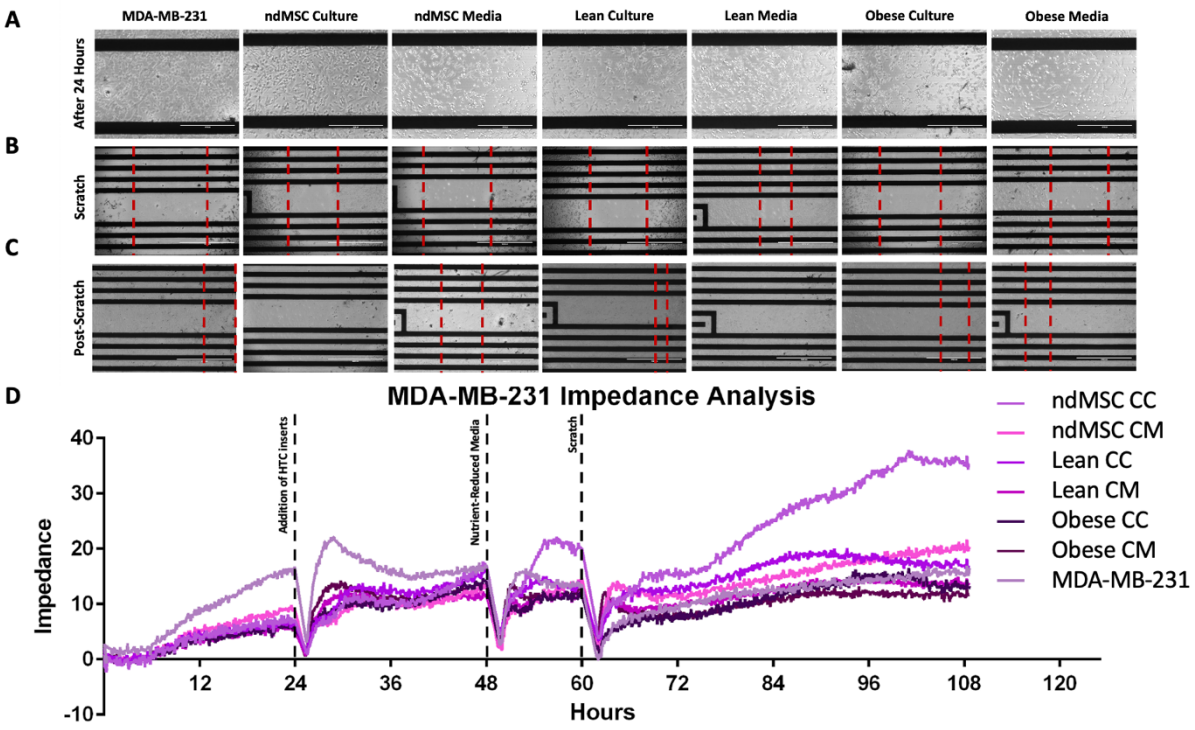

Figure 4.17. MDA-MB-231 breast cancer cell line co-culture and conditioned media analysis visualized (A) 24 hours after seeding, (B) after scratching the culture and (C) 36 hours after the scratch where (D) the impedance values recorded at real-time for the entire duration of the study.

At 60 hours, a scratch was created to observe the migratory capabilities of the cancer cells in the presence of adipocytes, or the conditioned medias as seen in Figure 4.17B. Immediately after the scratch, there was a slight drop in impedance, followed by a gradual increase until the end of the study (Figure 4.17D). The dotted line at 1.0 in Figure 4.18C signifies complete wound closure exhibited by the unscratched groups. About 50% wound closure was observed in the treatment groups after 12 hours from the scratch, while some treatment groups were very close to the 1.0 complete wound closure mark (Figure 4.18C). The obese culture and the obese media group were also significantly lower ($p < 0.001$, $p < 0.0001$) than the unscratched mark compared to the other treatment groups. At the end of the study, all of the groups except the control group had

better wound closure rates (Figure 4.16D). The D1 growth culture, the lean culture and lean conditioned media groups were the closest to complete wound coverage, which is also seen in Figure 4.16D. The obese culture and obese conditioned media were significantly below the complete wound closure mark at 1.0 ($p < 0.001$, $p < 0.01$).

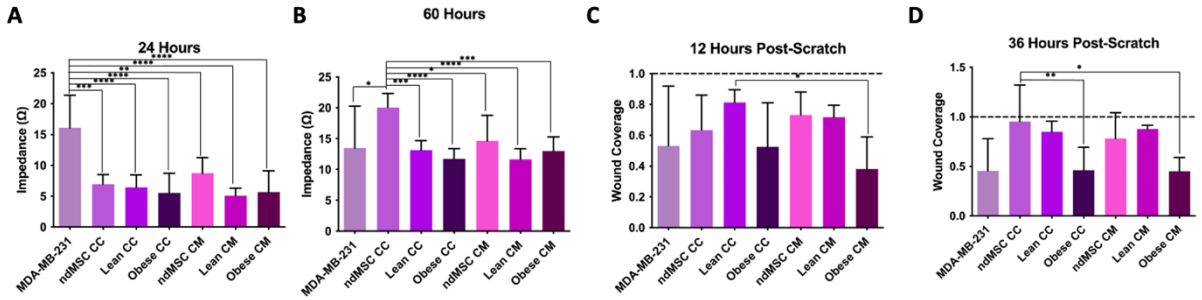

Figure 4.18. Impedance of MDA-MB-231 assessed (A) after 24 hours of seeding, (B) at 60 hours (prior to scratch), (C) at 12 hours post-scratch and (D) at 36 hours post-scratch (end of study).

4.3.3 Barrier Index Analysis

The barrier index measurements based on the trans-epithelial electrical resistance (TEER) measurements were collected to assess the epithelial-to-mesenchymal transition (EMT) of the cancer cells. The low barrier index values signify less tight junctions between the cells which correlate to the epithelial-to-mesenchymal transition of the cancer cells.

The MCF-10A fibrocystic disease cells exhibit epithelial or cobblestone-like structures and are not expected to exhibit cancer cell-like behaviors. 24 hours after the addition of adipogenic cells and medias, there was a slight increase in barrier index values until 36 hours of the study. Then there was a slight decrease in barrier index values observed until the scratch was induced at

60 hours, but not significantly different between the different groups (Figure 4.19A-B). Prior to the scratch, the obese cell and conditioned media cultures had higher barrier index values compared to the lean cultures and the MCF-10A control culture, but not significantly different (Figure 4.19B). After the scratch, increased barrier index values were observed in the MCF-10A control group and was significantly higher than the obese co-cultures ($p < 0.05$). By the end of the study, the barrier index values of the MCF-10A control group were higher than the treatment groups, but was not significantly different. Though not significantly different, the obese cell culture had lower barrier index values compared to the lean cell culture whereas the obese conditioned media culture had higher barrier index values compared to the lean conditioned media culture. Thus, suggesting an slight impact in barrier permeability of the MCF-10A but not significant enough to cause the EMT transition of the fibrocystic disease cells.

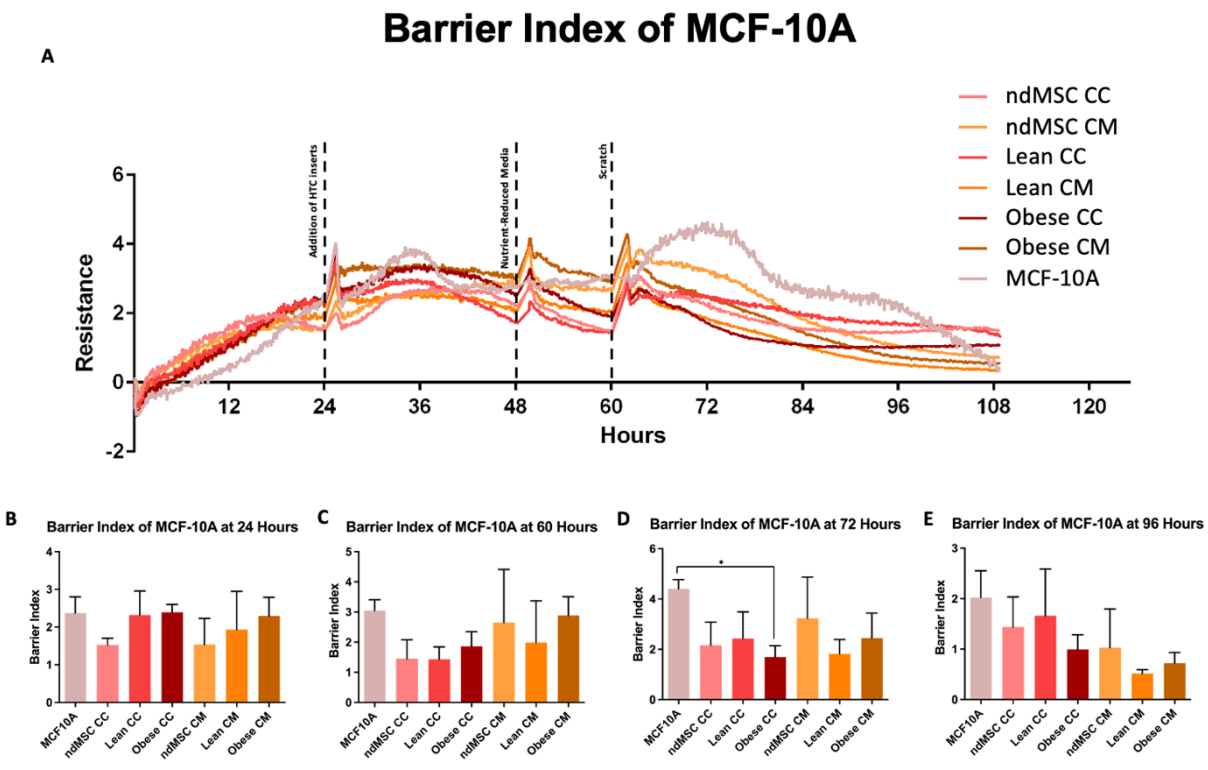

Figure 4.19. The (A) barrier index of the MCF-10A benign breast cell line was observed throughout the study and analyzed at (B) 24 hours, (C) 48 hours, (D) 60 hours, and (E) 72 hours.

The MCF-7 also are more epithelial-like in structure and are known to have a better prognosis. The barrier index values of the cancer cell co-cultures and conditioned media cultures were higher than the MCF-7 control group throughout the duration of the study. After adding the adipogenic cells and conditioned medias to the MCF-7, there was a gradual increase in barrier index values (Figure 4.20A). Prior to the scratch, the barrier index of the treatment groups showed slightly higher values compared to the MCF-7 control groups. More specifically, the obese cells and conditioned medias showed slightly higher values compared to the control group, suggesting no changes in barrier permeability and tight junctions between the cancer cells. After the scratch was induced during the wound healing assay, the barrier index values of the co-cultures and

conditioned media cultures remained higher than the MCF-7 control group suggesting no significant effect in hindering the barrier permeability of the cancer cells. When the cultures were observed 12 hours after the scratch, the lean culture and lean conditioned media groups were significantly ($p < 0.05$, $p < 0.01$) different from the ndMSC culture group (Figure 4.20D). However, closer to hour 96, the values of a majority of the groups started to stabilize at higher barrier index values compared to the MCF-7 control group. The barrier index values were very close in proximity for the different groups, but the conditioned media groups were slightly higher than the co-culture groups suggesting no impact in the cancer cell transition from an epithelial structure to a mesenchymal structure.

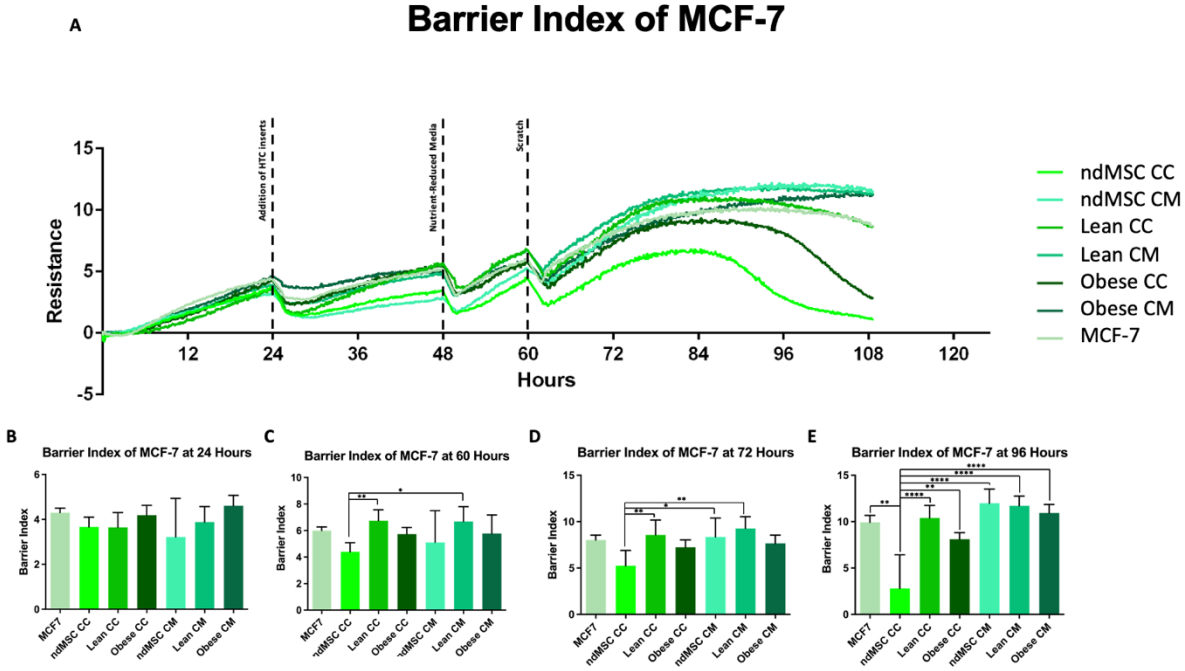

Figure 4.20. The (A) barrier index of the MCF-7 breast cancer cell line was observed throughout the study and analyzed at (B) 24 hours, (C) 48 hours, (D) 60 hours, and (E) 72 hours.

Unlike the MCF-7 cancer cells, the HCC-1806 cancer cells are basal-like structures and are known to have a worse prognosis of cancer. The barrier index values of the HCC-1806 cancer cells were impacted by addition of the adipogenic cell and conditioned media cultures (Figure 4.21A). Prior to the scratch, at 60 hours, the adipogenic conditioned media cultures were slightly higher than the adipogenic cell cultures, more specifically the lean cultures ($p < 0.01$) (Figure 4.21D). Overall, there were low barrier index values observed in the obese cell and conditioned media cultures compared to the lean cultures suggesting an impact on the barrier function of the cancer cells. During the wound healing assay, after 12 hours from the scratch, the HCC-1806 control group had negative barrier index values (Figure 4.21). By the end of the study, there were low barrier index values in the co-cultures and positive values in the conditioned media cultures. The presence of the adipocyte cells impacted the cancer cells more than the conditioned media. Thus, suggesting that the HCC-1806 cancer cells had less tight junctions and were more mesenchymal in structure.

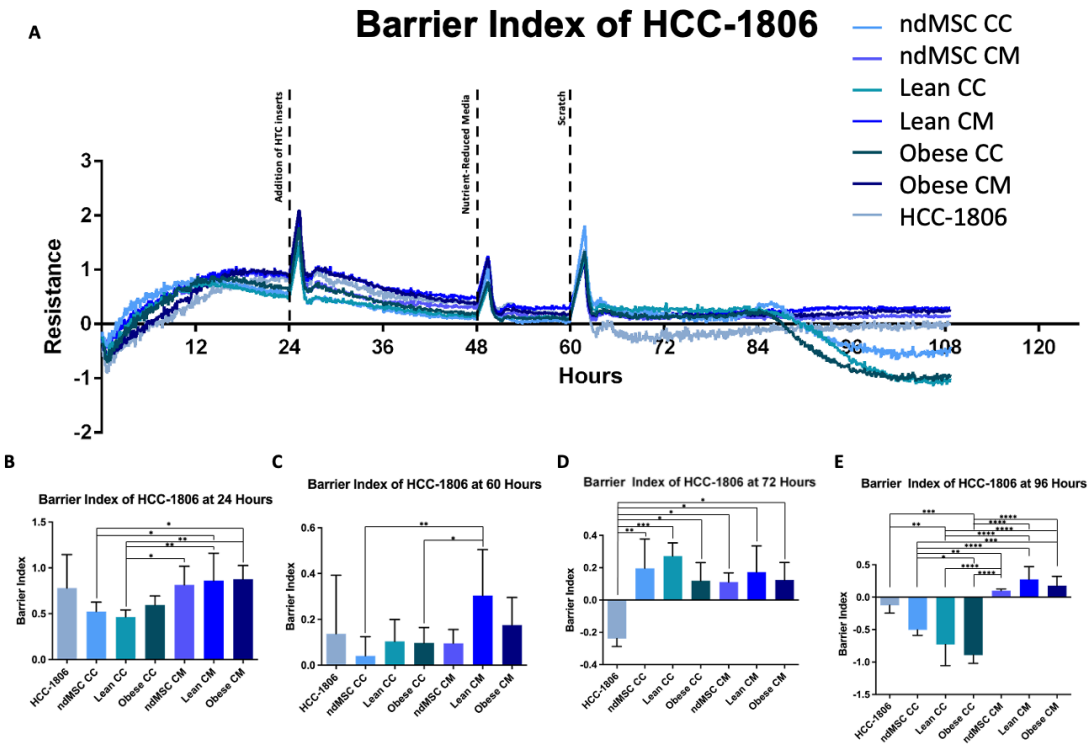

Figure 4.21. The (A) barrier index of the HCC-1806 breast cancer cell line was observed throughout the study and analyzed at (B) 24 hours, (C) 60 hours, (D) 72 hours, and (E) 96 hours.

Though both HCC-1806 and MDA-MB-231 are triple negative breast cancer cell line and exhibit basal-like structures, the MDA-MB-231 cancer cells have more elongated mesenchymal-like appearance compared to the HCC-1806 cells. The barrier index values of the MDA-MB-231 cultures were negative throughout the entire study. The addition of adipogenic cell and conditioned medias initially caused lower barrier index values compared to the MDA-MB-231 control group (Figure 4.22B-C). However, prior to the scratch, the barrier index values were slightly higher ($p < 0.05$) compared to the control group. During the wound healing assay, 12 hours after the scratch the barrier index values of the treatment groups were not significantly different but were slightly lower compared to the MDA-MB-231 control group (Figure 4.22D). By the end of the study, the

barrier index values of the obese cell culture was similar to the MDA-MB-231 control group, whereas the obese conditioned media group was slightly lower than the control group though not significant (Figure 4.22E). This suggests that the MDA-MB-231 are more mesenchymal in structure which is supported by the adipogenic conditions.

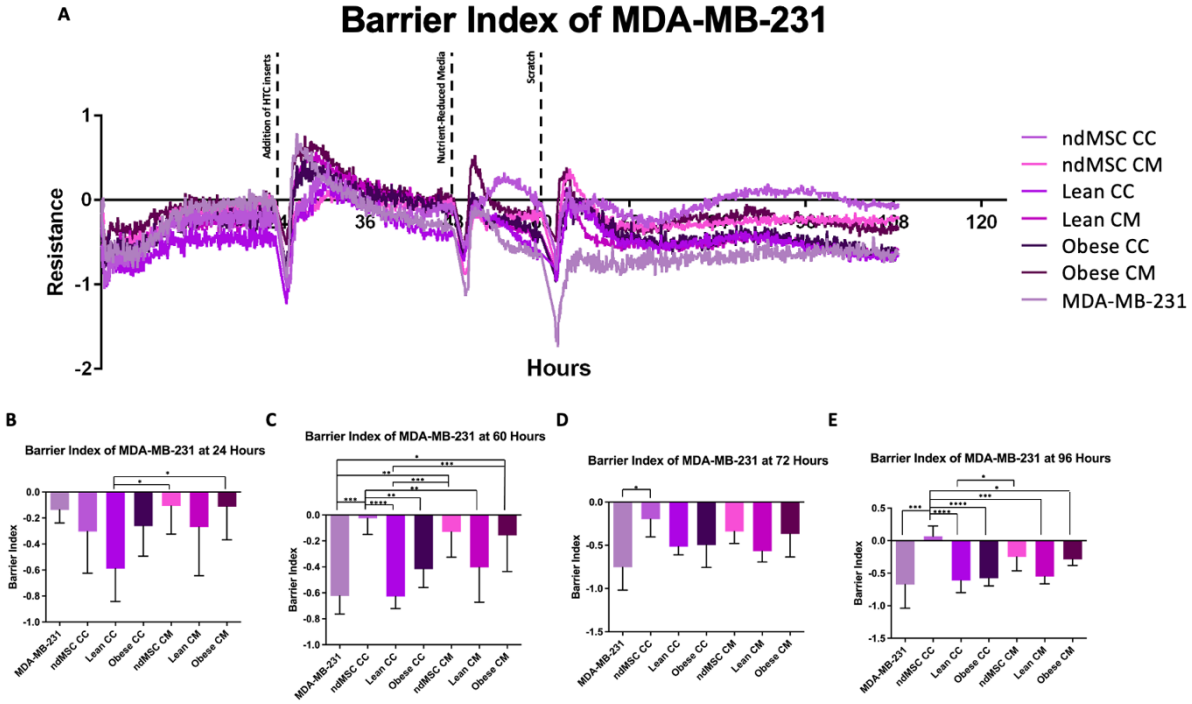

Figure 4.21. The (A) barrier index of the MDA-MB-231 breast cancer cell line was observed throughout the study and analyzed at (B) 24 hours, (C) 60 hours, (D) 72 hours, and (E) 96 hours.

4.4 Discussion

The nutrients in the breast tumor microenvironment significantly impact the tumor progression. The breast is primarily composed of adipose tissue that is a connective tissue comprising of lymphatic vessels, immune cells, and extracellular matrices. Adipocytes are the main type of cells in the adipose tissue and play a crucial role in the breast tumor microenvironment

[15]. Any small changes to the adipocytes or the adipocyte-secreted factors directly impact the estrogen metabolic pathway [55]. Estrogen is one of the main receptors that determines the breast cancer tumor subtype [102]. Likewise, previous studies have also shown enhanced breast cancer cell proliferation and migration due to the presence of adipocytes [40]. Therefore, it is important to understand the adipocyte-breast cancer cell interactions to profile the impact of conditions like obesity on breast cancer metastasis.

The impact of obese adipocytes on breast cancer progression slightly varies based on the subtype. The presence of obese adipocytes was observed to heavily impact triple negative breast cancer (TNBC) and lead to a worse prognosis of cancer [103]. The energy imbalance and dysregulated adipokine signaling during obesity promotes tumor progression TNBC [104]. The adipocyte secreted factors in obese conditions also influence the PR expression of the Luminal A breast cancer tumor, enhancing cell proliferation [105]. However, the impact of the adipocytes is not as severe as TNBC. Overall, as breast cancer originates and develops in an adipose environment, it is important to understand the different factors that influence tumor progression. A model that demonstrates breast cancer progression in the presence of lean and obese conditions will assist in profiling the disease to develop more personalized treatments.

4.4.1 Secretome Analysis

Many studies have shown fluctuations in adipocyte-secreted factors in obese conditions [28, 57]. To achieve the goal this study, the adipocyte-secreted factors involved in the chronic low-grade inflammation of the adipose tissue and breast cancer tumor progression were closely studied. The lean and obese media from adipogenic cultures were assessed to determine the levels of seven

different inflammatory markers: leptin, adiponectin, IL-6, IL-8, TNF-α, TGF-β1, and angiopoietin-2.

Leptin is a hormone released by the adipose tissue to regulate energy balance by inhibiting hunger and reducing the storage of fat in adipocytes [106]. It activates a receptor in the brain to decrease food intake and increase energy expenditure to maintain a balance in the body [107]. During obese conditions, the body becomes resistant to leptin causing irregular activation of the leptin receptor in the brain [108, 109]. Thus, resulting in high levels of leptin in obese adipose tissue [109]. This phenomenon was observed during the 10-day differentiation period in the obese media samples. The high signal intensities correlate to high levels of leptin in the obese cultures on Day 10 compared to the lean cultures. When adipocytes are in the breast cancer tumor microenvironment, they support the migration of cancer cells. Leptin levels also impact the levels of other inflammatory markers further promoting the estrogen metabolic pathway and promoting breast cancer cell activity [43].

Pro-inflammatory cytokines such as IL-6, TGF-β1, IL-8, TNF-α, and angiopoietin-2 are critical in cell-to-cell communication and inflammation in adipocytes. Interleukin-6 (IL-6) is a cytokine known to have pro- and anti-inflammatory effects depending on the context. It plays a role in various immune and hematopoietic processes [110]. In lean conditions, IL-6 is known to aid in B-cell differentiation to produce antibodies and inhibit the growth of diseased cells [111]. However, in obese conditions, IL-6 activates T-cells and macrophages influencing the inflammation of the adipose tissue. Additionally, IL-6 was observed to induce insulin resistance and suppress glucose uptake [112]. Though high levels of IL-6 were present in the obese media compared to the lean media, high levels of IL-6 were not observed throughout the 10-day differentiation period. Obesity-associated alterations to the adipose tissue cause different

fluctuations in the level of secreted factors. This could be due to the complexity of the cytokine or due to the impact of other cytokines that were secreted into the environment.

TGF-β1 is another multifunctional cytokine capable in promoting inflammation, regulating tissue remodeling, and maintaining homeostasis [113]. In normal conditions, it maintains homeostasis, and prevents excess inflammation. However, the excessive levels of other pro-inflammatory cytokines, TGF-β1 converts into a pro-inflammatory cytokine. Advanced stages of obesity cause an increase in TGF-β1 secretion which can further impact other diseased cells in the microenvironment, which was not observed in the study. In breast cancer, it can also promote epithelial to mesenchymal transition (EMT), thus increasing cancer cell motility and metastatic behavior [114].

IL-8 is a chemokine known to signal several inflammatory pathways. It acts as a chemoattractant to recruit and activate neutrophils to the adipose tissue during obese conditions [115]. Studies have observed that the release of IL-8 is supported by the release of TNF-α and IL-β1 [116]. TNF-α is another pro-inflammatory cytokine that is critical in obesity and breast cancer. It initiates lipolysis in adipocytes which directly trigger the inflammatory pathways in adipocytes [117]. Therefore, during obese conditions, high levels of IL-8, which were not observed in the study. High levels of TNF-α are observed in obese conditions which was seen in the study. Additionally, though not a pro-inflammatory cytokine, angopoietin-2 supports the inflammatory response of IL-8 and TNF-α. Obese conditions elevate the levels of angiopoietin-2 secreted into the environment [118]. The elevated levels, as seen in this study, cause a drastic decrease in vascular density and unstable blood vessels. Altogether, the abnormal vasculature and chronic inflammation of the adipose tissue during obese conditions create an adaptable environment for breast cancer tumor progression [118].

Contrary to leptin and pro-inflammatory cytokines, adiponectin is an anti-inflammatory cytokine that regulates insulin sensitivity and inflammation. It also controls glucose levels and plays an important role in cell morphology and hypertrophy [44]. The lipid formation in adipocytes causes high insulin levels. Adiponectin works to maintain the insulin sensitivity in adipocytes by signaling metabolic pathways like MAPK and PPARα [119]. Thus, high levels of adiponectin are observed in normal conditions. As the adipose tissue goes through chronic low-grade inflammation, the leptin and pro-inflammatory cytokine levels increase, which directly inhibit adiponectin transcription [119]. Thus, establishing a negative correlation between adiponectin and obesity which was not clearly established in this study. The low levels of adiponectin pose a risk for breast cancer metastasis as the inhibition of adiponectin can cause the tumor to go through vascular and lymphatic invasion and eventually reach a metastatic level [119].

4.4.2 Evaluating Adipocyte-Breast Cancer Cell Interactions

Adipokines have been observed to mediate the stimulation of cancer cell migration and invasiveness [120]. The secretome analysis proves the presence of adipocyte secreted factors in obese adipocytes and obese conditioned media. Though all of the factors did not fluctuate as expected, there were noticeable differences supporting the influence on the progression of obesity as well as the poor prognosis of breast cancer [121].

The impact of the adipocytes was evaluated on fibrocystic disease cell line, MCF-10A, which showed significantly high proliferation rates in the co-culture and conditioned media cultures [122]. The obese culture had higher impedance values compared to the other co-cultures and the MCF-10A fibrocystic cells. However, the lean conditioned media culture had slightly higher impedance values compared to the obese conditioned media. Thus, suggesting that the

presence of the adipocyte cells having a bigger impact on the growth of breast cells rather than the adipocyte-secreted factors in the media environment. However, the barrier permeability of the MCF-10A was not hindered due to the presence of the adipogenic cells. Thus, proving that the MCF-10A are still epithelial-like in structure even with the adipocytes in the microenvironment. The images obtained from the wound healing assay prove successful wound closures as shown through the results of this study, which was not expected. By the end of the wound healing assay, the obese co-cultures exhibited almost complete wound closure. The presence of adipocyte-secreted factors or adipocytes promotes the prostate derived Ets factor (PDEF), an overexpressed transcription factor in breast cancer [123]. PDEF is also known to enhance cell motility and growth in tumorigenic epithelial cells such as MCF-10A breast cells [124]. However, the MCF-10A are not expected to exhibit high migratory rates as seen in the study. As the adipocytes impacted the MCF-10A cancer cells, the barrier permeability became weaker suggesting a decrease in tight junctions in the cancer cells.

As for the Luminal A breast cancer cells, the MCF-7 cancer cells show low proliferation rates and a better prognosis, and the adipocyte cultures and conditioned medias support the progress of the cancer cell growth [125]. However, the MCF-7 cells exhibited higher impedance based on their epithelial like morphology and their growth patterns. The adipocyte co-cultures cause low impedance or proliferation compared to the MCF-7 cancer cells alone. Compared to the obese cultures, the lean cultures show better impedance values, suggesting better proliferation rates of the MCF-7 cancer cells with lean adipogenic conditions. As the cancer cells were proliferating with the adipogenic conditions, the barrier permeability was not impacted, nor low tight junctions were observed. The MCF-7 were expected to not show high migratory rates, which was clearly exhibited after the scratch was induced during the wound healing assay. By the end of the study,

the wounds of all of the treatment groups were still open suggesting the presence of the different cells or conditioned medias did not have a significant effect on cancer cell migration.

Both triple negative breast cancer cells, the HCC-1806 and MDA-MB-231, are basal-like in structure but the MDA-MB-231 are more elongated and mesenchymal in structure. The HCC-1806 are known to be very sensitive to changes. The adipocyte co-cultures exhibited higher impedance compared to the controls, indicating higher proliferation rates. Thus, suggesting the influence of the adipocyte-secreted factors in promoting the estrogen levels and inflammation of the tissue. The secreted adipokines enhance the EMT markers in TNBC to promote tumor cell proliferation [126]. However, compared to the co-culture of obese adipocytes, the obese conditioned media showed slightly better proliferation rates in the MDA-MB-231 cancer cells. Likewise, the low barrier index values during the proliferation stage suggest that the adipocytes and conditioned medias were impacting the cancer cell transition towards becoming more mesenchymal in structure.

The triple negative breast cancer cells are known to have high migratory capabilities, which would be reflected by a complete wound closure during the wound healing assay. Though the adipocyte and conditioned media groups exhibited better wound closures compared to the control group, there was no complete wound closure in the HCC-1806 and MDA-MB-231 cultures. This could have been due to the interference between the cells, the small sample sizes not reflecting the full potential of the TNBC or the cancer cells going into shock from the nutrient-reduced media or the induced scratch. Though HCC-1806 and MDA-MB-231 are TNBC cells, there were differences in impedance values during the proliferation and migratory stages of the study. The slight changes in morphology between HCC-1806 and MDA-MB-231 cancer cells could have caused differences in the interactions between adipocytes and the cancer cells [127]. Overall,

though the obese adipocytes supported the growth of breast cancer cells, the extent of the impact differed among the different breast cancer subtypes.

4.5 Conclusion

In this study, an adipocyte co-culture and conditioned media cultures were successfully created to show the adipocyte-breast cancer cell interactions. The adipocyte-secreted factors involved in obesity and breast cancer metastasis were identified and compared between lean and obese cultures. The characterized medias were used to create co-cultures and used to culture different breast cancer subtypes. The impedance studies prove that the presence of obese adipocytes impact breast cancer cell proliferation and migration in different extents depending on the subtypes. More importantly, the adipocyte-secreted factors significantly supported the TNBC cells in becoming more mesenchymal in structure compared to the Luminal A breast cancer. The obese adipogenic conditions also caused low barrier index values supporting the transition of the cancer cells from an epithelial-like structure to a mesenchymal-like structure. The study creates a model to identify the impact of obesity on breast cancer metastasis. Future work of this study will focus on developing a 3D *in vitro* model to incorporate environmental aspects and analyzation of adipocytes for cancer-like behavior to better profile the adipocyte-breast cancer cell interactions. A better adipocyte-breast cancer cell model will eventually assist in developing more personalized treatments that account for obesity while curing breast cancer metastasis.

CHAPTER 5

SUMMARY AND RECCOMENDATIONS

Through this work, a successful co-culture model was created using adipocytes and breast cancer cells to evaluate the impact of obesity on breast cancer metastasis. Additionally, conditioned media models of breast cancer cell cultures were also created to further support the understanding of adipocyte-breast cancer cell interactions. Cancer cells of various subtypes were analyzed to observe the impact across different cases of breast cancer under different tumor microenvironment conditions.

The proof-of-concept study work performed in Chapter 3 successfully identified a media formulation to culture obese adipocytes using stearic acid. Various aspects of the adipogenic cell culture were evaluated using assays and analysis techniques to confirm the growth of obese adipocytes and compare them to lean adipocytes. First, the proliferation and differentiation potential of the culture were evaluated by using AlamarBlue™ and impedance analysis, which showed stable metabolic activity and low impedance in the obese cultures. Thus, suggesting the low proliferation rates and of the cells in the obese cultures. Then, Oil Red O staining was done to the cultures to observe the formation of lipid droplets that signify the adipogenicity of the culture. The images taken of the stained culture were used to assess the hypertrophy of the lipid droplets which showed larger sized droplets in the obese cultures. Likewise, the barrier index of the culture supported the hypertrophy results by assessing the barrier integrity of the adipocytes. Lastly, the triglyceride content and glucose uptake levels of the culture were assessed as they are two important aspects of adipocytes. The obese cultures showed high triglyceride contents and

low glucose uptake levels. Overall, all of the assays have supported the growth of obese adipocytes in the cultures with stearic acid. More specifically, the obese culture with 700 μM stearic acid showcased the different aspects with better differentiation proving to be the best media formula to grow obese adipocytes.

The media formulation determined from the proof-of-concept study was used to grow obese adipocytes for a co-culture study conducted in Chapter 4. The first part of the study was to determine the adipocyte-secreted factor levels in the lean and obese adipogenic media. The analysis did show high levels of leptin and some pro-inflammatory cytokines as well as low levels of adiponectin in the obese media, though not significantly different between the lean and obese condition. However, the visible differences between the adipocyte-secreted levels support the obese adipogenicity of the cultures grown in that media. The second part of the study was observing the interactions between breast cancer cells and the adipocytes. Four different breast cancer cell lines of different subtypes were used along with lean and obese adipocytes. Overall, the conditioned media cultures showed better adipocyte-breast cancer cell interactions compared to the co-cultures. The presence of lean and obese adipocytes significantly impacted the proliferation and migration rates of triple negative breast cancer cells (MDA-MB-231 and HCC-1806). The cultures with obese adipocytes or obese conditioned media had higher impedance and low barrier index values compared to the TNBC control cultures. However, the presence of lean and obese adipocytes did not impact the Luminal A breast cancer (MCF-7) proliferation rates as much as the TNBC. Lastly, the adipocytes also made a significant impact on the proliferation and migration rates of the benign breast cells (MCF-10A). The impedance values of the cultures and conditioned media groups were higher than the control group. Thus, proving that the presence of adipocytes supporting the proliferation of breast cancer cells regardless of the subtype. More

specifically, the adipocyte-secreted factors released by the adipocytes during differentiation act as nutrients for the cancer cells to become a larger tumor and lead to the cancer cells becoming more mesenchymal in structure, especially the triple negative breast cancer cells.

Recommendations for the future would be to repeat the glucose uptake assay and triglyceride assay with larger sample sizes. The glucose uptake assay can be conducted with a longer incubation time to allow the fluorescence marker to fully tag the culture prior to adding the glucose buffer solution. Likewise, larger sample sizes for the triglyceride assay can be helpful in using a small sample-to-reagent ratio to better identify the differences in triglyceride content between the cultures.

The co-culture and conditioned media culture studies can be repeated with larger sample sizes and incorporate a proliferation assay to further support the impedance study conducted with the TrayZ. Likewise, the impact of the adipocyte-secreted factors on the cancer cells can be further studied by developing a protocol to add two or more of these factors to the cancer cell growth media. This would provide a better picture about the impact of the adipocyte-secreted factors only, rather than the adipocyte cells themselves. Likewise, the adipocytes should be tested with a specific cancer marker, whether it is a gene or a hormone, to identify the cancerous potential of the adipocytes as well.

This study can also be scaled to a 3D *in vitro* model to better mimic the environment in which the breast cancer cells grow. Different materials can be tested to develop a hydrogel, a scaffold or a microfluidic device to culture adipocytes and breast cancer cells together to observe migratory and proliferative capabilities of the cells. The 3D *in vitro* co-culture model would further support the findings of this study to understand the impact of environmental aspects in addition to adipocytes on breast cancer progression.

Future studies are necessary to improve a breast cancer model that incorporates various factors that could allow the tumor to develop a metastatic behavior. The model would provide a better understanding about the adipose environment in which the breast cancer cells grow as well. The model can also be used to test different breast cancer therapeutics to understand how specific subtypes react to different therapies. It would also allow for better personalized therapies as it would take into account conditions like obesity that impact the adipose tissue of the breast.

APPENDIX

A. ImageJ calibration and procedure to calculate average area of lipid droplets

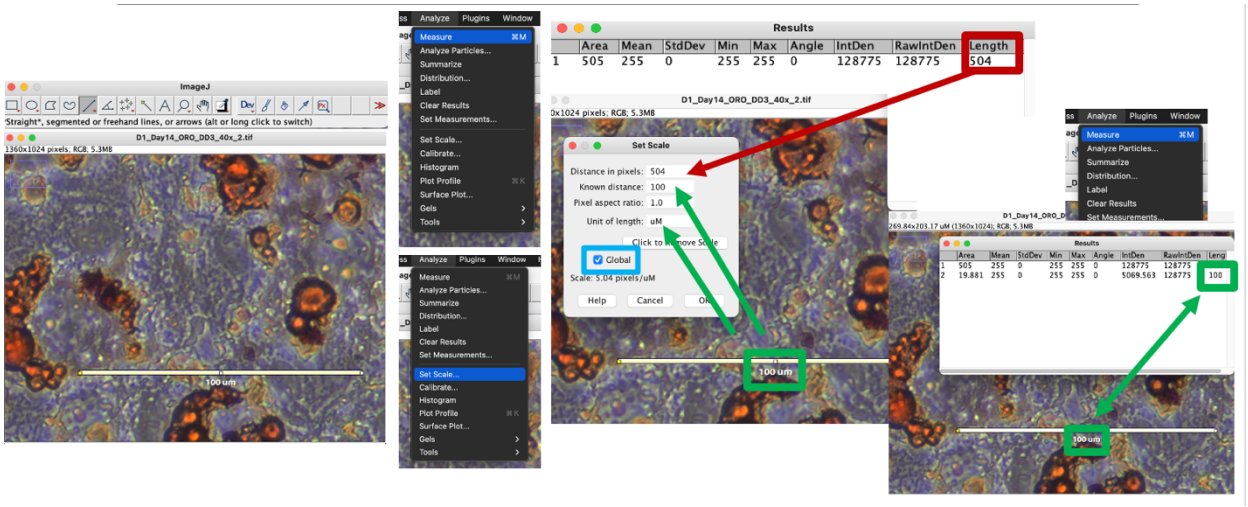

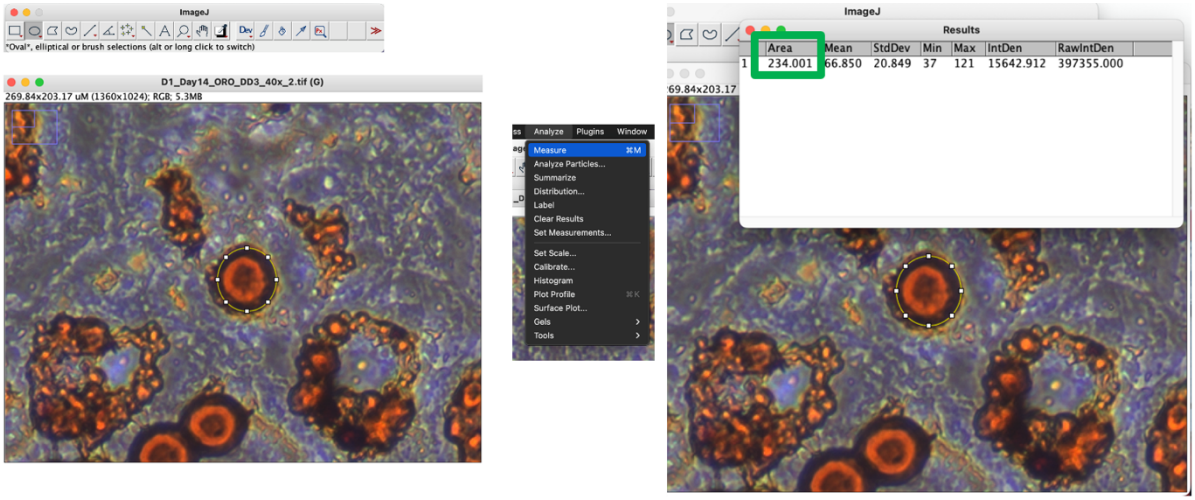

B. AlamarBlue™ Analysis

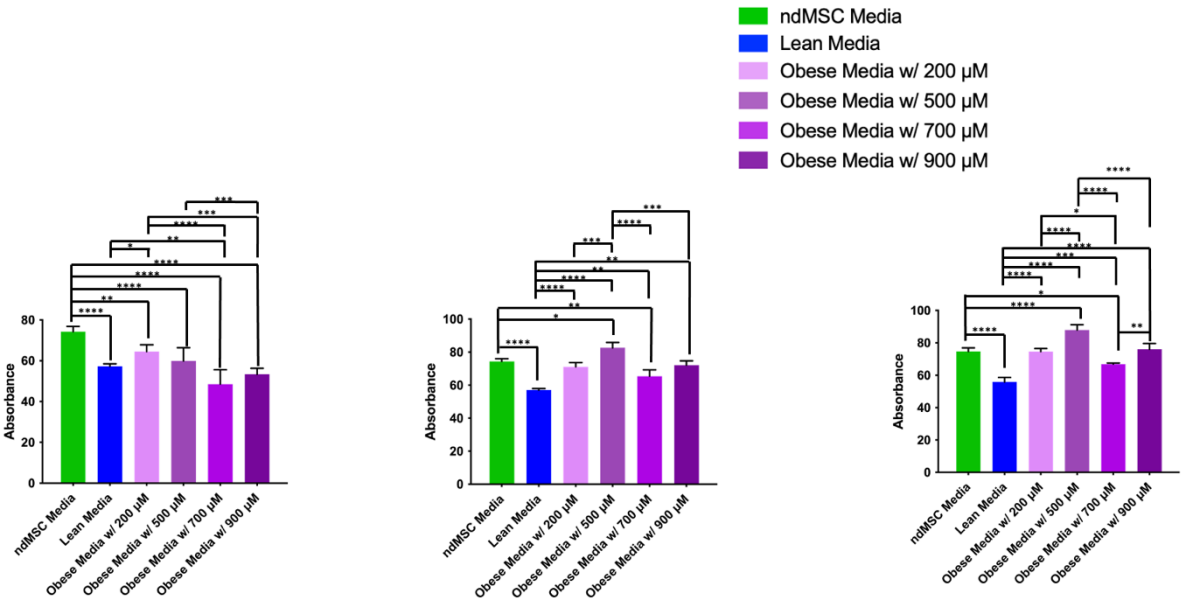

C. MCF-10A Impedance Analysis at (A) 12 hours, (B) 48 hours, and (C) 36 hours of proliferation study as well as (D) 24 hours post-scratch of the migration study.

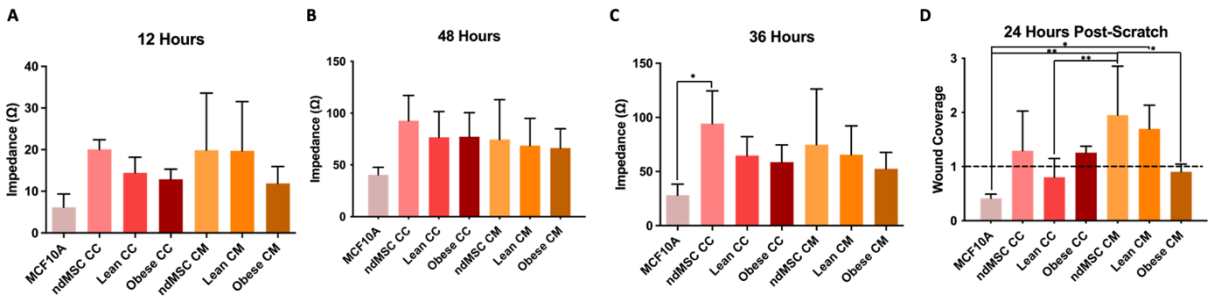

D. MCF-7 Impedance Analysis at (A) 12 hours, (B) 48 hours, and (C) 36 hours of proliferation study as well as (D) 24 hours post-scratch of the migration study.

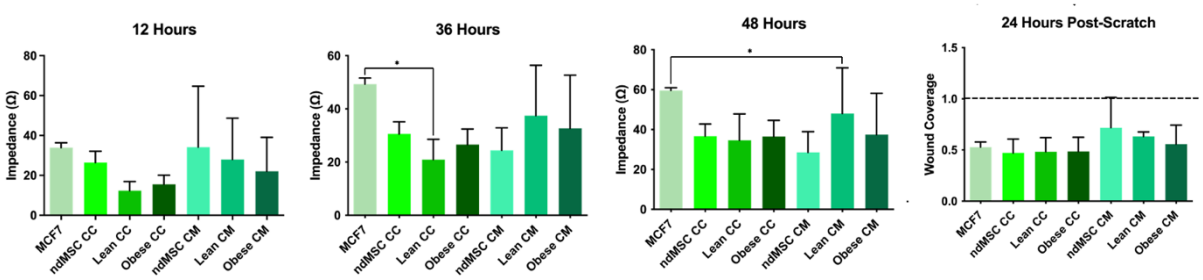

E. HCC-1806 Impedance Analysis at (A) 12 hours, (B) 48 hours, and (C) 36 hours of proliferation study as well as (D) 24 hours post-scratch of the migration study.

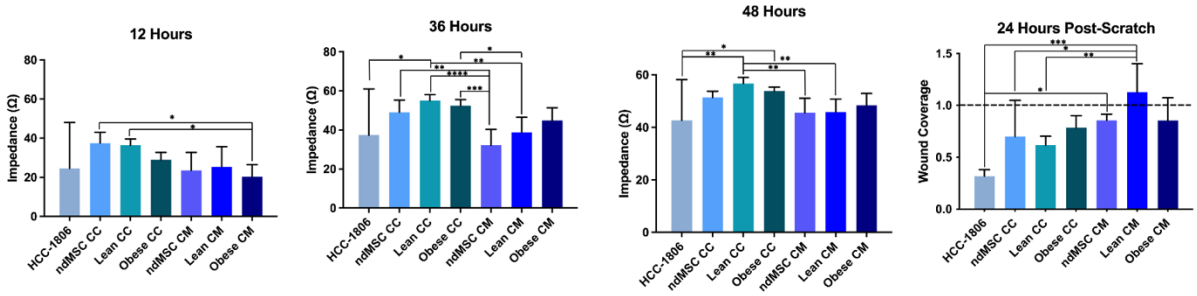

F. MDA- MB-231 Impedance Analysis at (A) 12 hours, (B) 48 hours, and (C) 36 hours of proliferation study as well as (D) 24 hours post-scratch of the migration study.

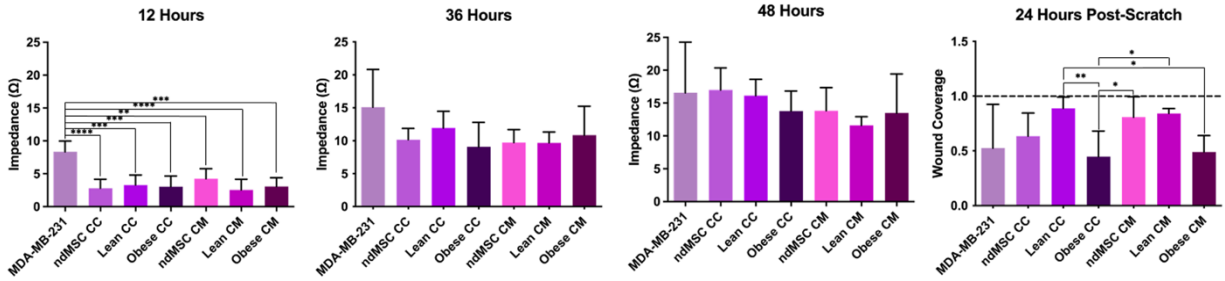

G. Cytokine Analysis raw normalization results from RayBiotech

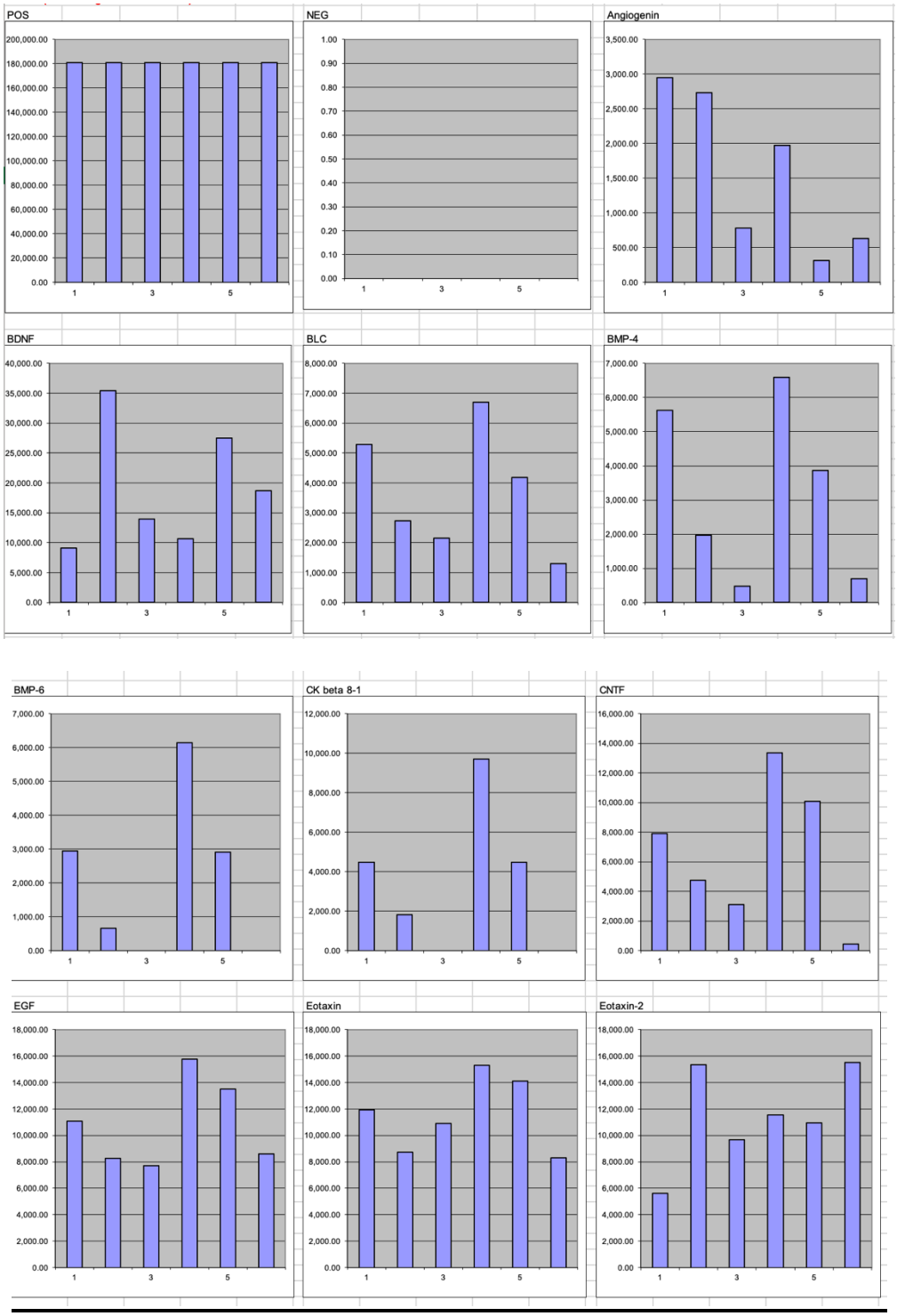

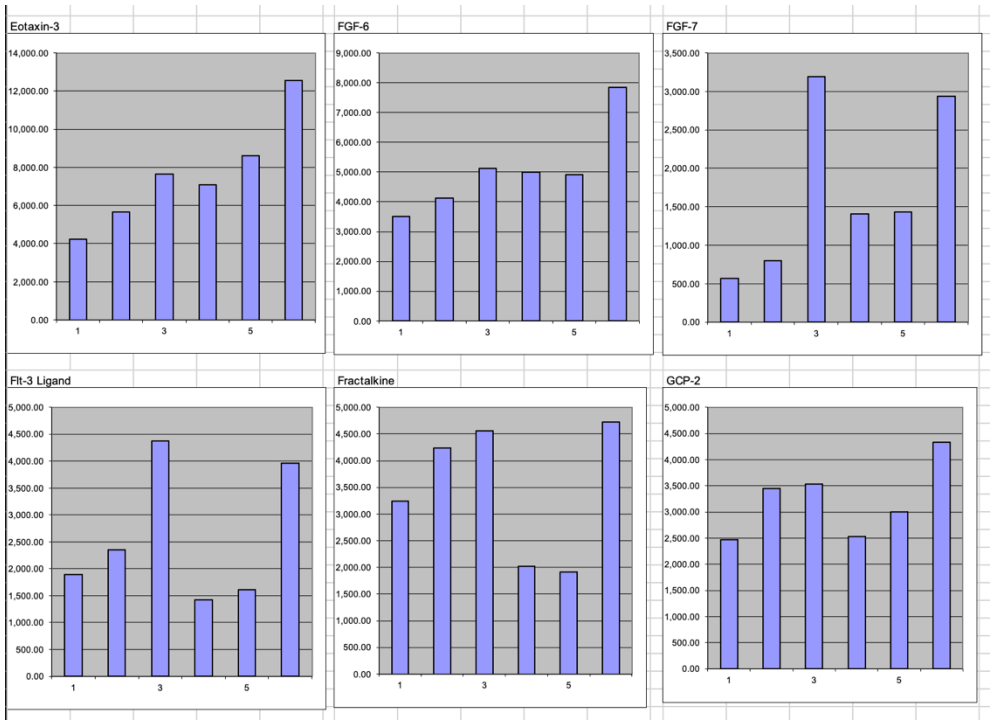
Eotaxin-3
FGF-6
FGF-7
Flt-3 Ligand
Fractalkine
GCP-2

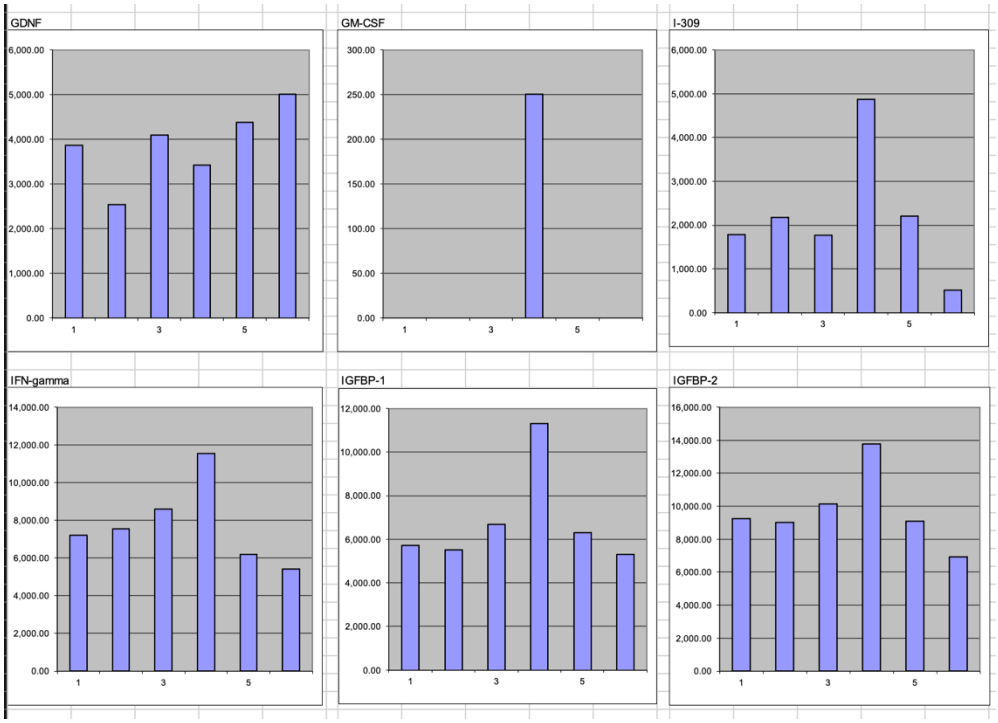
GDNF
GM-CSF
I-309
IFN-gamma
IGFBP-1
IGFBP-2

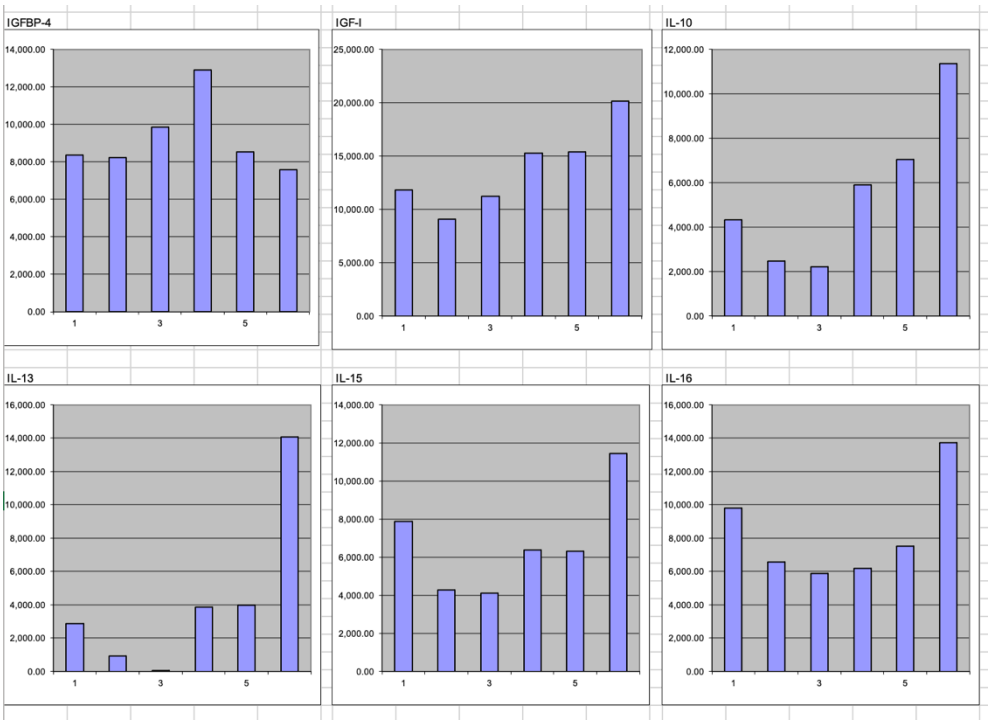
IGFBP-4
14,000.00
12,000.00
10,000.00
8,000.00
6,000.00
4,000.00
2,000.00
0.00
1
3
5
IGF-I
25,000.00
20,000.00
15,000.00
10,000.00
5,000.00
0.00
1
3
5
IL-10
12,000.00
10,000.00
8,000.00
6,000.00
4,000.00
2,000.00
0.00
1
3
5
IL-13
16,000.00
14,000.00
12,000.00
10,000.00
8,000.00
6,000.00
4,000.00
2,000.00
0.00
1
3
5
IL-15
14,000.00
12,000.00
10,000.00
8,000.00
6,000.00
4,000.00
2,000.00
0.00
1
3
5
IL-16
16,000.00
14,000.00
12,000.00
10,000.00
8,000.00
6,000.00
4,000.00
2,000.00
0.00
1
3
5

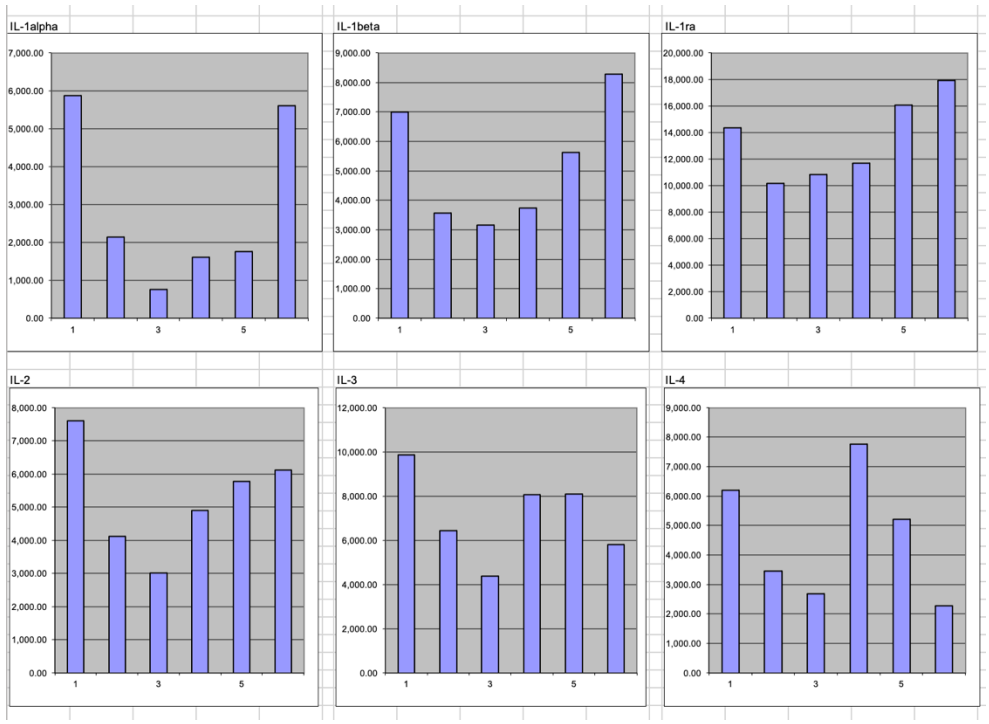
IL-1alpha
7,000.00
6,000.00
5,000.00
4,000.00
3,000.00
2,000.00
1,000.00
0.00
1
3
5
IL-1beta
9,000.00
8,000.00
7,000.00
6,000.00
5,000.00
4,000.00
3,000.00
2,000.00
1,000.00
0.00
1
3
5
IL-1ra
20,000.00
18,000.00
16,000.00
14,000.00
12,000.00
10,000.00
8,000.00
6,000.00
4,000.00
2,000.00
0.00
1
3
5
IL-2
8,000.00
7,000.00
6,000.00
5,000.00
4,000.00
3,000.00
2,000.00
1,000.00
0.00
1
3
5
IL-3
12,000.00
10,000.00
8,000.00
6,000.00
4,000.00
2,000.00
0.00
1
3
5
IL-4
9,000.00
8,000.00
7,000.00
6,000.00
5,000.00
4,000.00
3,000.00
2,000.00
1,000.00
0.00
1
3
5

REFERENCES

1. *Global Cancer Facts & Figures*. Available from: https://www.cancer.org/research/cancer-facts-statistics/global.html#:~:text=According%20to%20estimates%20from%20the,9.5%20million%20cancer%20deaths%20worldwide.
2. *Why men get cancer more than women and how they can manage their risk*. 2022; Available from: https://www.cancercenter.com/community/blog/2022/02/men-and-cancer-risk#:~:text=Men%20have%20a%20one%20in,National%20Cancer%20Institute%20(NCI).
3. *Breast Cancer In Young Women*. Division of Cancer Prevention and Control, Centers for Disease Control and Prevention [cited 2023; Available from: https://www.cdc.gov/cancer/breast/young_women/bringyourbrave/breast_cancer_young_women/index.htm#:~:text=About%201%20in%208%20women,than%2045%20years%20of%20age.
4. *Survival Rates for Breast Cancer*. Available from: https://www.cancer.org/cancer/breast-cancer/understanding-a-breast-cancer-diagnosis/breast-cancer-survival-rates.html.
5. Dillekas, H., M.S. Rogers, and O. Straume, *Are 90% of deaths from cancer caused by metastases?* Cancer Med, 2019. **8**(12): p. 5574-5576.
6. Picon-Ruiz, M., et al., *Obesity and adverse breast cancer risk and outcome: Mechanistic insights and strategies for intervention.* CA Cancer J Clin, 2017. **67**(5): p. 378-397.
7. Blucher, C. and S.C. Stadler, *Obesity and Breast Cancer: Current Insights on the Role of Fatty Acids and Lipid Metabolism in Promoting Breast Cancer Growth and Progression.* Front Endocrinol (Lausanne), 2017. **8**: p. 293.
8. Lukong, K.E., *Understanding breast cancer - The long and winding road.* BBA Clin, 2017. **7**: p. 64-77.
9. Burguin, A., C. Diorio, and F. Durocher, *Breast Cancer Treatments: Updates and New Challenges.* J Pers Med, 2021. **11**(8).
10. Jubelin, C., et al., *Three-dimensional in vitro culture models in oncology research.* Cell Biosci, 2022. **12**(1): p. 155.
11. Chu, D.T., et al., *The Effects of Adipocytes on the Regulation of Breast Cancer in the Tumor Microenvironment: An Update.* Cells, 2019. **8**(8).
12. Harold Ellis, V.M., *Anatomy and physiology of the breast.* Surgery, 2013. **31**(1): p. 11-14.
13. Patrick Mallucci, G.B., *Anatomy and physiology of the breast.* Plastic and reconstructive surgery, 2015: p. 477-485.
14. *Breast Anatomy*. 2020.
15. Kothari, C., C. Diorio, and F. Durocher, *The Importance of Breast Adipose Tissue in Breast Cancer.* Int J Mol Sci, 2020. **21**(16).
16. *What is Menopause?* ; Available from: https://www.nia.nih.gov/health/what-menopause#:~:text=Menopause%20is%20a%20point%20in,between%20ages%2045%20and%2055.

17. Surakasula, A., G.C. Nagarjunapu, and K.V. Raghavaiah, *A comparative study of pre- and post-menopausal breast cancer: Risk factors, presentation, characteristics and management.* J Res Pharm Pract, 2014. **3**(1): p. 12-8.
18. Pillay, J. and T.J. Davis, *Physiology, Lactation*, in *StatPearls*. 2022: Treasure Island (FL).
19. Sriraman, N.K., *The Nuts and Bolts of Breastfeeding: Anatomy and Physiology of Lactation.* Curr Probl Pediatr Adolesc Health Care, 2017. **47**(12): p. 305-310.
20. Bhushan, A., A. Gonsalves, and J.U. Menon, *Current State of Breast Cancer Diagnosis, Treatment, and Theranostics.* Pharmaceutics, 2021. **13**(5).
21. Wang, L., *Early Diagnosis of Breast Cancer.* Sensors (Basel), 2017. **17**(7).
22. *What is Cancer?* ; Available from: https://www.cancer.gov/about-cancer/understanding/what-is-cancer#:~:text=Cancer%20is%20a%20disease%20caused,are%20also%20called%20genetic%20changes.
23. *carcinoma in situ*. Available from: https://www.cancer.gov/publications/dictionaries/cancer-terms/def/carcinoma-in-situ.
24. *What is Breast Cancer?* ; Available from: https://www.cdc.gov/cancer/breast/basic_info/what-is-breast-cancer.htm#:~:text=Most%20breast%20cancers%20begin%20in,is%20said%20to%20have%20metastasized.
25. Roarty, K. and G.V. Echeverria, *Laboratory Models for Investigating Breast Cancer Therapy Resistance and Metastasis.* Front Oncol, 2021. **11**: p. 645698.
26. Lui, D. *Breast Cancer Stages*. 2022 [cited 2023; Available from: https://www.cancercenter.com/cancer-types/breast-cancer/stages#:~:text=Stage%201%20breast%20cancer%20means,spread%20to%20the%20lymph%20nodes.
27. Anderson, B.O., et al., *Early detection of breast cancer in countries with limited resources.* Breast J, 2003. **9 Suppl 2**: p. S51-9.
28. Gupta, G.P. and J. Massague, *Cancer metastasis: building a framework.* Cell, 2006. **127**(4): p. 679-95.
29. Hapach, L.A., et al., *Engineered models to parse apart the metastatic cascade.* NPJ Precis Oncol, 2019. **3**: p. 20.
30. Jin, X. and P. Mu, *Targeting Breast Cancer Metastasis.* Breast Cancer (Auckl), 2015. **9**(Suppl 1): p. 23-34.
31. Scully, O.J., et al., *Breast cancer metastasis.* Cancer Genomics Proteomics, 2012. **9**(5): p. 311-20.
32. Lai, X., et al., *Epithelial-Mesenchymal Transition and Metabolic Switching in Cancer: Lessons From Somatic Cell Reprogramming.* Front Cell Dev Biol, 2020. **8**: p. 760.
33. Jin, X., P.J.B.c.b. Mu, and c. research, *Targeting breast cancer metastasis.* 2015. **9**: p. BCBCR. S25460.
34. Oskarsson, T., *Extracellular matrix components in breast cancer progression and metastasis.* Breast, 2013. **22 Suppl 2**: p. S66-72.
35. Bernard-Marty, C., F. Cardoso, and M.J. Piccart, *Facts and controversies in systemic treatment of metastatic breast cancer.* Oncologist, 2004. **9**(6): p. 617-32.

36. Vandeweyer, E. and D. Hertens, *Quantification of glands and fat in breast tissue: an experimental determination.* Ann Anat, 2002. **184**(2): p. 181-4.
37. Lorusso, G. and C. Ruegg, *New insights into the mechanisms of organ-specific breast cancer metastasis.* Seminars in Cancer Biology, 2012. **22**(3): p. 226-233.
38. Hernández, A., Singh, A., Miklush, L., Lin, A. *Adipose Tissue*. Available from: https://www.osmosis.org/answers/adipose-tissue#:~:text=Adipose%20tissue%2C%20also%20known%20as,a%20structural%20network%20of%20fibers.
39. Gomez-Hernandez, A., et al., *Differential Role of Adipose Tissues in Obesity and Related Metabolic and Vascular Complications.* Int J Endocrinol, 2016. **2016**: p. 1216783.
40. Nickel, A., et al., *Adipocytes induce distinct gene expression profiles in mammary tumor cells and enhance inflammatory signaling in invasive breast cancer cells.* Sci Rep, 2018. **8**(1): p. 9482.
41. Kaul, K., et al., *Contribution of the tumor and obese microenvironment to triple negative breast cancer.* 2021.
42. Perez-Perez, A., et al., *Role of Leptin in Inflammation and Vice Versa.* Int J Mol Sci, 2020. **21**(16).
43. Shouman, S., M. Wagih, and M. Kamel, *Leptin influences estrogen metabolism and increases DNA adduct formation in breast cancer cells.* Cancer Biol Med, 2016. **13**(4): p. 505-513.
44. Achari, A.E. and S.K. Jain, *Adiponectin, a Therapeutic Target for Obesity, Diabetes, and Endothelial Dysfunction.* Int J Mol Sci, 2017. **18**(6).
45. Nehme, R., et al., *Targeting Adiponectin in Breast Cancer.* Biomedicines, 2022. **10**(11): p. 2958.
46. Ando, S., et al., *Obesity, Leptin and Breast Cancer: Epidemiological Evidence and Proposed Mechanisms.* Cancers (Basel), 2019. **11**(1).
47. Ward, Z.J., et al., *Excess mortality associated with elevated body weight in the USA by state and demographic subgroup: A modelling study.* EClinicalMedicine, 2022. **48**: p. 101429.
48. Sun, L., et al., *Body mass index and prognosis of breast cancer: An analysis by menstruation status when breast cancer diagnosis.* Medicine (Baltimore), 2018. **97**(26): p. e11220.
49. Calle, E.E., et al., *Overweight, obesity, and mortality from cancer in a prospectively studied cohort of U.S. adults.* N Engl J Med, 2003. **348**(17): p. 1625-38.
50. Fruh, S.M., *Obesity: Risk factors, complications, and strategies for sustainable long-term weight management.* J Am Assoc Nurse Pract, 2017. **29**(S1): p. S3-S14.
51. *Defining Adult Overweight & Obesity*. 2022 [cited 2022.
52. Ee, C., et al., *Weight before and after a diagnosis of breast cancer or ductal carcinoma in situ: a national Australian survey.* Bmc Cancer, 2020. **20**(1).
53. Rubin, R., *Postmenopausal Women With a "Normal" BMI Might Be Overweight or Even Obese.* Jama-Journal of the American Medical Association, 2018. **319**(12): p. 1185-1187.
54. Banack, H.R., et al., *Is BMI a valid measure of obesity in postmenopausal women?* Menopause-the Journal of the North American Menopause Society, 2018. **25**(3): p. 307-313.

55. Lee, H.R., T.H. Kim, and K.C. Choi, *Functions and physiological roles of two types of estrogen receptors, ERalpha and ERbeta, identified by estrogen receptor knockout mouse.* Lab Anim Res, 2012. **28**(2): p. 71-6.
56. Cleary, M.P. and M.E. Grossmann, *Minireview: Obesity and breast cancer: the estrogen connection.* Endocrinology, 2009. **150**(6): p. 2537-42.
57. Rose, D.P. and L. Vona-Davis, *Biochemical and molecular mechanisms for the association between obesity, chronic inflammation, and breast cancer.* Biofactors, 2014. **40**(1): p. 1-12.
58. Sanchez-Jimenez, F., et al., *Obesity and Breast Cancer: Role of Leptin.* Front Oncol, 2019. **9**: p. 596.
59. *Adiponectin*. [cited 2022.
60. Webb, D.R., *Animal models of human disease: inflammation.* Biochem Pharmacol, 2014. **87**(1): p. 121-30.
61. Levy, N., *The use of animal as models: ethical considerations.* International Journal of Stroke, 2012. **7**(5): p. 440-442.
62. Tang, C. *In Vitro vs. In Vivo: Is One Better?* ; Available from: https://www.uhnresearch.ca/news/vitro-vs-vivo-one-better.
63. *2D Versus 3D Cell Cultures: Advantages and Disadvantages*. Available from: https://www.mimetas.com/en/blogs/315/2d-versus-3d-cell-cultures-advantages-and-disadvantages.html#:~:text=2D%20cell%20cultures%20have%20been,more%20accurate%20models%20of%20tissues.
64. Guo, J., et al., *Conditioned Medium from Malignant Breast Cancer Cells Induces an EMT-Like Phenotype and an Altered N-Glycan Profile in Normal Epithelial MCF10A Cells.* Int J Mol Sci, 2017. **18**(8).
65. Boix-Montesinos, P., et al., *The past, present, and future of breast cancer models for nanomedicine development.* Advanced Drug Delivery Reviews, 2021. **173**: p. 306-330.
66. Arrigoni, C., et al., *In Vitro Co-Culture Models of Breast Cancer Metastatic Progression towards Bone.* Int J Mol Sci, 2016. **17**(9).
67. Mai, J.a.S., H., *Use of Transwell® Cell Culture Inserts to Study Trans-endothelial Transport of Polymeric Doxorubicin Nanoparticles Derived from an Injectable Nanoparticle Generator*. 2017, Department of Nanomedicine Houston Methodist Research Institute: Houston, TX.
68. Bogdanowicz, D.R. and H.H. Lu, *Multifunction co-culture model for evaluating cell-cell interactions.* Methods Mol Biol, 2014. **1202**: p. 29-36.
69. Lee Isla Crake, R., et al., *Co-culture With Human Breast Adipocytes Differentially Regulates Protein Abundance in Breast Cancer Cells.* Cancer Genomics Proteomics, 2019. **16**(5): p. 319-332.
70. Sforza, L. *More than half the global population will be overweight or obese by 2035: report*. 2023; Available from: https://thehill.com/policy/healthcare/3881302-more-than-half-the-global-population-will-be-overweight-or-obese-by-2035-report/#:~:text=In%202020%2C%2038%20percent%20of,obese%2C%20according%20to%20the%20report.
71. *Adult Obesity Facts*. Available from: https://www.cdc.gov/obesity/data/adult.html.

72. *Overweight & Obesity Statistics*. 2021; Available from: https://www.niddk.nih.gov/health-information/health-statistics/overweight-obesity.
73. *Obesity and overweight*. 2021; Available from: https://www.who.int/news-room/fact-sheets/detail/obesity-and-overweight.
74. Zhang, R., et al., *FSP1-positive fibroblasts are adipogenic niche and regulate adipose homeostasis.* PLoS Biol, 2018. **16**(8): p. e2001493.
75. Malodobra-Mazur, M., et al., *Metabolic Differences between Subcutaneous and Visceral Adipocytes Differentiated with an Excess of Saturated and Monounsaturated Fatty Acids.* Genes (Basel), 2020. **11**(9).
76. Kinkel, A.D., et al., *Oil red-O stains non-adipogenic cells: a precautionary note.* Cytotechnology, 2004. **46**(1): p. 49-56.
77. *Adipose Tissue (Body Fat)*. Available from: https://my.clevelandclinic.org/health/body/24052-adipose-tissue-body-fat.
78. Hruby, A. and F.B. Hu, *The Epidemiology of Obesity: A Big Picture.* Pharmacoeconomics, 2015. **33**(7): p. 673-89.
79. Choe, S.S., et al., *Adipose Tissue Remodeling: Its Role in Energy Metabolism and Metabolic Disorders.* Front Endocrinol (Lausanne), 2016. **7**: p. 30.
80. Janderova, L., et al., *Human mesenchymal stem cells as an in vitro model for human adipogenesis.* Obes Res, 2003. **11**(1): p. 65-74.
81. Contador, D., et al., *Dexamethasone and rosiglitazone are sufficient and necessary for producing functional adipocytes from mesenchymal stem cells.* Exp Biol Med (Maywood), 2015. **240**(9): p. 1235-46.
82. Li, H., et al., *AMPK-PPARgamma-Cidec Axis Drives the Fasting-Induced Lipid Droplet Aggregation in the Liver of Obese Mice.* Front Nutr, 2022. **9**: p. 917801.
83. Moriyama, K., et al., *Oleic acid to stearic acid ratio might be a potential marker for insulin resistance in non-obese Japanese.* J Clin Biochem Nutr, 2021. **68**(2): p. 164-168.
84. Caron-Jobin, M., et al., *Stearic acid content of abdominal adipose tissues in obese women.* Nutr Diabetes, 2012. **2**(1): p. e23.
85. Maxson, S. and K.J. Burg, *Conditioned media cause increases in select osteogenic and adipogenic differentiation markers in mesenchymal stem cell cultures.* J Tissue Eng Regen Med, 2008. **2**(2-3): p. 147-54.
86. Taura, D., et al., *Adipogenic differentiation of human induced pluripotent stem cells: comparison with that of human embryonic stem cells.* FEBS Lett, 2009. **583**(6): p. 1029-33.
87. Kraus, N.A., et al., *Quantitative assessment of adipocyte differentiation in cell culture.* Adipocyte, 2016. **5**(4): p. 351-358.
88. Kim, J.I., et al., *Lipid-overloaded enlarged adipocytes provoke insulin resistance independent of inflammation.* Mol Cell Biol, 2015. **35**(10): p. 1686-99.
89. Weidlich, D., et al., *Lipid droplet-size mapping in human adipose tissue using a clinical 3T system.* Magn Reson Med, 2021. **86**(3): p. 1256-1270.
90. *Barrier Function*. Available from: https://updates.axionbiosystems.com/applications/cellular-kinetics/barrier-function.
91. Chadt, A. and H. Al-Hasani, *Glucose transporters in adipose tissue, liver, and skeletal muscle in metabolic health and disease.* Pflugers Arch, 2020. **472**(9): p. 1273-1298.

92. Luo, L. and M. Liu, *Adipose tissue in control of metabolism.* J Endocrinol, 2016. **231**(3): p. R77-R99.
93. Gastaldelli, A., M. Gaggini, and R.A. DeFronzo, *Role of Adipose Tissue Insulin Resistance in the Natural History of Type 2 Diabetes: Results From the San Antonio Metabolism Study.* Diabetes, 2017. **66**(4): p. 815-822.
94. Stolic, M., et al., *Glucose uptake and insulin action in human adipose tissue--influence of BMI, anatomical depot and body fat distribution.* Int J Obes Relat Metab Disord, 2002. **26**(1): p. 17-23.
95. Krycer, J.R., et al., *Insulin signaling requires glucose to promote lipid anabolism in adipocytes.* J Biol Chem, 2020. **295**(38): p. 13250-13266.
96. Ahmadian, M., et al., *Triacylglycerol metabolism in adipose tissue.* Future Lipidol, 2007. **2**(2): p. 229-237.
97. Kershaw, E.E., et al., *Adipose triglyceride lipase: function, regulation by insulin, and comparison with adiponutrin.* Diabetes, 2006. **55**(1): p. 148-57.
98. van de Woestijne, A.P., et al., *Adipose tissue dysfunction and hypertriglyceridemia: mechanisms and management.* Obes Rev, 2011. **12**(10): p. 829-40.
99. *Key Statistics of Breast Cancer*. Available from: https://www.cancer.org/cancer/types/breast-cancer/about/how-common-is-breast-cancer.html.
100. Kabala-Dzik, A., et al., *Migration Rate Inhibition of Breast Cancer Cells Treated by Caffeic Acid and Caffeic Acid Phenethyl Ester: An In Vitro Comparison Study.* Nutrients, 2017. **9**(10).
101. Kauanova, S., A. Urazbayev, and I. Vorobjev, *The Frequent Sampling of Wound Scratch Assay Reveals the "Opportunity" Window for Quantitative Evaluation of Cell Motility-Impeding Drugs.* Front Cell Dev Biol, 2021. **9**: p. 640972.
102. DePolo, J. *Molecular Subtypes of Breast Cancer*. Available from: https://www.breastcancer.org/types/molecular-subtypes.
103. Oshi, M., et al., *Adipogenesis in triple-negative breast cancer is associated with unfavorable tumor immune microenvironment and with worse survival.* Sci Rep, 2021. **11**(1): p. 12541.
104. Berger, E.R. and N.M. Iyengar, *Obesity and Energy Balance Considerations in Triple-Negative Breast Cancer.* Cancer J, 2021. **27**(1): p. 17-24.
105. Tong, Y., et al., *Association of Obesity and Luminal Subtypes in Prognosis and Adjuvant Endocrine Treatment Effectiveness Prediction in Chinese Breast Cancer Patients.* Front Oncol, 2022. **12**: p. 862224.
106. Dornbush, S. and N.R. Aeddula, *Physiology, Leptin*, in *StatPearls*. 2023: Treasure Island (FL).
107. Myers, M.G., Jr., et al., *Obesity and leptin resistance: distinguishing cause from effect.* Trends Endocrinol Metab, 2010. **21**(11): p. 643-51.
108. Dubern, B. and K. Clement, *Leptin and leptin receptor-related monogenic obesity.* Biochimie, 2012. **94**(10): p. 2111-5.
109. Izquierdo, A.G., et al., *Leptin, Obesity, and Leptin Resistance: Where Are We 25 Years Later?* Nutrients, 2019. **11**(11).

110. Fuster, J.J. and K. Walsh, *The good, the bad, and the ugly of interleukin-6 signaling.* EMBO J, 2014. **33**(13): p. 1425-7.
111. Tanaka, T., M. Narazaki, and T. Kishimoto, *IL-6 in inflammation, immunity, and disease.* Cold Spring Harb Perspect Biol, 2014. **6**(10): p. a016295.
112. Shi, J., et al., *Cytokines and Abnormal Glucose and Lipid Metabolism.* Front Endocrinol (Lausanne), 2019. **10**: p. 703.
113. Ramirez, H., S.B. Patel, and I. Pastar, *The Role of TGFbeta Signaling in Wound Epithelialization.* Adv Wound Care (New Rochelle), 2014. **3**(7): p. 482-491.
114. Zarzynska, J.M., *Two faces of TGF-beta1 in breast cancer.* Mediators Inflamm, 2014. **2014**: p. 141747.
115. Bernhard, S., et al., *Interleukin 8 Elicits Rapid Physiological Changes in Neutrophils That Are Altered by Inflammatory Conditions.* J Innate Immun, 2021. **13**(4): p. 225-241.
116. Bruun, J.M., S.B. Pedersen, and B. Richelsen, *Regulation of interleukin 8 production and gene expression in human adipose tissue in vitro.* J Clin Endocrinol Metab, 2001. **86**(3): p. 1267-73.
117. Anto Michel, N., et al., *Inflammatory Pathways Regulated by Tumor Necrosis Receptor-Associated Factor 1 Protect From Metabolic Consequences in Diet-Induced Obesity.* Circ Res, 2018. **122**(5): p. 693-700.
118. Muramoto, A., et al., *Angiopoietin-like protein 2 sensitively responds to weight reduction induced by lifestyle intervention on overweight Japanese men.* Nutr Diabetes, 2011. **1**(11): p. e20.
119. Parida, S., S. Siddharth, and D. Sharma, *Adiponectin, Obesity, and Cancer: Clash of the Bigwigs in Health and Disease.* Int J Mol Sci, 2019. **20**(10).
120. Moreira, A., et al., *Adipocyte secreted factors enhance aggressiveness of prostate carcinoma cells.* PLoS One, 2015. **10**(4): p. e0123217.
121. Nicolini, A., A. Carpi, and G. Rossi, *Cytokines in breast cancer.* Cytokine Growth Factor Rev, 2006. **17**(5): p. 325-37.
122. Vale, N., et al., *Normal breast epithelial MCF-10A cells to evaluate the safety of carbon dots.* RSC Med Chem, 2021. **12**(2): p. 245-253.
123. Fontana, F., et al., *Adipocyte-Derived Extracellular Vesicles Promote Prostate Cancer Cell Aggressiveness by Enabling Multiple Phenotypic and Metabolic Changes.* Cells, 2022. **11**(15).
124. Gunawardane, R.N., et al., *Novel role for PDEF in epithelial cell migration and invasion.* Cancer Res, 2005. **65**(24): p. 11572-80.
125. Yersal, O. and S. Barutca, *Biological subtypes of breast cancer: Prognostic and therapeutic implications.* World J Clin Oncol, 2014. **5**(3): p. 412-24.
126. Asante, E.C., et al., *Adipose Tissue from Lean and Obese Mice Induces a Mesenchymal to Epithelial Transition-Like Effect in Triple Negative Breast Cancers Cells Grown in 3-Dimensional Culture.* Int J Mol Sci, 2020. **21**(17).
127. Del Bano, J., et al., *A Bispecific Antibody-Based Approach for Targeting Mesothelin in Triple Negative Breast Cancer.* Front Immunol, 2019. **10**: p. 1593.